

The role of TrkB and Nav1.9 in activity-dependent axon  
growth in motoneurons



Die Rolle von TrkB und Nav1.9 in aktivitätsabhängigem  
Axonwachstum von Motoneuronen



Doctoral thesis for a doctoral degree  
at the Institute for Clinical Neurobiology,  
University hospital Würzburg  
and Graduate School of Life Sciences,  
Julius-Maximilians-Universität Würzburg  
Section: Neuroscience

Submitted by

**Andrea Wetzel**

from Erfurt

Würzburg, December 2013



Submitted on:.....

**Members of the *Promotionskomitee*:**

Chairperson: Prof. Dr. Utz Fischer

Primary Supervisor: PD Dr. Robert Blum

Supervisor (Second): Prof. Dr. Erhard Wischmeyer

Supervisor (Third): Prof. Dr. Michael Sendtner

Date of Public Defence:.....

Date of receipt of Certificates:.....

---

For my parents

# Table of contents

<b>Table of contents</b> .....	<b>4</b>
<b>List of figures</b> .....	<b>6</b>
<b>List of tables</b> .....	<b>8</b>
<b>Abbreviations</b> .....	<b>9</b>
<b>Zusammenfassung</b> .....	<b>12</b>
<b>Abstract</b> .....	<b>13</b>
<b>1 Introduction</b> .....	<b>14</b>
1.1 Neurotrophic factors and their receptors .....	14
1.1.1 Trk receptor-mediated signalling cascades.....	16
1.1.2 Trk receptor-mediated activation of ion channels .....	18
1.1.3 Transactivation of Trk receptors.....	19
1.2 The motoneuron disease spinal muscular atrophy (SMA) .....	20
1.3 Spontaneous neuronal activity regulates axonal growth.....	22
1.4 Voltage-gated sodium channels.....	25
1.4.1 The voltage-gated sodium channel Na <sub>v</sub> 1.9.....	26
1.4.2 BDNF - TrkB - Na <sub>v</sub> 1.9 .....	27
1.5 Aims of the thesis.....	29
<b>2 Material and Methods</b> .....	<b>30</b>
2.1 Material .....	30
2.1.1 Animals .....	30
2.1.2 Cell lines.....	30
2.1.3 Chemicals for cell culture .....	31
2.1.4 Chemicals for DNA and RNA techniques.....	32
2.1.5 Chemicals for protein analysis .....	33
2.1.6 Buffers, media and solutions.....	34
2.1.7 Antibodies and labelling dyes.....	35
2.1.8 Plasmids and primers.....	37
2.1.9 Commercial kits.....	38
2.1.10 Software .....	38
2.2 Methods .....	40
2.2.1 Cell culture .....	40
2.2.2 DNA and RNA techniques.....	41
2.2.3 Protein analysis techniques .....	45
2.2.4 Axon length measurement .....	48
2.2.5 Survival assay .....	48

2.2.6	Calcium imaging.....	49
<b>3</b>	<b>Results .....</b>	<b>50</b>
3.1	Na <sub>v</sub> 1.9 is expressed in spinal cord and motoneurons.....	50
3.2	Na <sub>v</sub> 1.9 protein is localized in cultured embryonic motoneurons and at the node of Ranvier of motor and sensory nerve fibres .....	52
3.2.1	Generation of a stable Na <sub>v</sub> 1.9 expressing cell line .....	53
3.2.2	Verification of the anti-mouse Na <sub>v</sub> 1.9 antibody .....	55
3.2.3	Detection of Na <sub>v</sub> 1.9 protein in cultured embryonic motoneurons.....	57
3.2.4	Localization of Na <sub>v</sub> 1.9 protein in motor and sensory nerve fibres.....	58
3.3	The axons of motoneurons from Na <sub>v</sub> 1.9 <sup>-/-</sup> mice are shorter .....	60
3.4	Reduced axon growth of Na <sub>v</sub> 1.9 <sup>-/-</sup> motoneurons can be rescued by a Na <sub>v</sub> 1.9 encoding virus .....	61
3.5	Na <sub>v</sub> 1.9 protein is present in growth cones of motoneurons from <i>Smn</i> <sup>-/-</sup> - <i>SMN2tg</i> mice.....	62
3.6	Mutant Na <sub>v</sub> 1.9 is expressed in DRGs from <i>Scn11a</i> <sup>+L788P</sup> mice.....	63
3.7	TrkB protein is localized in cultured embryonic motoneurons and at the node of Ranvier of facial nerve fibres.....	65
3.7.1	Detection of TrkB protein in cultured embryonic motoneurons .....	65
3.7.2	Localization of TrkB protein in facial nerve fibres.....	67
3.8	Spontaneous activity is reduced in motoneurons from TrkB <sup>-/-</sup> mice .....	68
3.9	The axons of motoneurons from TrkB <sup>-/-</sup> mice are shorter.....	69
3.10	BDNF and TrkB mediate motoneuron survival by two independent mechanisms .....	70
<b>4</b>	<b>Discussion .....</b>	<b>72</b>
4.1	The Na <sub>v</sub> 1.9 channel is found in motoneurons .....	73
4.2	Is Na <sub>v</sub> 1.9 a therapeutic target for motor defects? .....	74
4.3	Na <sub>v</sub> 1.5 might act downstream of Na <sub>v</sub> 1.9-mediated excitation.....	75
4.4	Is TrkB upstream of Na <sub>v</sub> 1.9-mediated excitation?.....	75
4.5	TrpC channels and motoneuron excitation at growth cones .....	76
	<b>References .....</b>	<b>78</b>
	<b>Affidavit/Eidesstattliche Erklärung.....</b>	<b>90</b>
	<b>Curriculum Vitae.....</b>	<b>91</b>
	<b>Acknowledgements.....</b>	<b>93</b>

## List of figures

Figure 1: Neurotrophic factors and their receptors.....	15
Figure 2: Neurotrophins and their receptors .....	15
Figure 3: BDNF-TrkB binding activates three major signalling pathways: PI3K, MAPK and PLC $\gamma$ .....	17
Figure 4: BDNF/TrkB-mediated activation of ion channels .....	19
Figure 5: Reduced Ca <sup>2+</sup> transients and axon length in <i>Smn</i> <sup>-/-</sup> - <i>SMN2</i> motoneurons.....	22
Figure 6: VGSC pore blockers reduce spontaneous calcium transients in soma and growth cone of wild type motoneurons .....	23
Figure 7: VGSC pore blockers reduce axon growth of wild type motoneurons.....	24
Figure 8: Structure of voltage-gated sodium channels.....	25
Figure 9: BDNF/TrkB mediated rapid opening of Na <sub>v</sub> 1.9 .....	28
Figure 10: Reaction mix and PCR program for genotyping.....	42
Figure 11: qRT-PCR components and cycling conditions.....	44
Figure 12: Expression pattern of TTX-resistant VGSCs in spinal cord, DRGs and motoneurons .....	51
Figure 13: Isolation process to generate stable Na <sub>v</sub> 1.9 expressing cells.....	53
Figure 14: Verification of the stable Na <sub>v</sub> 1.9 expressing cell line .....	54
Figure 15: Verification of the specificity of anti-mouse Na <sub>v</sub> 1.9 antibody .....	56
Figure 16: Immunohistochemistry of Na <sub>v</sub> 1.9 in dorsal root ganglia.....	57
Figure 17: Detection of Na <sub>v</sub> 1.9 protein in cultured embryonic motoneurons.....	58
Figure 18: Detection of Na <sub>v</sub> 1.9 protein in femoral quadriceps nerve fibres.....	59
Figure 19: Detection of Na <sub>v</sub> 1.9 protein in facial nerve fibres.....	59
Figure 20: Axon length of motoneurons from Na <sub>v</sub> 1.9 wild type and knock-out mice.....	61
Figure 21: Axon length of motoneurons from Na <sub>v</sub> 1.9 wild type and knock-out mice with and without Na <sub>v</sub> 1.9 virus infection .....	62
Figure 22: Na <sub>v</sub> 1.9 labelling in motoneurons from <i>Smn</i> <sup>-/-</sup> - <i>SMN2tg</i> mice .....	63
Figure 23: Detection of mutant Na <sub>v</sub> 1.9 transcripts and Na <sub>v</sub> 1.9 protein in dorsal root ganglia from wild type and mutant mice.....	64
Figure 24: Recognition of TrkB protein in cultured embryonic motoneurons .....	66
Figure 25: Labelling of TrkB protein at the node of Ranvier of facial nerve fibres.....	67

Figure 26: Spontaneous activity of motoneurons from wild type and  $\text{TrkB}^{-/-}$  mice .....68

Figure 27: Axon length of cultured motoneurons from wild type and  $\text{TrkB}^{-/-}$  mice.....69

Figure 28: Survival of cultured motoneurons from  $\text{TrkB}^{+/+}$  and  $\text{TrkB}^{-/-}$  mice .....70

Figure 29: Model for the interplay of regulators for axon elongation at the growth cone of  
developing motoneurons .....76

## List of tables

Table 1: Chemicals for cell culture .....	31
Table 2: Chemicals for DNA and RNA techniques.....	32
Table 3: Chemicals for protein analysis .....	33
Table 4: Buffers, media and solutions.....	34
Table 5: Primary antibodies .....	35
Table 6: Secondary antibodies and labelling dyes.....	36
Table 7: Plasmids.....	37
Table 8: Primers for genotyping .....	37
Table 9: Primers for cDNA amplification .....	37
Table 10: Commercial kits.....	38
Table 11: Software .....	38



## Abbreviations

ACSF	Artificial cerebrospinal fluid
Akt/PKB	Akt kinase / protein kinase B
ALS	Amyotrophic lateral sclerosis
AMPA	$\alpha$ -Amino-3-hydroxy-5-methyl-4-isoxazole propionic acid receptor
ATP	Adenosine triphosphate
BCA	Bicinchoninic acid
BDNF	Brain-derived neurotrophic factor
bp, kb	Base pair(s); kilo base pairs
BSA	Bovine serum albumin
BSS	Balanced Salt Solution
CaM	Calmodulin
CaMK	Ca <sup>2+</sup> -CaM-dependent kinase
Caspr	Contactin-associated protein
CNS	Central nervous system
CNTF	Ciliary neurotrophic factor
CREB	cAMP response element-binding protein
CTP	Cytidine triphosphate
Da	Dalton
DAG	Diacylglycerol
DAPI	4', 6-diamidino-2-phenylindole
DMEM	Dulbecco's modified essential medium
DMSO	Dimethyl sulfoxide
DNA	Deoxyribonucleic acid
dNTP	Deoxyribonucleotide
DTT	Dithiothreitol
E. coli	Escherichia coli
ECL	Enhanced chemiluminescence
EDTA	Ethylenediaminetetraacetic acid
EGF	Epidermal growth factor
ERK	Extracellular signal-regulated kinase
FCS	Fetal calf serum
Fyn	FYN oncogene related to SRC, FGR, YES
GABA	$\gamma$ -Aminobutyric acid
GAPDH	Glyceraldehyde 3-phosphate dehydrogenase
GDP	Guanosine diphosphate

---

GPCR	G protein-coupled receptors
DRG	Dorsal root ganglia
GTP	Guanosine triphosphate
HBSS	Hanks' balanced salt solution
HEK	Human embryonic kidney
HPLC	High performance liquid chromatography
HRP	Horseradish peroxidase
IFM	Isoleucine, phenylalanine, and methionine
IP <sub>3</sub>	Inositol 1,4,5-trisphosphate
KO	Knock-out
LIF	Leukemia inhibitory factor
LTP	Long-term potentiation
MAPK	Mitogen-activated protein kinase
MEK	Mitogen-activated ERK activating kinase
MND	Motoneuron diseases
NaF	Sodium fluoride
NFL	Neurofilament
NGF	Nerve growth factor
NMDAR	<i>N</i> -methyl-D-aspartate receptor
NT	Neurotrophin
PACAP	Pituitary adenylate cyclaseactivating polypeptide
PAGE	Polyacrylamid gel electrophoresis
PBS	Phosphate buffered saline
PCR	Polymerase chain reaction
PFA	Paraformaldehyde
PI3K	Phosphatidylinositol 3-kinase
PIP <sub>2</sub>	Phosphatidylinositol 4,5-bisphosphate
PKC	Protein kinase C
PLC $\gamma$	Phospholipase C $\gamma$
PNS	Peripheral nervous system
PORN	Poly-DL-ornithine hydrobromide
PP1	4-amino-5-(4-methylphenyl)-7-( <i>t</i> -butyl)pyrazolol-[3,4- <i>d</i> ]-pyrimidine
PVDF	Polyvinylidene difluoride
Ras	Rat sarcoma; small GTP-binding protein Ras
RNA	Ribonucleic acid
ROI	Region of interest
rpm	Revolutions per minute
SDS	Sodium dodecyl sulfate

Shc	Src homology 2/ $\alpha$ -collagen-related protein
SEM	Standard error of the mean
SMA	Spinal muscular atrophy
SMN	Survival motor neuron
Src	v-src sarcoma
STED	Stimulated emission depletion
STX	Saxitoxin
TAE	Tris acetate EDTA
TBE	Tris borate EDTA
TBS	Tris buffered saline
tg	Transgene
Trk	Tropomyosin receptor kinase
TTP	Thymidine triphosphate
TTX	Tetrodotoxin
VGCC	Voltage-gated calcium channels
VGSC	Voltage-gated sodium channels
VOCC	Voltage-operated calcium channels
VSVG	Glycoproteins of vesicular stomatitis virus
wt	Wild type

## Zusammenfassung

Während der Entwicklung des Nervensystems lassen sich bei Motoneuronen aktivitätsabhängige Kalziumströme beobachten, die das Axonwachstum regulieren. Diese Form der neuronalen Spontanaktivität sowie das Auswachsen von Axonen sind bei Motoneuronen, die aus Tiermodellen der Spinalen Muskelatrophie isoliert werden, gestört. Experimente aus unserer Arbeitsgruppe haben gezeigt, dass spontane Erregbarkeit und aktivitätsabhängiges Axonwachstum von kultivierten Motoneuronen auch unter Verwendung von Toxinen beeinträchtigt sind, welche die Aktivität von spannungsabhängigen Natriumkanälen blockieren. In diesen Versuchen war die Wirkung von Saxitoxin effizienter als die Wirkung von Tetrodotoxin. Wir identifizierten den Saxitoxin-sensitiven/Tetrodotoxin-insensitiven spannungsabhängigen Natriumkanal  $Na_v1.9$  als Trigger für das Öffnen spannungsabhängiger Kalziumkanäle. Die Expression von  $Na_v1.9$  in Motoneuronen konnte über quantitative RT-PCR nachgewiesen werden und Antikörperfärbungen offenbarten eine Anreicherung des Kanals im axonalen Wachstumskegel sowie an Ranvier'schen Schnürringen von isolierten Nervenfasern wildtypischer Mäuse. Motoneurone von  $Na_v1.9$  *knock-out* Mäusen zeigen reduzierte Spontanaktivität und eine Reduktion des Axonwachstums, welche durch  $Na_v1.9$  Überexpression normalisiert werden kann. In Motoneuronen von *Smn*-defizienten Mäusen konnte keine Abweichung der  $Na_v1.9$  Proteinverteilung nachgewiesen werden.

Kürzlich wurden Patienten identifiziert, die eine *missense*-Mutation im  $Na_v1.9$  kodierenden *SCN11A* Gen tragen. Diese Patienten können keinerlei Schmerz empfinden und leiden zudem an Muskelschwäche in Kombination mit einer verzögerten motorischen Entwicklung. Im Rahmen dieser Doktorarbeit konnten molekularbiologische Untersuchungen an Mäusen, welche die Mutation im orthologen *Scn11a* Gen tragen, zur Aufklärung des Krankheitsmechanismus beitragen. Die Kooperationsstudie zeigte, dass eine gesteigerte Funktion von  $Na_v1.9$  diese spezifische Kanalerkrankung auslöst, was die Wichtigkeit von  $Na_v1.9$  in menschlichen Motoneuronen unterstreicht.

Eine frühere Studie beschrieb an hippocampalen Neuronen, dass die Rezeptortyrosinkinase *tropomyosin receptor kinase B* (TrkB) den  $Na_v1.9$  Kanal öffnen kann. Im Wachstumskegel von Motoneuronen ist TrkB nachweisbar und folglich in räumlicher Nähe zu  $Na_v1.9$  zu finden. Um zu prüfen, ob TrkB in die spontane Erregbarkeit von Motoneuronen involviert ist, wurden TrkB *knock-out* Mäuse untersucht. Isolierte Motoneurone von TrkB *knock-out* Mäusen weisen eine Reduktion der Spontanaktivität und eine Verringerung des Axonwachstums auf. Ob TrkB und  $Na_v1.9$  hierbei funktionell gekoppelt sind, ist Gegenstand künftiger Forschung.

## Abstract

During development of the nervous system, spontaneous  $\text{Ca}^{2+}$  transients are observed that regulate the axon growth of motoneurons. This form of spontaneous neuronal activity is reduced in motoneurons from a mouse model of spinal muscular atrophy and this defect correlates with reduced axon elongation. Experiments from our group demonstrated that voltage-gated sodium channel pore blockers decrease spontaneous neuronal activity and axon growth in cultured motoneurons, too. In these experiments, saxitoxin was more potent than tetrodotoxin. We identified the saxitoxin-sensitive/tetrodotoxin-insensitive voltage-gated sodium channel  $\text{Na}_v1.9$  as trigger for the opening of voltage-gated calcium channels. In motoneurons, expression of  $\text{Na}_v1.9$  was verified via quantitative RT-PCR. Immuno labelling experiments revealed enrichment of the channel in axonal growth cones and at the nodes of Ranvier of isolated nerve fibres from wild type mice. Motoneurons from  $\text{Na}_v1.9$  knock-out mice show decreased spontaneous activity and reduced axonal elongation. This growth defect can be rescued by  $\text{Na}_v1.9$  overexpression. In motoneurons from *Smn*-deficient mice,  $\text{Na}_v1.9$  distribution appeared to be normal.

Recently, patients carrying a missense mutation in the  $\text{Na}_v1.9$ -encoding gene *SCN11A* were identified. These patients are not able to feel pain and suffer from muscular weakness and a delayed motor development. Molecular biological work during this dissertation supported the analysis of this mutation in a mouse model carrying the orthologous alteration in the *Scn11a* locus. The cooperation study confirmed that a gain-of-function mechanism underlies the  $\text{Na}_v1.9$ -mediated channelopathy, thus suggesting a functional role of  $\text{Na}_v1.9$  in human motoneurons.

An earlier study showed in hippocampal neurons that the receptor tyrosine kinase tropomyosin receptor kinase B (TrkB) can open the  $\text{Na}_v1.9$  channel. TrkB is localized in growth cones of motoneurons and subsequently found in close proximity to  $\text{Na}_v1.9$ . In order to proof whether TrkB is involved in spontaneous excitability in motoneurons, TrkB knock-out mice were analysed. Isolated motoneurons from TrkB knock-out mice show a reduced spontaneous activity and axon elongation. It remains to be studied whether TrkB and  $\text{Na}_v1.9$  are functionally connected.

# 1 Introduction

During development of the nervous system, axons of motoneurons grow over long distances to make synaptic connections with the target tissue, the skeletal muscle (*Sanes & Lichtman 1999, Sendtner et al. 2000*). Very early experiments conducted in developing chick embryos showed that significant populations of motoneurons undergo a physiological cell death during this period of target finding (*Hamburger 1934, Hamburger 1975*). Studies on this physiological form of cell death led to the discovery of neurotrophic factors (for review see (*Sendtner et al. 2000, Dekkers et al. 2013*)) These factors have been identified to support motoneuron survival and maintenance as well as neurite elongation (*Arakawa et al. 1990, Thoenen 1993, Barde 1994, Sendtner et al. 2000, Zhou & Snider 2006*). According to the neurotrophic factor hypothesis, targets of innervation were postulated to secrete limiting amounts of survival factors that function to ensure a balance between the size of a target organ and the number of innervating neurons (*Huang & Reichardt 2001*). But in the course of time, neurotrophic factors have shown to be secreted proteins from various sources that act together in regulating multiple aspects of neural circuit development and function, including cell proliferation and differentiation, neurite outgrowth, synaptogenesis as well as synaptic function and activity-dependent forms of synaptic plasticity (*Sendtner et al. 2000, Lu et al. 2005, Reichardt 2006, Amaral & Pozzo-Miller 2007, Minichiello 2009*).

## 1.1 Neurotrophic factors and their receptors

Since the discovery of nerve growth factor (NGF) by Levi-Montalcini, Hamburger and Cohen, more than a dozen neurotrophic molecules have been characterized (*Levi-Montalcini 1987, Sendtner et al. 2000, Poo 2001*). The group of neurotrophic factors comprises the family of neurotrophins (NTs), the ciliary neurotrophic factor (CNTF)/leukemia inhibitory factor (LIF) family, the hepatocyte growth factor (HGF) family, the family of insulin-like growth factors (IGFs), as well as the family of glial-derived neurotrophic factors (*Sendtner et al. 2000*). A list of the members and their particular receptors is shown in Figure 1.

Among these neurotrophic factor families, neurotrophins comprise small and closely related proteins that are initially synthesized as precursors or pro-neurotrophins (*Hallbook 1999, Lessmann et al. 2003, Blum & Konnerth 2005, Skaper 2008*). The pre-peptide provides the signal for the translocation of the pro-neurotrophins into the lumen of the endoplasmic reticulum and is subsequently cleaved off. Further processing within the intracellular protein transport pathway includes the removal of the pro-domain, which precedes the generation of mature neurotrophins (*Blum & Konnerth 2005*).

Neurotrophic factors	Receptors
<b>1. Neurotrophins</b>	
Nerve growth factor (NGF)	p75 <sup>NTR</sup> , TrkA
Brain-derived neurotrophic factor (BDNF)	p75 <sup>NTR</sup> , TrkB
Neurotrophin-3 (NT-3)	p75 <sup>NTR</sup> , TrkC
Neurotrophin-4/5 (NT-4/5)	p75 <sup>NTR</sup> , TrkB
<b>2. CNTF/LIF family</b>	
Ciliary neurotrophic factor (CNTF)	CNTFR $\alpha$ , LIFR $\beta$ , gp130
Leukemia inhibitory factor (LIF)	LIFR $\beta$ , gp130
Cardiotrophin-1 (CT-1)	LIFR $\beta$ , gp130
Cardiotrophin-1-like cytokine (CLC)	LIFR $\beta$ , gp130
<b>3. Hepatocyte growth factor family</b>	
Hepatocyte growth factor/scatter factor (HGF/SF)	c-met
<b>4. Insulin-like growth factors</b>	
Insulin-like growth factor-I (IGF-I)	IGFR-1
Insulin-like growth factor-II (IGF-II)	IGFR-1, mannose-6P R
<b>5. Glial-derived neurotrophic factor and related factors</b>	
Glial-derived neurotrophic factor (GDNF)	GFR $\alpha$ 1, c-ret
Neurturin (NTR)	GFR $\alpha$ 2, c-ret
Persephin	GFR $\alpha$ 4, c-ret
Artemin	GFR $\alpha$ 3, c-ret

**Figure 1: Neurotrophic factors and their receptors**

(modified from (Sendtner et al. 2000))

GFR = GDNF family receptor; gp130 = glycoprotein 130; p75<sup>NTR</sup> = p75 neurotrophin receptor; Trk = tropomyosin receptor kinase

Biological effects of each of the four mammalian neurotrophins, NGF, brain-derived neurotrophic factor (BDNF), neurotrophin-3 (NT-3) and neurotrophin-4 (NT-4), are mediated through activation of one or more of the three members of the tropomyosin receptor kinase (Trk) family consisting of the proteins TrkA, TrkB and TrkC (Chao et al. 2006, Skaper 2008). NGF binds preferentially to TrkA, BDNF and NT-4 to TrkB, and NT-3 to TrkC (Figure 2) (Chao 2003, Huang & Reichardt 2003). Moreover, all neurotrophins activate the p75 neurotrophin receptor (p75<sup>NTR</sup>), a member of the tumour necrosis factor receptor superfamily (Rodriguez-Tebar et al. 1990, Dechant & Barde 1997, Dechant & Barde 2002, Skaper 2008).

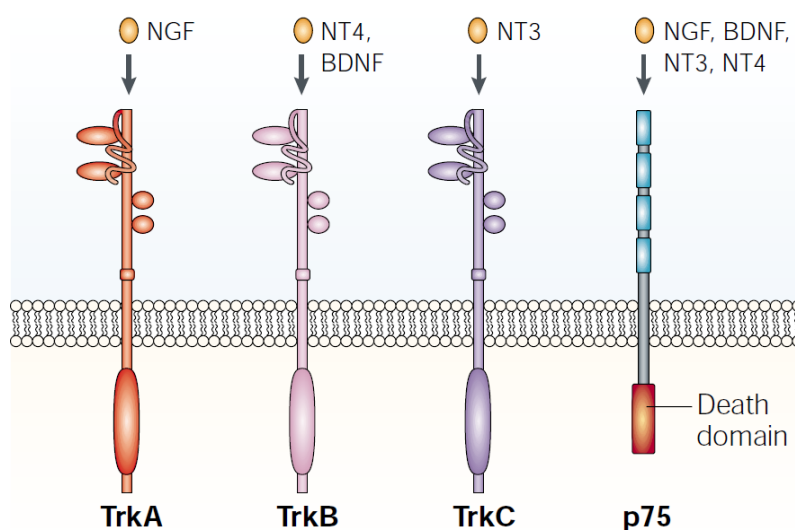


**Figure 2: Neurotrophins and their receptors**

Neurotrophins bind selectively to specific Trk receptors, whereas all neurotrophins bind to the p75 neurotrophin receptor. Trk receptors contain extracellular immunoglobulin G (IgG) domains for ligand binding and a catalytic tyrosine kinase sequence in the intracellular domain. The p75<sup>NTR</sup> receptor contains four extracellular cysteine-rich repeats and the intracellular part includes a "death" domain. (modified from (Chao 2003)) BDNF = brain-derived neurotrophic factor; NGF = nerve

growth factor; NT = neurotrophin; Trk = tropomyosin receptor kinase

Neurotrophin-mediated p75<sup>NTR</sup> signalling (Frade et al. 1996), which activates caspase-dependent apoptotic pathways, induces a negative signal for cell survival (Chao 2003, Reichardt 2006, Park & Poo 2013). The p75<sup>NTR</sup> receptor can further act as co-receptor for Trk

receptors and the expression of p75<sup>NTR</sup> can increase the affinity of TrkA for NGF and can enhance its specificity for cognate neurotrophins (*Hempstead et al. 1991, Bibel et al. 1999, Chao 2003*). A recent study using embryonic stem cells that express only one type of Trk receptor showed that cells expressing TrkA or TrkC readily die in the absence of the neurotrophin-binding partner of Trk, whereas the survival of TrkB-expressing cells is not affected by the absence of BDNF (*Nikoletopoulou et al. 2010*). However, the lack of the death-activating capability of TrkB does not imply that its activation by BDNF is not effective to prevent neuronal death during development of the peripheral nervous system (*Liu et al. 1995, Nikoletopoulou et al. 2010*). In the central nervous system, where BDNF is the most widely expressed neurotrophin, BDNF and the neurotrophic factor CNTF prevent the death of motoneurons after facial nerve transection (*Sendtner et al. 1990, Sendtner et al. 1992, Sendtner et al. 1996, Sendtner et al. 2000*). Moreover, cultured motoneurons survive by addition of BDNF and CNTF (*Arakawa et al. 1990, Sendtner et al. 1996, Wiese et al. 2010*).

### 1.1.1 Trk receptor-mediated signalling cascades

Trk receptors are typical receptor tyrosine kinases whose activation is stimulated by neurotrophin-mediated dimerization and trans-autophosphorylation of activation loop tyrosines (*Reichardt 2006*). In the case of TrkB, Figure 3 presents three main intracellular signalling pathways activated by BDNF binding: the phosphatidylinositol 3-kinase (PI3K)-Akt pathway, the Ras-mitogen-activated protein kinase (MAPK) pathway and the phospholipase C $\gamma$  (PLC $\gamma$ )-Ca<sup>2+</sup> pathway (*Kaplan & Miller 2000, Blum & Konnerth 2005, Minichiello 2009*). Ligand binding leads to phosphorylation of tyrosine residues in the juxtamembrane domain or the carboxyl terminus of the receptor, which act as docking sites for adaptor molecules like Src homologous and collagen-like (Shc) and PLC $\gamma$  (*Blum & Konnerth 2005, Minichiello 2009*). Recruitment and phosphorylation of Shc adaptors leads to the activation of PI3K, that generate 3-phosphoinositides and activate 3-phosphoinositide-dependent protein kinase 1 (PDK1). Together with these 3-phosphoinositides, PDK1 activates the protein kinase Akt, that phosphorylates several proteins (*Franke et al. 1997, Crowder & Freeman 1998*), resulting in survival signals in a wide range of neuronal cell types (*Brunet et al. 2001*).

The Shc adaptor protein also links activated Trk to the Ras-MAPK pathway. Thereby, phosphorylated Shc leads to an activation of the guanine nucleotide exchange factor son of sevenless (SOS) (*Yoshii & Constantine-Paton 2010*). SOS promotes the removal of GDP from Ras that subsequently binds GTP and becomes active. Ras activates the downstream kinases B-raf, Mitogen-activated ERK activating kinase (MEK), and MAPK (*Huang & Reichardt 2003, Reichardt 2006, Yoshii & Constantine-Paton 2010*). The Ras-MAPK pathway influences transcription events, such as the activation of the cAMP response



element-binding protein (CREB) transcription factor and therefore might play a role in BDNF induced long-term potentiation (LTP) (Finkbeiner et al. 1997, Shaywitz & Greenberg 1999, Blum & Konnerth 2005, Minichiello 2009, Park & Poo 2013).

Finally, phosphorylation of tyrosine 816 of TrkB leads to recruitment and phosphorylation of PLC $\gamma$  (Kaplan & Miller 2000). Active PLC $\gamma$  hydrolyses phosphatidylinositol 4,5-bisphosphate (PIP $_2$ ) to produce inositol 1,4,5-trisphosphate (IP $_3$ ) and diacylglycerol (DAG). IP $_3$  promotes release of Ca $^{2+}$  from internal stores, which results in the activation of enzymes like Ca $^{2+}$ /calmodulin-dependent protein kinases and DAG stimulates DAG-regulated PKC isoforms (Reichardt 2006, Minichiello 2009). The PLC $\gamma$ -Ca $^{2+}$  pathway influences the synthesis and activation of several proteins, which are involved in plasticity-dependent mechanisms of nerve cells (Minichiello et al. 2002, Gartner et al. 2006).

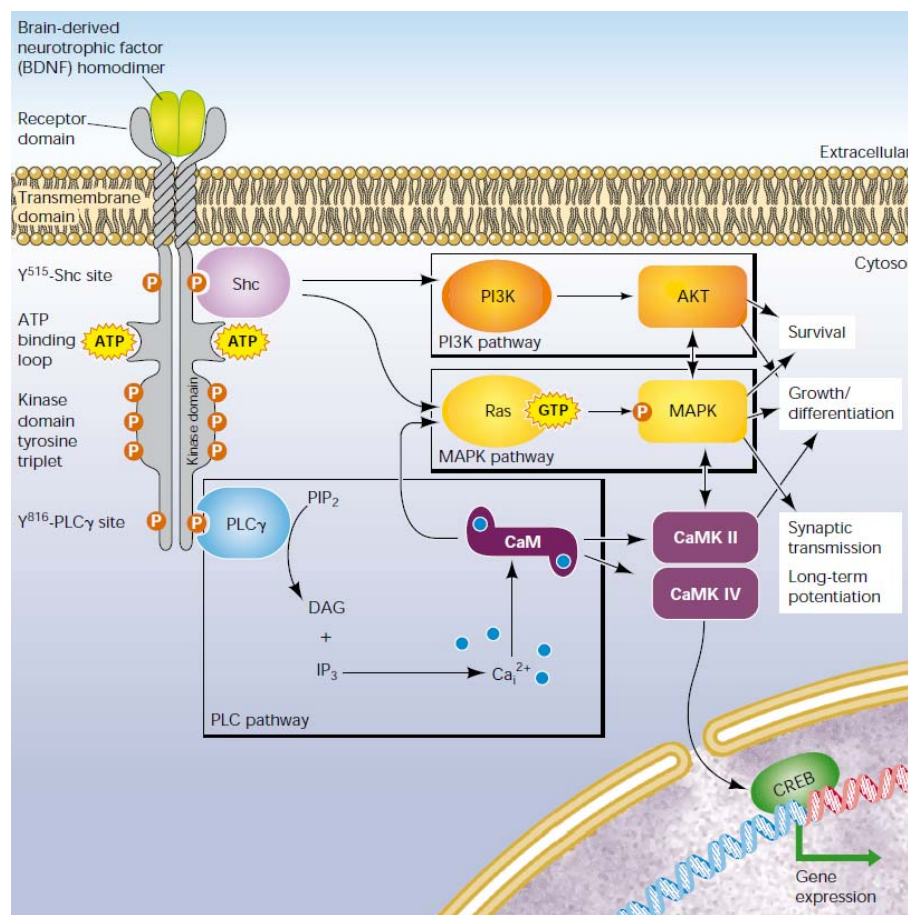


**Figure 3: BDNF-TrkB binding activates three major signalling pathways: PI3K, MAPK and PLC $\gamma$**  BDNF binding induces dimerization and autophosphorylation of TrkB<sup>FL</sup> receptors. Phosphorylation of tyrosine at position 515 (Y<sup>515</sup>) produces a binding site for Shc, whereas Y<sup>816</sup> forms the adaptor site for PLC $\gamma$ . The activated signalling pathways mediate effects on neuronal survival, differentiation, gene expression as well as acute effects on synaptic transmission and long-term potentiation. (from (Blum & Konnerth 2005)) Akt = Akt kinase; ATP = adenosine triphosphate; BDNF = brain-derived neurotrophic factor; Ca $_i^{2+}$  = intracellular Ca $^{2+}$ ; CaM = calmodulin; CaMKII and IV = Ca $^{2+}$ -CaM-dependent kinase II and IV; CREB = cAMP response element-binding protein; DAG = diacylglycerol; IP $_3$  = inositol 1,4,5-trisphosphate; MAPK = mitogen-activated protein kinase; P = phosphorylation; PI3K = phosphatidylinositol 3-kinase; PIP $_2$  = phosphatidylinositol 4,5-bisphosphate; PLC $\gamma$  = phospholipase C $\gamma$ ; Ras = rat sarcoma, small GTP-binding protein Ras; Shc = Src homology 2/ $\alpha$ -collagen-related protein; TrkB<sup>FL</sup> = full-length tropomyosin receptor tyrosine kinase B; Y = tyrosine residue

### 1.1.2 Trk receptor-mediated activation of ion channels

The neurotrophic factor BDNF influences the frequency and amplitude of synaptic currents (Lohof et al. 1993, Kang & Schuman 1995, Korte et al. 1995, Levine et al. 1995, Chao 2003). These findings indicate a link between neurotrophin-receptor signalling and ion channel function. Li et al. found that 30 seconds after a brief application of BDNF, pontine neurons show a PLC $\gamma$ /IP $_3$ -dependent, non-selective cation current (Li et al. 1999). This ion current was mediated by the non-voltage-gated, store operated cation channel transient receptor potential (Trp) C3 (Li et al. 2010). TrpC3 belongs to the Trp ion channel superfamily (Montell et al. 2002). These channels are generally activated through signalling pathways in contrast to voltage activation (Clapham 2003). TrpC5 regulates neurite growth and growth cone morphology in hippocampal neurons (Greka et al. 2003) and is highly expressed in motoneurons, where Trk receptors are found (Jablonka et al. 2007). TrpC3 contributes to BDNF-mediated survival and growth cone guidance in cerebellar granule neurons (Li et al. 2005). Co-expression analysis showed that activation of TrkB and PLC $\gamma$  leads to an IP $_3$ -dependent, store-operated influx of Ca $^{2+}$  and Na $^+$  through TrpC3, indicating that ion channels are closely associated with receptor tyrosine kinases (Figure 4A) (Li et al. 1999, Chao 2003, Blum & Konnerth 2005). Moreover, the interplay between neurotrophins and Trp channels might be involved in synaptic transmission by altering membrane potentials, which in turn facilitate synaptic Ca $^{2+}$  entry through *N*-methyl-D-aspartate (NMDA) glutamate receptors or voltage-gated channels (Li et al. 1999, Blum & Konnerth 2005). There is good evidence that BDNF regulates ionotropic glutamate receptors at synapses as well. BDNF treatment causes increased tyrosine phosphorylation of NMDA receptors and voltage-gated potassium channels (Levine et al. 1995, Lin et al. 1998, Tucker & Fadool 2002). Phosphorylation of the NMDA receptor subunits NR1 (Suen et al. 1997) and NR2B (Lin et al. 1998) by BDNF/TrkB increases the open probability of NMDA receptors (Levine et al. 1998) and is mediated by a direct interaction between TrkB and NMDAR through the non-receptor Src family tyrosine kinase Fyn (Figure 4B). Thereby, TrkB and the NMDAR are members of the same protein complex, as verified by co-immunoprecipitation of TrkB and the NR2B subunit (Mizuno et al. 2003). These data identified a postsynaptic signalling cascade that is likely to contribute to hippocampal spatial memory formation (Minichiello 2009, Park & Poo 2013).

Another line of evidence suggests fast effects of the neurotrophin BDNF on non-NMDA receptors. Electrophysiological measurements in sensory relay neurons showed that BDNF can block postsynaptic  $\alpha$ -amino-3-hydroxy-5-methyl-4-isoxazole propionic acid (AMPA) receptor-mediated currents (Balkowiec et al. 2000). The catalytic activity of TrkB receptors is required for the decrease in AMPA receptor activity, implying a close association between TrkB and AMPA receptors (Chao 2003). On the other hand, the exo- and endocytosis of

AMPA receptors (Carroll *et al.* 2001) determine activity-dependent changes of synaptic efficacy and are influenced by BDNF signalling (Chao 2003). Furthermore, an interaction between TrkB and the voltage-gated sodium channel  $\text{Na}_v1.9$  was described (Blum *et al.* 2002). This interaction is part of this thesis and will be present later under "1.4.2 BDNF - TrkB -  $\text{Na}_v1.9$ ".

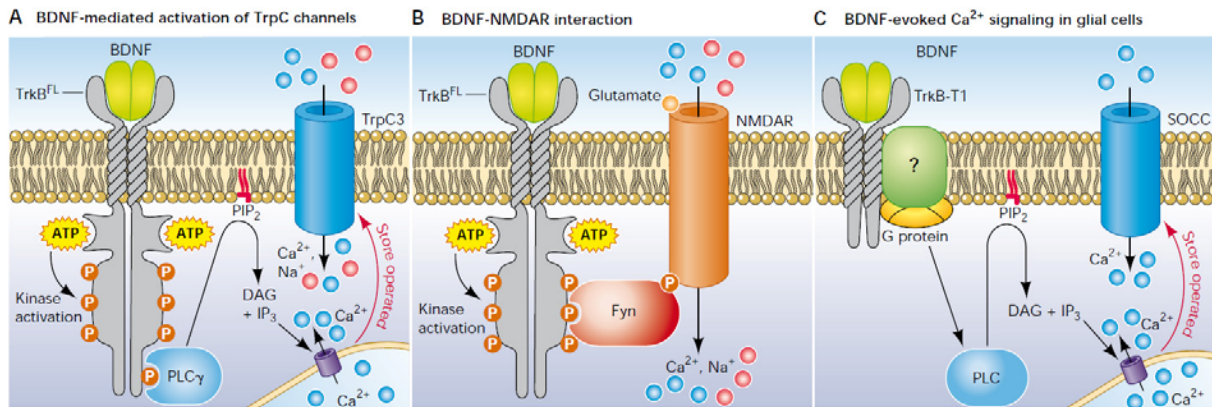


**Figure 4: BDNF/TrkB-mediated activation of ion channels**

(A)  $\text{TrkB}^{\text{FL}}$ /PLC $\gamma$ -mediated,  $\text{IP}_3$ -dependent  $\text{Ca}^{2+}$  store depletion activates ion influx through TrpC3. (B)  $\text{TrkB}^{\text{FL}}$ -dependent phosphorylation activates Fyn kinase that increases the open probability of postsynaptic NMDARs. (C) Truncated TrkB-T1 mediates G protein-dependent PLC activation,  $\text{IP}_3$ -dependent  $\text{Ca}^{2+}$  release from  $\text{Ca}^{2+}$  stores, and following activation of store-operated ion channels. (modified from (Blum & Konnerth 2005)) ATP = adenosine triphosphate; BDNF = brain-derived neurotrophic factor; DAG = diacylglycerol; Fyn = FYN oncogene related to SRC, FGR, YES;  $\text{IP}_3$  = inositol 1,4,5-trisphosphate; NMDAR = *N*-methyl-D-aspartate receptor; P = phosphorylation;  $\text{PIP}_2$  = phosphatidylinositol 4,5-bisphosphate; PLC = phospholipase C; Trk = tropomyosin receptor kinase; TrpC = transient receptor potential C; SOCC = store-operated calcium channels

Beside full-length TrkB receptors, truncated splice variants of TrkB also regulate signalling pathways and modulate ion channel functions. In glial cells the truncated TrkB receptor T1 is the predominant Trk receptor version and BDNF binding to TrkB-T1 can induce PLC/ $\text{IP}_3$ -dependent release of  $\text{Ca}^{2+}$  from intracellular stores, followed by  $\text{Ca}^{2+}$  entry through store-operated  $\text{Ca}^{2+}$  channels (Figure 4C) (Rose *et al.* 2003, Blum & Konnerth 2005). Glial cells are thought to be potent modulators of synaptic function, a model called the tripartite synapse concept (Araque & Perea 2004, Christensen *et al.* 2013). BDNF may act as a mediator between neurons and glial cells, thus acting as a modulator of neuronal activity (Bezzi & Volterra 2001, Reichardt 2003, Rose *et al.* 2003, Blum & Konnerth 2005).

### 1.1.3 Transactivation of Trk receptors

Many transmembrane receptors (Linseman *et al.* 1995, Daub *et al.* 1996, Luttrell *et al.* 1999) as well as Trk receptors can be activated in absence of their principal binding ligands through transactivation by G protein-coupled receptors and other receptor tyrosine kinases (Lee & Chao 2001, Lee *et al.* 2002, Huang & Reichardt 2003, Puehringer *et al.* 2013). A potent inducer of Trk transactivation is adenosine. This neuromodulator can initiate Trk receptor

autophosphorylation in PC12 cells and hippocampal neurons through the adenosine 2A ( $A_{2A}$ ) receptor (Lee & Chao 2001). The increased Trk activity may be inhibited by protein kinase inhibitors, such as PP1 (specific for Src family members) or K-252a. Another neuropeptide, the pituitary adenylate cyclaseactivating polypeptide (PACAP) is able to transactivate Trk receptors as well by interaction of PACAP with the PAC1 receptor (Lee et al. 2002). Adenosine and PACAP require a long period of time (hours, not minutes) to activate Trk tyrosine kinase activity. Both ligands produce an activation of the PI3K/Akt cascade, resulting in enhanced cell survival (Lee & Chao 2001, Lee et al. 2002). These results offer an explanation for the neuroprotective actions of adenosine and PACAP, and point to a therapeutic use for small-molecule GPCR agonists in neurodegenerative disorders (Chao 2003). This neuroprotective action was further demonstrated by (Wiese et al. 2007), who showed that a well established  $A_{2A}$  receptor agonist, CGS21680, is able to rescue motoneurons from cell death. This survival effect was caused by transactivation of TrkB and included an increase in Akt activity in motoneurons (Wiese et al. 2007). Unexpected was that the majority of transactivated Trk receptors resided in intracellular membranes, where the transactivation process may occur (Rajagopal et al. 2004, Rajagopal & Chao 2006, Wiese et al. 2007). In a recent study, it was shown that TrkB and TrkC of embryonic mouse cortical precursor cells are transactivated within minutes by epidermal growth factor receptor (EGFR) signalling (Puehringer et al. 2013). This transactivation procedure was shown to regulate the migration of early neuronal cells to their final position in the developing cortex. Transactivation by EGF leads to the membrane translocation of TrkB, hence promoting its signalling responsiveness to its natural ligand BDNF (Puehringer et al. 2013).

## 1.2 The motoneuron disease spinal muscular atrophy (SMA)

Neurological disorders that are caused by selective cell death of motoneurons are defined as motoneuron diseases (MND). Two major forms of motoneuron disease are amyotrophic lateral sclerosis (ALS) and proximal spinal muscular atrophy (SMA) (Kariya et al. 2012). While incidence of ALS peaks in the sixth decade of life (Kwiatkowski et al. 2009), proximal spinal muscular atrophy is a classical autosomal recessive disorder that is the most predominant form of motoneuron disease in children and young adults (Crawford & Pardo 1996, Sendtner 2010). Based on the clinical severity and age at onset, childhood SMA has been subdivided into three types: Type I SMA as the most severe form with a disease onset before 6 months and death occurring by the age of 2 years, Type II SMA as intermediate in severity with an onset before 18 months of age and patients never gaining the ability to walk and Type III SMA as the mildest form with onset after 18 months and patients that are able to walk (Monani et al. 2000). One type with adult onset, developing the first clinical symptoms

after the age of 30 (Type IV SMA), and very severe cases with prenatal onset and early neonatal death (Type 0 SMA) are further classified (Pearn et al. 1978, Dubowitz 1999, Briese et al. 2005). Spinal muscular atrophy is caused by insufficient levels of the survival motor neuron (SMN) protein leading to muscle paralysis and respiratory failure (Michaud et al. 2010). The loss of SMN protein correlates with the severity of the SMA disease. The most severe form of SMA (Type I) expresses less SMN protein than the milder forms (Type II and III) (Lefebvre et al. 1995, Coover et al. 1997, Burlet et al. 1998). The SMN gene exists in two copies, termed SMN1 and SMN2, on human chromosome 5q13 (Lefebvre et al. 1995, Jablonka et al. 2002, Jablonka et al. 2006). Whereas the SMN1 gene allows expression of the functional full-length protein, the major product of SMN2 is differentially spliced, thus lacking a specific exon (exon 7) (Lorson et al. 1999, Jablonka et al. 2002). Only the homozygous absence of SMN1 is responsible for spinal muscular atrophy, whereas homozygous absence of SMN2, found in about 5% of controls, has no clinical phenotype (Wirth 2000, Jablonka et al. 2002). The SMN protein is ubiquitously expressed and is localized to nuclear complexes known as Gemini or coiled bodies (Gems), which are involved in small nuclear ribonucleoprotein processing and recycling (Burghes & Beattie 2009, Sendtner 2010). In motoneurons the SMN protein is also found at relatively high quantities in the cytoplasm of the cell bodies, in axons and in axon terminals (Rossoll et al. 2002, Sendtner 2010).

To mimic the disease situation in a model organism, transgenic mice were created that express two copies of human SMN2 gene and these mice were mated onto a *Smn*<sup>-/-</sup> background (Monani et al. 2000). *Smn*<sup>-/-</sup>-SMN2tg mice normally die within 5 days after birth, but isolated motoneurons from these mice survive normal and show defects in axonal growth and growth cone morphology (Rossoll et al. 2003). Interestingly, reduced axon elongation of *Smn*-deficient motoneurons correlates with reduced numbers of spontaneous Ca<sup>2+</sup> transients in axons and axonal growth cones (Figure 5) (Jablonka et al. 2007). Several lines of evidence support the view that disturbed neuromuscular endplate development and function is responsible for abnormalities in synaptic transmission, hence causing muscle weakness in SMA patients (Chan et al. 2003, Monani 2005, Jablonka et al. 2007, McGovern et al. 2008, Kong et al. 2009, Murray et al. 2010, Sendtner 2010). SMN protein is able to form a complex with heterogeneous nuclear ribonucleoprotein (hnRNP) R (Rossoll et al. 2002), that can associate with the 3' untranslated region (UTR) of the  $\beta$ -actin mRNA and supports its transport into axons and growth cones of motoneurons (Rossoll et al. 2002, Rossoll et al. 2003). A reduced number of  $\beta$ -actin mRNA and locally synthesised  $\beta$ -actin protein molecules was found in distal parts of the axon and in the growth cone of *Smn*-deficient motoneurons (Rossoll et al. 2003, Rathod et al. 2012). This cytoskeletal defects in growth cones of *Smn*<sup>-/-</sup>-SMN2tg motoneurons cause defects in cell-surface clustering of the N-type calcium channel

Ca<sub>v</sub>2.2. As a consequence, local voltage-dependent calcium ion influx is reduced (Figure 5) (Jablonka et al. 2007, Ruiz et al. 2010, Wetzel et al. 2013).

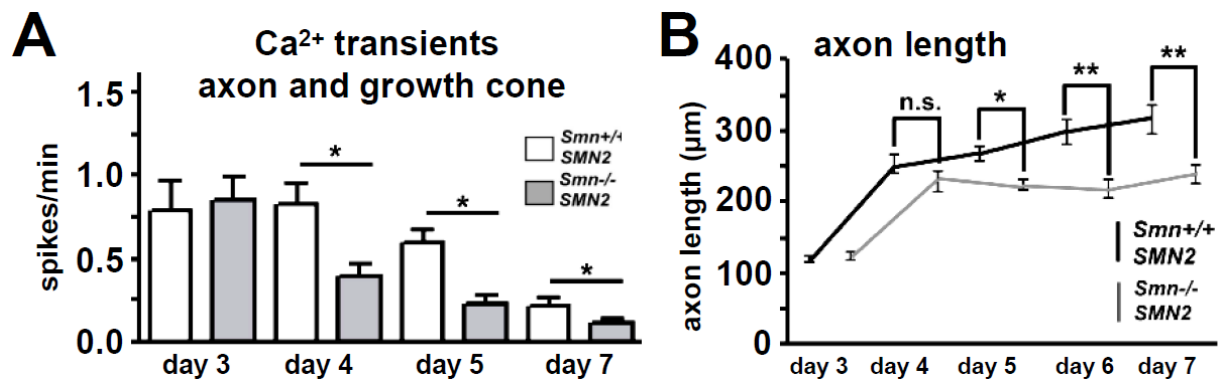


**Figure 5: Reduced Ca<sup>2+</sup> transients and axon length in Smn<sup>-/-</sup>-SMN2 motoneurons**  
**(A)** In axons and axonal growth cones of cultured embryonic motoneurons from Smn<sup>-/-</sup>-SMN2tg mice, spontaneous Ca<sup>2+</sup> transients are decreased compared to wild type motoneurons after four, five and seven days in culture. **(B)** Cultured motoneurons from Smn<sup>-/-</sup>-SMN2tg mice show significantly shorter axons compared to motoneurons from Smn<sup>+/+</sup>-SMN2tg mice after five, six and seven days *in vitro*. (modified from (Jablonka et al. 2007)) SMN = survival motor neuron

### 1.3 Spontaneous neuronal activity regulates axonal growth

Spontaneous activity is an evolutionary conserved process that plays an important role during development of the nervous system (O'Donovan & Landmesser 1987, Gu & Spitzer 1995, Spitzer et al. 2000, Hanson & Landmesser 2004, Spitzer 2006, Wang et al. 2009, Rosenberg & Spitzer 2011). It regulates developmental processes like proliferation of neural stem cells, migration of these neural precursors, neural differentiation and survival (Spitzer 2006). Furthermore, neurite outgrowth and the refinement of synaptic connections are involved (Spitzer 2006, Spitzer 2008, Vizard et al. 2008). In many cases the neuronal depolarization goes along with spontaneous influx of calcium ions into the neuronal cytosol. The analysis of molecular mechanisms underlying spontaneous calcium influx revealed two principle mechanisms of how neural activity is initiated. On the one hand, this excitability can be ligand-dependent and caused by the non-synaptic release of transmitters such as glutamate or  $\gamma$ -aminobutyric acid (GABA) (Milner & Landmesser 1999). On the other hand, excitability is part of a developmental program and consequently a cell-autonomous feature of a young neuron (Wetzel et al. 2013). Spontaneous Ca<sup>2+</sup> transients in embryonic motoneurons are either locally restricted to discrete domains in the entire cell, for example the growth cone, distal or proximal axons, or they are globally distributed over the whole cell (Jablonka et al. 2007, Subramanian et al. 2012). Furthermore, experiments in *Xenopus* spinal neurons characterized calcium transients as fast-rising global calcium spikes with characteristics of action potentials and slower wave like calcium transients, which are

generated in growth cones and are likely to regulate neurite extension (*Gu et al. 1994, Gomez & Spitzer 1999*).

At early stages during development, embryonic motoneurons exhibit spontaneous activity, while they are growing over long distances to make synaptic connections with the skeletal muscle (*O'Donovan & Landmesser 1987, Nishimaru et al. 1996, Milner & Landmesser 1999, Ciccolini et al. 2003, Hanson & Landmesser 2003, Spitzer 2006*). When embryonic motoneurons from mice are cultured at low density, so that these cells do not form any synaptic contact with each other, spontaneous excitation is preserved and spontaneous  $\text{Ca}^{2+}$  transients are preferentially observed in axons and axonal growth cones (*Jablonka et al. 2007, Subramanian et al. 2012*). In motoneurons, this spontaneous activity contributes to axon growth and presynaptic differentiation (*Jablonka et al. 2007*). The spontaneous electrical activity is driven by voltage-gated ion channels that are present at presynaptic sites in motoneurons. For example the N-type calcium channel  $\text{Ca}_v2.2$  and the P/Q-type channel  $\text{Ca}_v2.1$  that normally require a strong depolarization for activation (*Catterall et al. 2005, Wetzel et al. 2013*). This activation presupposes a specific trigger molecule that has to be expressed in motoneurons, especially in axons and axonal growth cones, with a low activation threshold and a spontaneous opening at voltages close to the resting membrane potential (*Wetzel et al. 2013*).

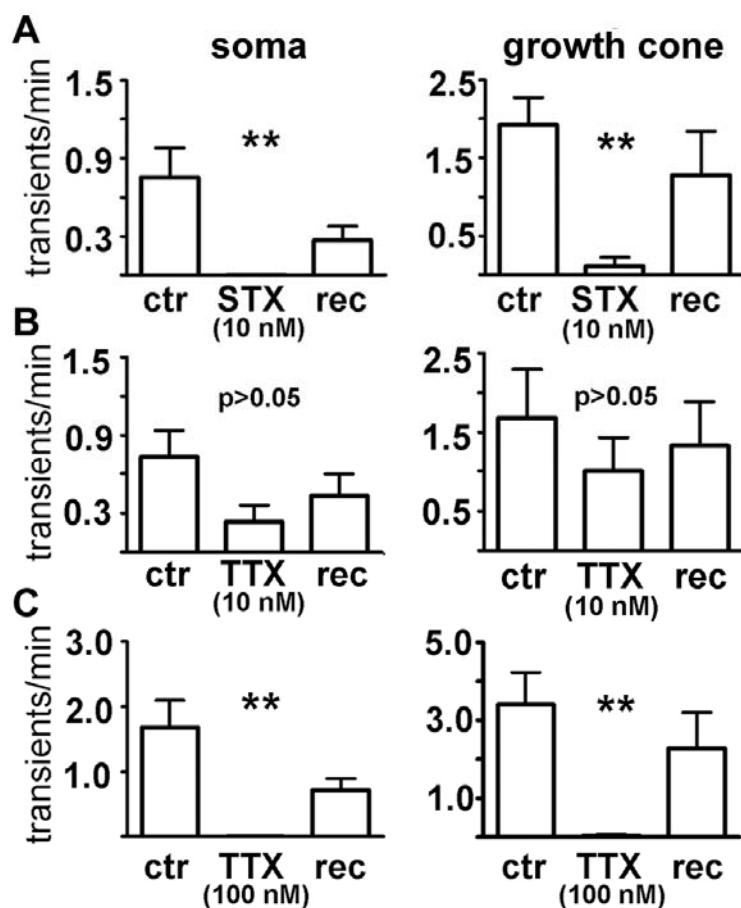


**Figure 6: VGSC pore blockers reduce spontaneous calcium transients in soma and growth cone of wild type motoneurons (A - C)** Live cell imaging analysis performed with wild type cultured motoneurons show that in soma and growth cones, spontaneous  $\text{Ca}^{2+}$  transients are reduced after perfusion with the voltage-gated sodium channel pore blockers saxitoxin and tetrodotoxin. STX (A) is more potent than TTX (B and C) and the blockage is reversible. (modified from (*Subramanian et al. 2012*)) ACSF = artificial cerebrospinal fluid; STX = saxitoxin; TTX = tetrodotoxin

In parallel to this dissertation, my colleagues observed that cultured embryonic motoneurons from wild type mice show a significantly reduced spontaneous calcium ion influx into the soma and axonal growth cone in presence of voltage-gated sodium channel pore blockers like saxitoxin (STX) and tetrodotoxin (TTX) (Figure 6) (Subramanian *et al.* 2012). Moreover, my colleagues found that the blockage of voltage-gated sodium channels caused a decreased axon growth of motoneurons which were cultured at low density for seven days *in vitro* (Figure 7) (Subramanian *et al.* 2012).

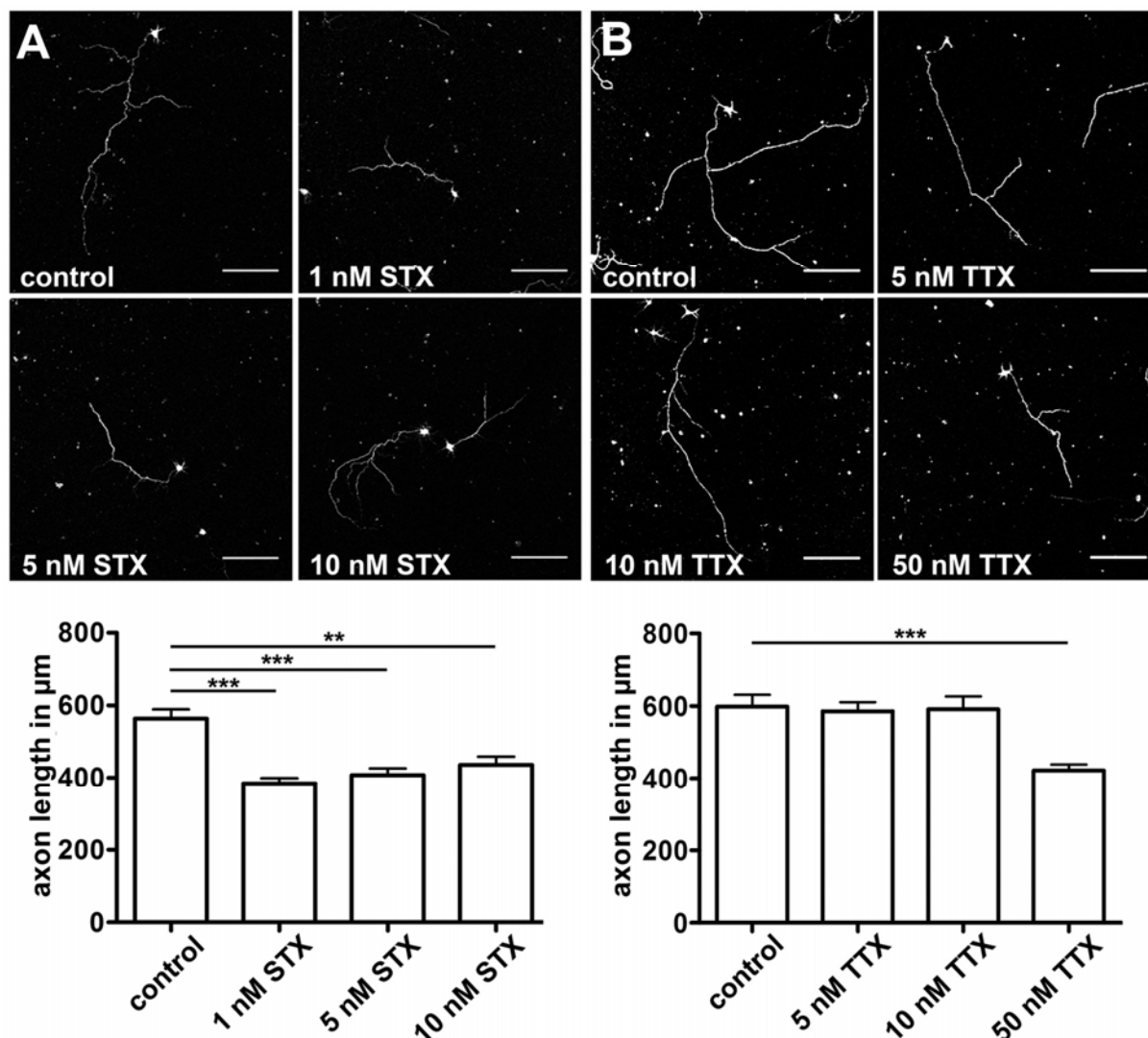


**Figure 7: VGSC pore blockers reduce axon growth of wild type motoneurons**

(A and B) Axon length of wild type, DIV 7 motoneurons is decreased after treatment with the voltage-gated sodium channel pore blockers: saxitoxin and tetrodotoxin. A significant reduction of axon elongation is observed in presence of 1, 5 and 10 nM of STX and 50 nM of TTX. STX is more potent than TTX. (modified from (Subramanian *et al.* 2012)) STX = saxitoxin; TTX = tetrodotoxin; VGSC = voltage-gated sodium channel



## 1.4 Voltage-gated sodium channels

The family of voltage-gated sodium channels (VGSC) comprises nine members, classified as  $\text{Na}_v1.1$  to  $\text{Na}_v1.9$  (Goldin *et al.* 2000). They are important for the initiation of action potentials in excitable cells and show similarities in structure and function. VGSCs are expressed with a pronounced tissue specificity and possess differences in their regulatory and pharmacological properties (Catterall 2000, Catterall *et al.* 2005, Catterall 2010, Catterall 2012).

Voltage-gated sodium channels consist of a pore-forming  $\alpha$  subunit of about 260 kDa and smaller  $\beta$  subunits, which are important for the kinetics and regulation of cell surface expression as well as for voltage dependence of the channel gating (Isom 2001, Patino & Isom 2010). An outline of the domain structure of voltage-gated sodium channels is presented in Figure 8.

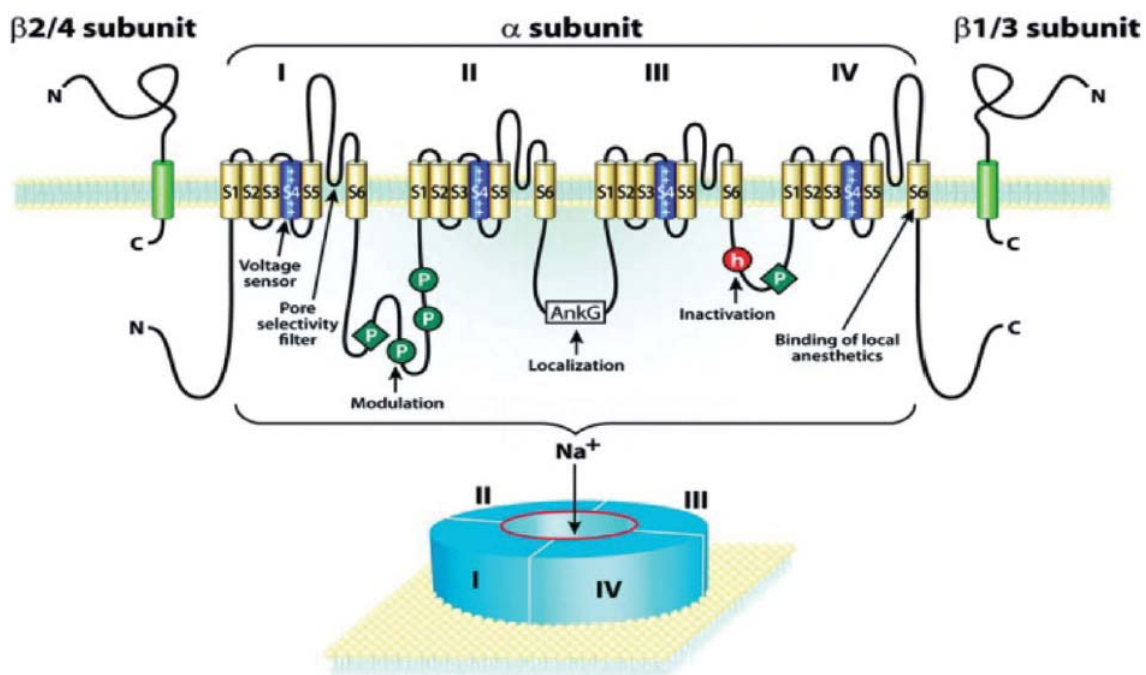


**Figure 8: Structure of voltage-gated sodium channels**

The  $\alpha$  subunit is organized in four homologous domains (I–IV), each with six  $\alpha$  helical transmembrane segments (S1–S6). The S4 segment of each domain plays an important role for the voltage sensitivity and gating and contains positive-charged amino acid residues at every third position. Depolarization of the membrane leads to a movement of the 4<sup>th</sup> segment outwards to initiate channel activation by conformational changes. The linker that connects S5 and S6 forms the external mouth of the channel pore and the selectivity filter. The cytoplasmic linker between domain III and IV acts as a “hinged lid” (h) and is responsible for fast inactivation. Residues in the inner cavity of the channel pore involving the S6 segment of domains I, III, and IV form the binding site for some local anesthetic, antiepileptic, and antiarrhythmic drugs. (from (Liu & Wood 2011)) P = phosphorylation

Pharmacological agents like neurotoxins and local anesthetics as well as related drugs have at least six distinct receptor sites on the  $\alpha$  subunits of VGSCs (Cestele & Catterall 2000, Stevens *et al.* 2011). Especially the neurotoxin tetrodotoxin (TTX) and the close relative saxitoxin (STX) played an important role in the early discovery and first analysis of sodium

channel proteins (Agnew *et al.* 1980, Noda *et al.* 1986, Heinemann *et al.* 1992). Both toxins use the same receptor binding site. The Na<sub>v</sub>1.9 channel exhibits an amino acid exchange from tyrosine or phenylalanine to serine at a critical position, leading to a more than 200-fold decrease in TTX affinity, whereas STX-sensitivity remains unaffected (Penzotti *et al.* 1998, Blum *et al.* 2002). Sodium channels are distinguishable by their affinity to TTX. Only the Na<sub>v</sub>1.5, which is described to be expressed in heart and the close relative Na<sub>v</sub>1.8 and Na<sub>v</sub>1.9 channel, known to be expressed predominantly in dorsal root ganglia are TTX-insensitive (Satin *et al.* 1992, Fozzard & Hanck 1996, Sivilotti *et al.* 1997, Catterall *et al.* 2005). Conservation of the TTX-resistant phenotype, and the proximity of the genes encoding Na<sub>v</sub>1.5, Na<sub>v</sub>1.8 and Na<sub>v</sub>1.9 on the same chromosome (Dib-Hajj *et al.* 1999), indicate that there is an evolutionary link between these three channels, but Na<sub>v</sub>1.9 is a voltage-gated sodium channel with unique properties (Dib-Hajj *et al.* 2002).

#### 1.4.1 The voltage-gated sodium channel Na<sub>v</sub>1.9

The discovery of the Na<sub>v</sub>1.9 channel, also known as NaN, occurred in 1998 using a PCR-based assay (Dib-Hajj *et al.* 1998). Na<sub>v</sub>1.9 exhibits all the hallmarks of voltage-gated sodium channels, including the inactivation tripeptide Ile-Phe-Met (West *et al.* 1992), multiple predicted phosphorylation sites in the intracellular loops, N-glycosylation sites in the extracellular linkers as well as sequences for the positively charged S4 and pore-lining SS1-SS2 segments at expected positions (Figure 8) (Dib-Hajj *et al.* 1998, Dib-Hajj *et al.* 2002). In humans, the Na<sub>v</sub>1.9 encoding gene *SCN11a*, maps to chromosome 3 (3p21–24), while in mice *Scn11a* is found in the analogous region on chromosome 9 (Dib-Hajj *et al.* 1999). It was demonstrated that Na<sub>v</sub>1.9 is preferentially expressed in small (<30 μm diameter) nociceptive neurons of the dorsal root ganglia and trigeminal ganglia (Dib-Hajj *et al.* 2002, Fang *et al.* 2002). In accordance with its predominant expression in nociceptive neurons, Na<sub>v</sub>1.9 is involved in nociception and even in pain transmission, at least in humans (Waxman *et al.* 1999, Fjell *et al.* 2000, Fang *et al.* 2002, Wood *et al.* 2004, Priest *et al.* 2005, Amaya *et al.* 2006, Ostman *et al.* 2008, Smith & Momin 2008, Dib-Hajj *et al.* 2010, Leo *et al.* 2010, Liu & Wood 2011, Leipold *et al.* 2013). Furthermore, Na<sub>v</sub>1.9 is expressed in myenteric neurons (Rugiero *et al.* 2003) and within free nerve terminals of the skin and the cornea (Dib-Hajj *et al.* 2002). No or only low expression levels of Na<sub>v</sub>1.9 were found in the central nervous system via quantitative RT-PCR and northern blot analysis (Dib-Hajj *et al.* 1998, Jeong *et al.* 2000, Ogata *et al.* 2000, Blum *et al.* 2002).

Na<sub>v</sub>1.9 has unique electrophysiological and pharmacological properties. The channel produces a persistent, TTX-resistant current with a substantial overlap of activation and steady-state inactivation, very slow activation and inactivation kinetics, as well as a negative threshold of activation close to normal resting potential (Cummins *et al.* 1999, Herzog *et al.*

2001, *Rugiero et al. 2003, Ostman et al. 2008*). Therefore,  $\text{Na}_v1.9$  is not a major contributor to the rapid depolarizing phase of the action potential, but regulates the electrogenic properties of nociceptor dorsal root ganglia and myenteric sensory neurons by modulating their resting potentials and by amplifying their responses to subthreshold stimuli (*Herzog et al. 2001, Rugiero et al. 2003, Waxman & Estacion 2008*). This characteristic is special for the  $\text{Na}_v1.9$  channel and gives him the ability to open spontaneously at resting membrane potentials. Studies focused on the role of inflammatory mediators that act through G protein-coupled receptors found that  $\text{Na}_v1.9$  contributes to the setting of inflammatory pain thresholds (*Baker et al. 2003, Rush & Waxman 2004, Ostman et al. 2008*). This model is supported by behavioral studies on  $\text{Na}_v1.9$  knock-out mice lines (*Priest et al. 2005, Amaya et al. 2006*). Interestingly, Blum et al. found that the neurotrophin BDNF can trigger the opening of  $\text{Na}_v1.9$  in central principle neurons via the activation of TrkB receptors (*Blum et al. 2002*). These findings proposed a ligand-gated channel opening of  $\text{Na}_v1.9$  (see 1.4.2). The idea that the  $\text{Na}_v1.9$  channel may be gated by ligand binding rather than by voltage in brain neurons adds further complexity to the functional characterization of  $\text{Na}_v1.9$ . Several studies have revealed that a better understanding of  $\text{Na}_v1.9$  is disabled by the lack of functional data on recombinant  $\text{Na}_v1.9$ , since it has been quite difficult to achieve robust heterologous expression levels of  $\text{Na}_v1.9$  in transfected cell lines (*Ostman et al. 2008, Smith & Momin 2008, Waxman & Estacion 2008*).

#### 1.4.2 BDNF - TrkB - $\text{Na}_v1.9$

In 1999, Kafitz et al. reported that local and transient applications of BDNF and NT-4/5 to various types of central neurons lead to a depolarization of these neurons within milliseconds, resulting in trains of action potentials (*Kafitz et al. 1999*). BDNF and NT-4/5 were much more effective than glutamate. The rapid neurotrophin-evoked depolarization is a result of an immediate activation of sodium channels, which are insensitive to the voltage-gated sodium channel pore blocker tetrodotoxin (*Kafitz et al. 1999, Catterall 2000, Blum & Konnerth 2005*). By screening candidate transcripts with an antisense mRNA expression, the  $\text{Na}_v1.9$  channel and receptor tyrosine kinase TrkB were identified as key components for this fast BDNF-induced sodium inward current (*Blum et al. 2002, Blum & Konnerth 2005*). Blum et al., 2002 demonstrated that stimulation of recombinant TrkB receptors by BDNF induces sodium ion influx through the co-expressed  $\text{Na}_v1.9$  channel in HEK 293 cells. Expression of either  $\text{Na}_v1.9$  or TrkB alone failed to reconstitute the BDNF-evoked sodium current, which was insensitive to tetrodotoxin, but highly sensitive to voltage-gated sodium channel pore blocker saxitoxin (*Catterall 2000, Blum et al. 2002, Blum & Konnerth 2005*). The gating mechanism of  $\text{Na}_v1.9$  via TrkB activation is still unknown and became controversial, because the kinetics of BDNF release conflict with the much faster activation kinetics of the  $\text{Na}_v1.9$ -

mediated currents (Brigadski et al. 2005, Minichiello 2009). Blum et al. suggested that there is a direct interaction between TrkB and  $\text{Na}_v1.9$  leading to BDNF-elicited depolarisation, which activates voltage-gated calcium channels (Figure 9), resulting in calcium ion influx (Blum et al. 2002, Blum & Konnerth 2005).

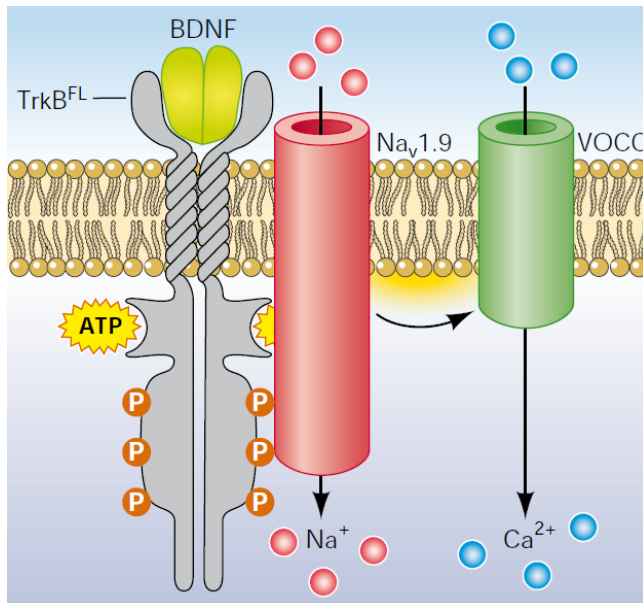


**Figure 9: BDNF/TrkB mediated rapid opening of  $\text{Na}_v1.9$**

Schematic model of the rapid opening of the sodium channel  $\text{Na}_v1.9$  (red) by activation through the binding of BDNF (light green) on TrkB (grey) with the subsequent dimerization and autophosphorylation of TrkB neurotrophic receptor. The resulting depolarization through the influx of sodium ions activates Voltage-operated calcium channels (VOCC) (green) and thus produces calcium ion influx. (modified from (Blum & Konnerth 2005)) BDNF = brain-derived neurotrophic factor; Trk = tropomyosin receptor kinase; VOCC = voltage-operated calcium channels

The existence of fast BDNF-induced currents have been reported only in a series of studies from the same group (Kafitz et al. 1999, Blum et al. 2002, Kovalchuk et al. 2002, Rose et al. 2003) and has only been confirmed indirectly by other studies (Cheng & Yeh 2003, Fujisawa et al. 2004, Kovalchuk et al. 2004, Blum & Konnerth 2005). Remarkably, the BDNF-mediated increase could only be blocked by the Trk kinase inhibitor K-252a, when cells were pre-incubated with the inhibitor for a longer time (Kafitz et al. 1999). These data imply that pre-phosphorylated TrkB receptors would be a structural prerequisite for the rapid activation of a TTX-insensitive sodium channel by BDNF (Blum & Konnerth 2005). The binding of BDNF and the subsequent dimerization of the “primed” receptors might then be sufficient for the gating of  $\text{Na}_v1.9$  (Figure 9) (Blum & Konnerth 2005). In 2007, Lang et al. provided strong evidence that developing hippocampal neurons intrinsically generate fast BDNF signalling in presence of TTX, which can be blocked by BDNF-specific antibodies or with K-252a (Lang et al. 2007). The onset kinetics of BDNF-evoked calcium transients were faster than 100 ms, suggesting that they are in the range of several tens of milliseconds or less (Lang et al. 2007). Thus, there is a lot of evidence that indeed  $\text{Na}_v1.9$  is a downstream mediator of fast neurotrophin action, however, it has not been tested yet whether fast excitation of neurons by BDNF is blocked in  $\text{Na}_v1.9$  knock-out mice.

## 1.5 Aims of the thesis

The aim of this thesis was to unravel regulators of spontaneous excitability in motoneurons. As outlined in the introduction, first experiments by my colleagues revealed that a blockage of voltage-gated sodium channels with STX and TTX leads to a reduced axonal elongation in young cultured motoneurons, indicating that a voltage-gated sodium channel is involved in spontaneous excitability of motoneurons. In these experiments, neurons were grown at very low density, so that these cells did not receive a synaptic input from each other. In addition, experiments by our group demonstrated that STX was more potent than TTX in blocking spontaneous excitation and activity-dependent axon growth of motoneurons.

These observations raised the question whether TTX-resistant voltage-gated sodium channels are responsible for the activity-dependent axon growth in motoneurons. Basing on these findings, the present study aimed to:

- support the molecular identification of a voltage-gated sodium channel involved in early motoneuron excitation and axon elongation.
- localize this sodium channel at the node of Ranvier, the principle site of action potential generation in axons of adult motoneurons.
- work out evidences how the here identified candidate is linked to the disease mechanism in spinal muscular atrophy.
- clarify whether there is a link between neurotrophin signalling and spontaneous excitability which regulates axon growth in motoneurons.

## 2 Material and Methods

### 2.1 Material

#### 2.1.1 Animals

All mice, except of *Scn11a*<sup>+L799P</sup> knock-in mice, were bred in the animal facility of the Institute for Clinical Neurobiology, University Hospital Würzburg. The animals (approximately 20 g) were housed three per cage (370 cm<sup>2</sup>) or 18 per cage (1829 cm<sup>2</sup>) in a colony room kept at 21 ± 1°C with humidity around 45 - 50%, and on a 12 h light-dark cycle. The mice had free access to food and water and in each standard polysulphone cage small autoclaved paper channels were available for environmental enrichment.

For the experiments C57BL/6J0laHsd mice (Harlan Laboratories, Germany, originated from Jackson Laboratory, Bar Harbor, Maine), Na<sub>v</sub>1.9<sup>-/-</sup> mice (*Ostman et al. 2008*) (kindly provided by John Wood, London), *Scn11a*<sup>+L799P</sup> mice (*Leipold et al. 2013*) (kindly provided by Ingo Kurth, Jena), *Smn*<sup>-/-</sup>-*SMN2tg* mice (*Monani et al. 2000*) and TrkB<sup>-/-</sup> mice (*Rohrer et al. 1999*) (Jackson Laboratory, Bar Harbor, Maine) were used.

The genotype of the transgenic mice was identified by PCR of tail DNA.

#### 2.1.2 Cell lines

In this study Human Embryonic Kidney (HEK 293T) cells were used to produce a stable Na<sub>v</sub>1.9 expressing cell line. These cells express the simian virus 40 (SV40) large T antigen, which enables to replicate plasmids carrying the SV40 origin (*Graham et al. 1977, Lebkowski et al. 1985*).

Furthermore, primary embryonic motoneurons were isolated from day 13.5 (14) embryos as described earlier (*Wiese et al. 2010*).

### 2.1.3 Chemicals for cell culture

**Table 1: Chemicals for cell culture**

DMEM = Dulbecco's modified eagle medium; DMSO = dimethyl sulfoxide; PBS = phosphate buffered saline; BSS = balanced salt solution; BDNF = brain-derived neurotrophic factor; CNTF = ciliary neurotrophic factor

substances	company; reference
B27 Supplement 50x	Invitrogen-Gibco; 17504-044
$\beta$ -mercaptoethanol	Sigma; M7154
Boric acid	Merck; 203667
DMEM high glucose, pyruvate, GlutaMax™	Invitrogen-Gibco; 31966-021
DMSO	Sigma; D8779
Dulbecco's PBS without Ca/Mg 1x	Invitrogen-Gibco; 14190-094
Fetal calf serum	Invitrogen-Gibco; 10270-106
Geneticin® selective antibiotic (G418 sulfate)	Invitrogen; 10131-027
GlutaMax	Invitrogen-Gibco; 35050-038
Hanks' BSS without Ca/Mg, with phenol red 1x	Invitrogen-Gibco; 14170-088
HEPES Pufferan, $\geq 99.5\%$ cell pure	Roth; HN77.4
Horse serum	Linaris; SHD3250ZK
Laminin	Invitrogen; 23017-015
Neurobasal® medium	Invitrogen-Gibco; 21103-049
Neurotrophic factors (BDNF and CNTF)	Institute for Clinical Neurobiology
Penicillin-streptomycin	Invitrogen; 15070-063
Pluronic® F-127	Invitrogen; P6867
Poly-DL-ornithine hydrobromide (PORN)	Sigma; P8638
Purified human merosin	Millipore; CC085
TrypLE™ Express	Invitrogen; 12605-028
Trypsin inhibitor	Sigma; T6522
Trypsin TRL3 1%	Worthington; LS003707
Water – Ampuwa® Aqua ad injectabilia	DeltaSelect; 8771004

## 2.1.4 Chemicals for DNA and RNA techniques

**Table 2: Chemicals for DNA and RNA techniques**

BSA = bovine serum albumin; ATP = adenosine triphosphate; CTP = cytidine triphosphate; GTP = guanosine triphosphate; TTP = thymidine triphosphate; DTT = dithiothreitol; DNA = deoxyribonucleic acid; HPLC = high performance liquid chromatography

substances	company; reference
Agarose	Biozym; 840004
Betaine 5 M	Sigma; 14300
BSA 100x	New England BioLabs; B9001
Chloroform	Sigma; 32211
dATP 100 mM	Fermentas; R0141
dCTP 100 mM	Fermentas; R0151
dGTP 100 mM	Fermentas; R0161
dTTP 100 mM	Fermentas; R0171
DTT 0.1 mM	Invitrogen; 90289
Ethanol absolute	Sigma; 32205
Ethidium bromide	Sigma; E1510
First strand buffer 5x	Invitrogen; Y00146
Formamide	Merck; 344205
Gene Ruler™ 100 bp DNA Ladder	Fermentas; SM0242
Gene Ruler™ 1 kb DNA Ladder	Fermentas; SM0311
HPLC water	Merck; 1153331000
MgCl <sub>2</sub> 25 mM	Roche; 11699113001
Primer, random pd(N) <sub>6</sub> 50 A <sub>260</sub> units	Roche; 11034731001
Proteinase K	Roche; 03115828001
RNasin® Plus RNase Inhibitor	Promega; N2611
SuperScript® III reverse transcriptase	Invitrogen; 18080-044
Taq buffer advanced 10x	5 Prime; 2201240
Taq DNA polymerase	5 Prime; 2200010



## 2.1.5 Chemicals for protein analysis

**Table 3: Chemicals for protein analysis**

BSA = bovine serum albumin; ECL = enhanced chemiluminescence; NaF = sodium fluoride; PVDF = polyvinylidene difluoride; SDS = sodium dodecyl sulfate

substances	company; reference
Aqua polymount	Polyscience; 18606
BSA	Sigma; A2153
Criterion XT Precast gel 3-8% Tris-Acetate	BioRad; 345-0129
ECL Prime Western Blotting Detection Reagent	GE Healthcare; RPN2232
Goat serum	Linaris; SGA3511KYA
High performance chemiluminescence Hyperfilm™	GE Healthcare; 28906836
Immuno-Blot PVDF membrane	BioRad; 162-0177
Methanol	Sigma; 32213
NaF	Sigma; S6776
Na-orthovanadate	Sigma; S6508
Na-pyrophosphate	Sigma; 221368
Nonidet P40 Substitute	Fluka Analytical; 74385
Powdered milk	Roth; T145.3
Precision Plus Protein™ All Blue Standards	BioRad; 161-0373
Roti®-Liquid Barrier Marker	Roth; AN92.1
SDS	BioRad; 161-0418
Tablet of complete Mini EDTA-free	Roche; 04693159001
Tissue-Tek® O.C.T™ Compound	Sakura; 4583
Triton X-100	Sigma; T8787
Tween 20	Sigma; P7949

## 2.1.6 Buffers, media and solutions

**Table 4: Buffers, media and solutions**

ACSF = artificial cerebrospinal fluid; DNA = deoxyribonucleic acid; BSA = bovine serum albumin; HEK = human embryonic kidney; PBS = phosphate buffered saline; PFA = paraformaldehyde; PORN = poly-DL-ornithine hydrobromide; TAE = Tris acetate EDTA; TBE = Tris borate EDTA; TBS = Tris buffered saline; EDTA = ethylenediaminetetraacetic acid; SDS = sodium dodecyl sulphate; DMEM = Dulbecco's modified eagle medium; HBSS = Hanks' balanced salt solution

name	composition
ACSF ringer solution	127 mM NaCl; 3 mM KCl; 2.5 mM NaH <sub>2</sub> PO <sub>4</sub> ; 2 mM CaCl <sub>2</sub> ; 2 mM MgCl <sub>2</sub> ; 23 mM NaHCO <sub>3</sub> ; 25 mM D-glucose  pH adjustment with CO <sub>2</sub>
Basic protein lysis buffer	150 mM NaCl; 10% glycerol; 50 mM HEPES pH 7.4  sterile filtered
Blocking solution for immunocytochemistry	1x PBS; 10% horse serum; 0.1% Tween 20; 0.3% Triton X-100
Blocking solution for protein detection after western blot	1x TBS-T; 5% powdered milk; 5% goat serum
Borate solution	150 mM boric acid dissolved in cell culture grade water  pH adjustment to pH 8.35 with NaOH, sterile filtered
Depolarization solution	30 mM KCl; 0.8% NaCl; 2 mM CaCl  sterile filtered
DNA loading buffer 6x (10 ml)	6 ml 50% glycerol; 1 ml 2% bromophenol blue; 1 ml 2% xylene cyanol solution; 2 ml H <sub>2</sub> O dest.
DNA lysis buffer	10 mM Tris pH 7.5; 100 mM EDTA pH 8.0; 150 mM NaCl; 0.5% SDS
EB-BSA	1 mg/ml BSA diluted in 10 mM Tris pH 8.0
Electrophoresis buffer 10x (1 l)	30.3 g Tris base; 144 g glycine; 10 g SDS  pH adjustment to 8.45
HEK 293T cell culture medium	DMEM with GlutaMax™; 10% FCS; 1% penicillin-streptomycin, 500 µg/ml geneticin
Laminin 2.5 µg/ml	21 µl aliquots diluted in 6 ml HBSS
Motoneuron complete medium	Neurobasal® medium; 2% horse serum; 1x GlutaMax™; 1x B27 supplement; 10 nM β-mercaptoethanol  sterile filtered

PBS 10x (1 l)	80 g NaCl; 2 g KCl; 2.4 g KH <sub>2</sub> PO <sub>4</sub> ; 14.4 g Na <sub>2</sub> HPO <sub>4</sub> ; H <sub>2</sub> O bidest.  autoclaved
PFA 4% (100 ml)	4 g paraformaldehyde dissolved in 50 ml H <sub>2</sub> O at 60°C; few drops of 2 M NaOH, filtered; 45 ml 0.2 M Na <sub>2</sub> HPO <sub>4</sub> ; 5 ml 0.2 M NaH <sub>2</sub> PO <sub>4</sub>  pH adjustment with to 7.4
PORN 0.5 mg/ml	Diluted in 150 mM borate solution pH 8.35
Sample buffer 4x (20 ml) (Laemmli)	4 ml 1M Tris HCl pH 6.8; 8 ml 20% SDS; 5 ml glycerol; 1.6 ml β-mercaptoethanol; 50 mg bromophenol blue; 1.4 ml H <sub>2</sub> O dest.
TAE 50x (1 l)	242 g Tris base; 57.1 ml glacial acetic acid, 100 ml 0.5 M EDTA; H <sub>2</sub> O dest.
TBE 10x	108 g/l Tris base; 55 g/l boric acid; 40 ml 0.5 M EDTA pH 8.0  pH adjustment to 8.4
TBS 10x (1 l)	12.1 g Tris base; 87.8 g NaCl  pH adjustment with 5 N HCl to pH 8.0
TBS-T	1x TBS; 0.2% Tween 20
Transfer buffer	1x electrophoresis buffer; 20% methanol
Trypsin 1%	1 g trypsin diluted in 100 ml HBSS
Trypsin inhibitor 1%	1 g trypsin inhibitor diluted in 98 ml HBSS and 2 ml of 1 M HEPES pH 7,4
Washing solution for immunocytochemistry	1x PBS; 0.1% Tween 20; 0.1% Triton X-100

## 2.1.7 Antibodies and labelling dyes

**Table 5: Primary antibodies**

Caspr = contactin-associated protein; NFL = neurofilament; Trk = tropomyosin receptor kinase

name	host	dilution	reference
mNa <sub>v</sub> 1.9 (71n)	Rabbit	IF-1:400, WB-1:1000	By PD Dr. R. Blum
panNa <sub>v</sub>	Mouse	IF-1:500	Sigma, S8809

NFL	Chicken	IF-1:10000	Millipore; AB5539
$\alpha$ -Tubulin	Mouse	IF-1:2000	Sigma, T5168
Caspr	Mouse	IF-1:300	Biocompare; 75-001
TrkB	Rabbit	IF-1:400	Millipore; 07-225
Trk	Rabbit	WB-1:1000	Santa Cruz; Sc-11
p75 <sup>NTR</sup>	Mouse	Panning: 15 ng/ml	Prof. R. Rush, Flinders University, Australia

**Table 6: Secondary antibodies and labelling dyes**

DAPI = 4', 6-diamidino-2-phenylindole; HRP = horseradish peroxidase

name	host	dilution	reference
mouse IgG affi-pure (H+L) Alexa 488	Goat	IF-1:800	Invitrogen; A11029
mouse IgG (H+L) DyLight 488	Goat	IF-1:800	Jackson Immuno; 115-485-146
rabbit IgG affi-pure (H+L) Alexa 488	Donkey	IF-1:800	Jackson Immuno; 711-545-152
rabbit IgG affi-pure (H+L) DyLight 488	Donkey	IF-1:800	Jackson Immuno; 711-485-152
mouse IgG affi-pure (H+L) Cy3	Goat	IF-1:800	Jackson Immuno; 115-165-146
rabbit IgG affi-pure (H+L) Cy3	Donkey	IF-1:800	Jackson Immuno; 711-165-152
chicken IgG affi-pure (H+L) DyLight 649	Donkey	IF-1:800	Jackson Immuno; 703-495-155
mouse IgG affi-pure (H+L) Cy5	Donkey	IF-1:600	Jackson Immuno; 715-175-150
rabbit IgG Atto647N	Goat	IF-1:100	Sigma; 40839
rabbit IgG affi-pure (H+L) HRP	Goat	WB-1:10000	Jackson Immuno; 111-035-003
Alexa Fluor® 546 phalloidin	-	IF-1:100	Invitogen, A22283
Alexa Fluor® 633 phalloidin	-	IF-1:100	Invitogen, A22284
DAPI	-	IF-1:5000	Sigma, D9542
Oregon Green 488 BAPTA-1, AM	-	5 $\mu$ M	Invitogen; O-6807

### 2.1.8 Plasmids and primers

**Table 7: Plasmids**

VSVG = glycoproteins of vesicular stomatitis virus

name	description	reference
719-pLVX1-ROP-mNav1-9	mouse Na <sub>v</sub> 1.9 expression vector	cloned by Steven Havlicek and PD Dr. Robert Blum
pMD.G VSVG	helper plasmids for the packaging of lentiviral particles	Addgene (Dull et al. 1998, Zufferey et al. 1998)
pRSV-REV		
pMDLg/pRRE		
pCMVΔR8.91		

**Table 8: Primers for genotyping**

KO = knock-out; SMN = survival motor neuron; tg = transgene; Trk = tropomyosin receptor kinase; wt = wild type

name	sequence	mouse line
Na <sub>v</sub> 1.9_antisense	5'-AACAGTCTTACGCTGTTCCGATG-3'	Na <sub>v</sub> 1.9 KO
Na <sub>v</sub> 1.9_sense	5-ATGTGGCACTGGGCTTGAAGTC-3	
neomycin gene	5-CTCGTCGTGACCCATGGCGAT-3	
sense	5-CTGGAATTCAATATGCTAGACTGGCCTG-3	Smn <sup>-/-</sup> -SMN2tg
KO primer	5-GATGTGCTGCAAGGCGATTAAGTTG-3	
wt primer 1049r	5-CAACTTTCCACTGTTTCAAGGGAGTTG-3	
trkb-n2	5'-ATGTCGCCCTGGCTGAAGTG-3'	Ntrk-2-ROHR
trkb-c8	5'-ACTGACATCCGTAAGCCAGT-3'	
pgk3-1	5'-GGTTCTAAGTACTGTGGTTTCC-3'	

**Table 9: Primers for cDNA amplification**

GAPDH = glyceraldehyde 3-phosphate dehydrogenase

name	sequence	PCR targets
712-for	5'-TTCACCGCCATCTACACCT-3'	mNa <sub>v</sub> 1.5 (NM_021544)
855-rev	5'-GAGCCGACAAATTGCCTAGC-3'	

2541-for	5'-CATTCCCTTCCTCGTCGTC-3'	mNa <sub>v</sub> 1.8 (NM_009134)
2676-rev	5'-AAAGCGATGAATAGGTTGAG-3'	
1992-for	5'-CCCTTGTGAGTCTCGCTGAC-3'	mNa <sub>v</sub> 1.9 (AF118044)
2114-rev	5'-GGAGTGGCCGATGATCTTAAT-3'	
2318U17-for	5'-GGGGAGTGGATCGAGAA-3'	Na <sub>v</sub> 1.9 <sup>L799P</sup> (NM_011887+LP)
2448L16-rev	5'-TTGCTGAAGGAATTGG-3'	
205-for	5'-GCAAATTCAACGGCACA-3'	GAPDH (NM_008084)
337-rev	5'-CACCAGTAGACTCCACGAC-3'	

### 2.1.9 Commercial kits

**Table 10: Commercial kits**

BCA = bicinchoninic acid

name	reference
LightCycler® FastStart DNA Master SYBR Green I	Roche; 12239264001
Pierce BCA Protein Assay Kit	Thermo Scientific; 23225
RNeasy Mini Kit	QIAGEN; 74104

### 2.1.10 Software

**Table 11: Software**

name	reference
ApE- A plasmid Editor v2.0.36	2003-2009 by M. Wayne Davis
BZ observation application	2007-2011 KEYENCE Corporation
GraphPad Prism 4.02	1992-2004 GraphPad Software, Inc., San Diego, California, USA
ImageJ 1.42i	Wayne Rasband, National Institutes of Health, USA, <a href="http://rsb.info.nih.gov/ij">http://rsb.info.nih.gov/ij</a> , Java 1.6.0_10-rc (32-bit) 1686K of 1500MB (<1%)
LAS AF Lite 2.2.1 build 4842	2005-2009 Leica Microsystems CMS GmbH
Microsoft Office 2003	1985-2003 Microsoft Corporation

---

Oligo 6.71	1989-2005 Wojciech Rychlik; Molecular Biology Insights, Inc., 8685 U.S. Highway 24 West Cascade, CO 80809, USA
OriginPro 9.0.0G	1991-2012 OriginLab Corporation, One Roundhouse Plaza Northampton, MA 01060 USA
Photoshop CS5	Adobe Systems, San Jose, CA, USA
StreamPix 4	NORPIX Digital Video Recording Software

## 2.2 Methods

### 2.2.1 Cell culture

#### 2.2.1.1 HEK 293T cells

HEK 293T cells were cultured in DMEM with GlutaMax, 10% heat-inactivated fetal calf serum (FCS), 1% penicillin-streptomycin and 500 µg/ml geneticin at 37°C and 5% CO<sub>2</sub> in a standard cell culture incubator. Confluent cells were washed two times with 1x PBS and detached with a 10% dilution of TrypLE Express in 1x PBS. After cell detachment trypsinization was stopped by addition of culture medium. A centrifugation step removed TrypLE Express solution and a defined part of the cell solution was transferred into a new cell culture flask with fresh culture medium.

For experiments cells were cultivated on 0.5 mg/ml Poly-DL-ornithine hydrobromide (PORN) coated cover glasses or cell culture dishes. PORN coating of cover glasses and dishes occurred over night at 4°C. Coated material was three times washed with HBSS before cells were plated at appropriate densities.

#### 2.2.1.2 Embryonic motoneurons

The isolation of primary embryonic motoneurons from spinal cord was performed according to the protocol described by Wiese et al. (2010). The lumbar spinal cord was dissected from day 14 embryos. Dorsal root ganglia were removed from spinal cord by displacing the ensheathing meninges and the spinal cord was stored in 180 µl of HBSS and kept on ice. Afterwards the tissue was trypsinized by addition of 20 µl of 1% Trypsin and incubation for 15 minutes at 37°C. Addition of 20 µl of 1% Trypsin inhibitor stopped the trypsinization process and gently trituration solved the cell aggregates completely. For enrichment of motoneurons, cells were transferred to a 24-well plate which was coated with p75<sup>NTR</sup> antibody (1.8 mg/ml) and washed three times with neurobasal medium containing GlutaMax. After incubation at room temperature for 45 minutes, the panning plate was gently washed for three times with pre-warmed neurobasal medium containing GlutaMax to remove p75<sup>NTR</sup> negative cells. To dissolve and collect the motoneurons from the panning plate, 150 µl of depolarization solution and 30 seconds later 450 µl of motoneuron complete medium were added. The cell solution was transferred into a 15 ml falcon tube and centrifuged for four minutes at 400 x g. Cells were resuspended in motoneuron complete medium and plated on PORN and laminin coated 10 mm cover glasses at a density of 1000 - 2000 cells/cover glass. Approximately 45 minutes later when cells have attached, they were fed with motoneuron complete medium



containing the neurotrophic factors BDNF and CNTF (both at 5 ng/ml). One day after motoneuron isolation and then every second day 40% of the medium were replaced.

## 2.2.2 DNA and RNA techniques

### 2.2.2.1 Isolation of DNA

Mouse tail biopsies of three-week-old mice or head biopsies of day 14 embryos were dispersed in 500 µl DNA lysis buffer with 20 µl of 20 mg/ml proteinase K at 60°C in a shaker at 550 rpm for over night. Next, 300 µl of 5% SDS and 120 µl of 3 M NaCl were added to each reaction tube. The samples were mixed until the solutions were uniform and viscous. After addition of 750 µl chloroform, samples were mixed again until the solution became homogenous. A 10 minutes centrifugation step followed at 4°C and 14 000 rpm. The upper phase of each sample was transferred to a new reaction tube and chloroform clearance was repeated until the phase became completely clear. Next, 1 ml of 100% ethanol was added to the supernatant and tubes were mixed carefully until a white DNA precipitate became visible. After 10 minutes centrifugation at 4°C and 14 000 rpm, the DNA pellet was washed with 70% ethanol. The supernatant was taken off and the pellet was dried on air for almost five minutes. DNA was resolved in 100 µl of 10 mM Tris pH 8.0 and stored at 4°C.

### 2.2.2.2 Isolation of RNA

Isolation of total RNA from spinal cord tissue, dorsal root ganglia tissue or cultured primary motoneurons was performed by using the RNeasy Mini Kit from QIAGEN, according to the manufactures' protocol. Briefly, frozen tissue was solved in RLT Plus buffer and homogenized using an autoclaved Silent Crusher S (Heidolph). After centrifugation the supernatant was transferred to a genomic DNA Eliminator spin column placed in a 2 ml collection tube. After a centrifugation step, a defined volume of 70% ethanol was added to the flow-through. The sample was mixed and 700 µl were transferred to a RNeasy spin column. After the next centrifugation step, the RNA containing column membrane was washed by adding RW1 and RPE buffer. To elute the RNA, the RNeasy spin column was placed in a new 1.5 ml collection tube and 30-50 µl RNase-free water was added directly to the spin column membrane. The lid of the tube was closed gently and centrifugation for one minute at 10000 rpm took place. Afterwards RNA concentration was measured using NanoDrop 1000 spectrophotometer from PeqLab. The purity of RNA was assessed by the calculated ratio of absorption at 260 nm and 280 nm. The Ration of 260/280 should be close to two for pure RNA. For an additional quality control, ribosomal 5S, 18S and 28S RNA was

visualized by electrophoresis using a 1.6% agarose gel in 1x TBE. Each RNA probe was mixed with 7  $\mu$ l formamide, 2x TBE and 1 mg/ml ethidium bromide and incubated for 10 minutes at 70°C before loading on the TBE gel. Electrophoresis was performed at 40-80 mA in a mini gel chamber treated with 3% H<sub>2</sub>O<sub>2</sub> for at least 15 minutes.

### 2.2.2.3 Polymerase chain reaction

DNA amplification by polymerase chain reaction (PCR) was performed using Taq polymerase and PCR reaction buffer from 5 Prime. Each reaction mix contained: DNA as template, forward and reverse primer, 2 mM dNTPs, 10x PCR buffer, Taq polymerase and water. In case 5 M betaine was used as enhancer.

#### A Genotyping of Na<sub>v</sub>1.9 KO mouse line

Reagents	Volume 1x [ $\mu$ l]
each primer (20 pMol)	0.25
Taq	0.3
DNA	1
dNTP (2 mM)	2.5
PCR buffer 10x	2.5
water	17.95
total reaction volume	25

Segment	Temperature	Time	Cycle
pre - denaturation	94°C	2 min	1x
denaturation	94°C	30 sec	
annealing	60°C	15 sec	35x amplification
elongation	72°C	1 min	
post - elongation	72°C	10 min	1x
cooling	4°C	$\infty$	1x

#### B Genotyping of *Smn*<sup>-/-</sup>-SMN2tg mouse line

Reagents	Volume 1x [ $\mu$ l]
each primer (100 pMol)	0.15
Taq	0.35
DNA	1
dNTP (2 mM)	5
PCR buffer 10x	5
water	38.35
total reaction volume	50

Segment	Temperature	Time	Cycle
pre - denaturation	94°C	3 min	1x
denaturation	94°C	30 sec	
annealing	57°C	30 sec	30x amplification
elongation	72°C	1 min 30 sec	
post - elongation	72°C	5 min	1x
cooling	4°C	$\infty$	1x

#### C Genotyping of *TrkB*<sup>-/-</sup> (Ntrk-2-ROHR) mouse line

Reagents	Volume 1x [ $\mu$ l]
each primer (10 pMol)	0.5
Taq	0.3
DNA	1
dNTP (2 mM)	2.5
PCR buffer 10x	2.5
betaine (5 M)	5
water	38.35
total reaction volume	25

Segment	Temperature	Time	Cycle
pre - denaturation	94°C	3 min	1x
denaturation	94°C	30 sec	
annealing	59°C	30 sec	30x amplification
elongation	68°C	30 sec	
post - elongation	68°C	3 min	1x
cooling	4°C	$\infty$	1x

#### Figure 10: Reaction mix and PCR program for genotyping

(A - C) Reaction mix (left) and PCR program (right) for genotyping of the Na<sub>v</sub>1.9 KO mouse line (A), the *Smn*<sup>-/-</sup>-SMN2tg mouse line (B), and the *TrkB*<sup>-/-</sup> (Ntrk-2-Rohr) mouse line (C). PCR = polymerase chain reaction; KO = knock-out; tg = transgene; dNTP = deoxyribonucleotide; DNA = deoxyribonucleic acid; SMN = survival motor neuron; Trk = tropomyosin receptor kinase

The DNA amplification process occurred in Eppendorf's Mastercycler® PCR machine. PCR was used for genotyping of the following mouse lines:  $Na_v1.9$  KO,  $Smn^{-/-}$ - $SMN2tg$  and  $TrkB^{-/-}$  ( $Ntrk-2$ -Rohr). The reaction mix and PCR program for each genotyping experiment is shown in Figure 10. After the PCR process DNA fragments were analysed by agarose gel electrophoresis.

#### 2.2.2.4 Agarose gel electrophoresis

Agarose gel electrophoresis was used to separate DNA fragments in a 1-2% agarose gel containing agarose, 1x TAE and 0.4  $\mu$ g/ml ethidium bromide. Samples were mixed with 1x DNA loading buffer and loaded on the gel together with 250 ng (5  $\mu$ l) of a 100 bp or 1 kb DNA size marker. The DNA loaded agarose gel was run in 1x TAE for 30 minutes at 120 V. Finally, the visualization of DNA bands was performed at 368 nm.

#### 2.2.2.5 Reverse transcriptase polymerase chain reaction

In this variant of PCR, RNA is reverse-transcribed into its DNA complement (cDNA) using the enzyme reverse transcriptase. To synthesize cDNA, 100-200 ng RNA were mixed with 2  $\mu$ l of 10 mM dNTPs, 1  $\mu$ l of 100 nmol/ $\mu$ l random hexamer primers and 1  $\mu$ l of 40 units RNasin. The solution was incubated for five minutes at 65°C and after a short placement on ice a master mix containing 4  $\mu$ l of 5x first strand buffer, 2  $\mu$ l of 0.1 mM DTT and 2  $\mu$ l of 25 mM  $MgCl_2$  was added. The reaction was further incubated for five minutes at 37°C. Subsequently, 1  $\mu$ l of SuperScript™ III Reverse Transcriptase was added to each reaction and reverse transcription occurred for two hours at 37°C. After 10 minutes of heat inactivation of the enzyme at 70°C, synthesized cDNA was diluted 1:10 in EB-BSA and stored at -20°C or used for qPCR immediately.

#### 2.2.2.6 Quantitative real time polymerase chain reaction

Quantitative real time polymerase chain reaction (qRT-PCR) was used to amplify and simultaneously quantify PCR products. This variant of PCR was performed using the LightCycler 1.5 Instrument (Roche) according to the protocol of the LightCycler® FastStart DNA Master SYBR Green I kit. The reaction took place in glass capillaries in a final volume of 20  $\mu$ l. Figure 11 shows the qRT-PCR components and cycling conditions for the quantitative amplification of  $Na_v1.5$ ,  $Na_v1.8$ ,  $Na_v1.9$ ,  $Na_v1.9^{L799P}$  and GAPDH as target in cDNA from several tissues and cultured motoneurons.

**A** qRT-PCR conditions for amplification of Na<sub>v</sub>1.5

Reagents	Volume 1x [μl]	Segment	Temperature	Time	Cycle
MgCl <sub>2</sub> (25 mM)	1.6	pre - denaturation	95°C	10 min	1x
each primer (20 pmol/μl)	2.5	denaturation	95°C	0 sec	
cDNA	2	annealing	59°C	5 sec	50x amplification
SYBR Green I	2	elongation	72°C	7 sec	
water	9.4	dissociation	85°C	5 sec	
total reaction volume	20	melting	65°C	15 sec	1x
		cooling	40°C	40 sec	1x

**B** qRT-PCR conditions for amplification of Na<sub>v</sub>1.8

Reagents	Volume 1x [μl]	Segment	Temperature	Time	Cycle
MgCl <sub>2</sub> (25 mM)	1.6	pre - denaturation	95°C	10 min	1x
each primer (20 pmol/μl)	1.5	denaturation	95°C	0 sec	
cDNA	2	annealing	58°C	5 sec	50x amplification
SYBR Green I	2	elongation	72°C	7 sec	
water	11.4	dissociation	85°C	5 sec	
total reaction volume	20	melting	65°C	15 sec	1x
		cooling	40°C	40 sec	1x

**C** qRT-PCR conditions for amplification of Na<sub>v</sub>1.9

Reagents	Volume 1x [μl]	Segment	Temperature	Time	Cycle
MgCl <sub>2</sub> (25 mM)	1.6	pre - denaturation	95°C	10 min	1x
each primer (20 pmol/μl)	1.5	denaturation	95°C	0 sec	
cDNA	2	annealing	59°C	5 sec	50x amplification
SYBR Green I	2	elongation	72°C	6 sec	
water	11.4	dissociation	83°C	5 sec	
total reaction volume	20	melting	65°C	15 sec	1x
		cooling	40°C	40 sec	1x

**D** qRT-PCR conditions for amplification of Na<sub>v</sub>1.9-L799P

Reagents	Volume 1x [μl]	Segment	Temperature	Time	Cycle
MgCl <sub>2</sub> (25 mM)	1.6	pre - denaturation	95°C	10 min	1x
each primer (20 pmol/μl)	1	denaturation	95°C	0 sec	
cDNA	2	annealing	62°C	5 sec	50x amplification
SYBR Green I	2	elongation	72°C	6 sec	
water	13.4	dissociation	80°C	5 sec	
total reaction volume	20	melting	65°C	15 sec	1x
		cooling	40°C	40 sec	1x

**E** qRT-PCR conditions for amplification of GAPDH

Reagents	Volume 1x [μl]	Segment	Temperature	Time	Cycle
MgCl <sub>2</sub> (25 mM)	2.4	pre - denaturation	95°C	10 min	1x
each primer (20 pmol/μl)	1.5	denaturation	95°C	0 sec	
cDNA	2	annealing	59°C	5 sec	50x amplification
SYBR Green I	2	elongation	72°C	6 sec	
water	10.6	dissociation	83°C	5 sec	
total reaction volume	20	melting	65°C	15 sec	1x
		cooling	40°C	40 sec	1x

**Figure 11: qRT-PCR components and cycling conditions**

(A - E) Reaction mix (left) and qRT-PCR program (right) for amplification of Na<sub>v</sub>1.5 (A), Na<sub>v</sub>1.8 (B), Na<sub>v</sub>1.9 (C), Na<sub>v</sub>1.9-L799P (D), and GAPDH (E). qRT-PCR = quantitative real time polymerase chain reaction; cDNA = copy or complementary Deoxyribonucleic acid; GAPDH = glyceraldehyde 3-phosphate dehydrogenase

Intron-spanning primers, producing a PCR product of around 150 bp, were selected with Oligo 6.71 software and PCR conditions, primer concentration and MgCl<sub>2</sub> concentration were optimized as described earlier (*Durand et al. 2006*). After polymerase chain reaction, products were further analysed by agarose gel electrophoresis, melting curve analysis, and control PCRs.

## 2.2.3 Protein analysis techniques

### 2.2.3.1 Protein isolation and measurement of protein concentration

For protein isolation, lumbar and thoracic dorsal root ganglia (DRG) were dissected from adult mice, collected in a 1.5 ml reaction tube, which was filled with 500 µl 1x PBS, and kept on ice. After short centrifugation, PBS was removed and the tissue was solved in 14 µl of 10% Nonidet P40 and 70 µl of protein lysis buffer composed of 2.5 ml basic protein lysis buffer (150 mM NaCl; 10% glycerol; 50 mM HEPES pH 7.4) together with one tablet of complete Mini (EDTA-free) and 25 µl 100 mM DTT. The tissue was homogenized using Hielscher UP50H ultrasonic homogenizer with a MS1/3 sonotrode. After several short pulses (5 s pulse with 85% amplitude; MS1 sonotrode) and incubation steps on ice, the sample was centrifuged and a part of the protein lysate was directly prepared for gel electrophoresis. Another part of the lysate was used for protein concentration determination and the rest of the lysate was stored at -20°C (or for long-term at -80°C).

To isolate proteins from cultured cells, a 6 cm cell culture dish with adherent cells was put on ice, cells were washed twice with 1x PBS and 200-300 µl of protein lysis buffer containing 4 ml basic protein lysis buffer (150 mM NaCl; 10% glycerol; 50 mM HEPES pH 7.4), 1 ml of 2% Nonidet P40, ½ tablet of complete Mini (EDTA-free), 1 mM NaF, 10 mM Na-pyrophosphate and 2 mM Na-orthovanadate, was added. Cells were scrapped from culture dishes, collected in 1.5 ml reaction tubes and incubated for 10 to 15 minutes on ice. Cells were further solubilised with Hielscher UP50H ultrasonic homogenizer and after centrifugation lysates were used in the same way as lysates from tissue samples.

The protein concentration was determined with the Pierce BCA Protein Assay kit according to the manufactures' protocol. Samples were diluted 1:10 in 1x PBS and mixed with 1 ml of BCA solution. After incubation for 30 minutes at 37°C, the absorption was measured at 562 nm with an Eppendorf photometer. To determine the protein amount of the samples, a BSA standard calibration curve was generated. Calculation occurred with Microsoft Excel 2003 software.

### 2.2.3.2 SDS-polyacrylamid gel electrophoresis and Western blot analysis

Sodium dodecyl sulphate (SDS) polyacrylamid gel electrophoresis (PAGE) was performed with 3-8% Tris-Acetate gradient gels from BioRad. Samples were mixed with 4x Laemmli sample buffer and boiled for 10 minutes at 50°C. After centrifugation a defined amount (40-60 µg) of each sample was loaded on the gel together with 8 µl of Precision Plus Protein™ All Blue Standards for size identification. The process of electrophoresis occurred in a Criterion™ Cell from BioRad, in 1x electrophoresis buffer (30.3 g/l Tris base; 144 g/l glycine; 10 g/l SDS, pH 8.45) at constant 150 V for 120 minutes.

To transfer the proteins from gel to a polyvinylidene difluoride (PVDF, BioRad, 162-0177) membrane, the gel and some filter papers (BioRad, 1703969) were equilibrated in transfer buffer (1x electrophoresis buffer; 20% methanol) for 30 minutes. The PVDF membrane was activated in methanol and then equilibrated in transfer buffer, too. Filter paper was placed on the anode of the Trans-Blot SD Semi-Dry Transfer Cell (BioRad), followed by PVDF membrane, gel, another filter paper and the lid containing the cathode plate. Proteins were blotted using the semi-dry western blot chamber under the conditions 20 V constant and 640 mA (5.5 mA/cm<sup>2</sup>) for 40 minutes.

### 2.2.3.3 Immunological detection of proteins

After blotting, the membrane was washed for 10 minutes in TBS-T (1x TBS, 0.2% Tween 20) and afterwards incubated in blocking solution (1x TBS-T, 5% powdered milk, 5% goat serum) over night at 4°C on a shaker. Next day, the membrane was transferred into blocking solution with primary antibody and incubated for three to four hours at room temperature. A three times washing step followed with TBS-T for 10 minutes and secondary antibody incubation occurred in 1x TBS-T with 5% powdered milk for another three hours at room temperature. The membrane was again washed three times with TBS-T for 10 minutes and finally protein visualisation took place in a dark room using ECL Prime Western Blotting Detection System (Amersham) according to the manufacturers' instructions. ECL was incubated, removed and the blots were exposed to X-ray Hyperfilm™ (Amersham) for detection of the chemiluminescence. Films were developed by Agfa HealthCare CP 1000 Medical X-Ray Film Processor. For loading control the membrane was washed with TBS-T for 10 minutes at room temperature, blocked over night at 4°C with blocking solution and re-probed with a primary and secondary antibody.

#### 2.2.3.4 Immunocytochemistry and immunohistochemistry

For immunocytochemistry, cells were fixed with pre-warmed 4% paraformaldehyde (PFA) for 10 minutes at room temperature, washed three times with 1x PBS and incubated in blocking solution containing 1x PBS, 10% horse serum, 0.1% Tween 20 and 0.3% Triton X-100 for 1.5 hours at room temperature. Afterwards, cells on cover glasses were transferred into a dark and wet chamber on a plastic paraffin film (Parafilm) and covered with 75  $\mu$ l of the primary antibody solution. Antibodies were diluted in blocking solution. After 2-3 hours of antibody incubation, cells were washed three times with washing solution (1x PBS; 0.1% Tween 20; 0.1% Triton X-100) and incubated with 75  $\mu$ l of the secondary antibody solution for another two hours at room temperature. Subsequently, cells were washed three times with washing solution and incubated with 75  $\mu$ l of 0.4  $\mu$ g/ml DAPI in 1x PBS for 10 to 15 minutes. Next, cells were washed three times with 1x PBS, cover glasses were dipped in water and after a short drying step the cells were embedded with aqua poly/mount on glass slides. Finally, the slides were used for staining analysis via microscopy or stored at 4°C in slide boxes or slide folders to protect them from light.

Immunohistochemistry was performed using teased nerve fibres or dorsal root ganglia cryostat slices. For preparation of teased nerve fibres, adult mice were deeply anesthetized with CO<sub>2</sub> and trans-cardially perfused with 2% PFA. For this, the thoracic cavity was opened, a perfusion needle was inserted into the left ventricle of the exposed heart and the right atrium was cut to allow the exchange of blood and PFA. After perfusion, nerves were dissected and separated, so called teased (*Kohl et al. 2010*) in 0.5x PBS on glass slides and dried over night at room temperature. Next morning, the tissue was surrounded with Roti®-Liquid Barrier Marker and after drying, PBS was added. The further procedure was same as used for immunocytochemistry. The tissue was fixed with 4% PFA, blocked for 1.5 hours, incubated with primary (over night at 4°C) and secondary antibodies, stained with DAPI and embedded with aqua polymount. Finally, a cover glass was put on the stained fibres.

For preparation of dorsal root ganglia cryostat slices, adult mice were anesthetized and trans-cardially perfusion was performed with 4% PFA. Dorsal root ganglia were dissected and incubated in 4% PFA over night at 4°C. Next day, fixed dorsal root ganglia were transferred into sucrose solutions in PBS with increasing sucrose concentration from 10% to 30%. When the tissue was submerged in the 30% sucrose solution, dorsal root ganglia were embedded into Tissue-Tek and frozen with the help of dry ice. Afterwards, the embedded DRGs were stored at -20°C over night. Next day, the tissue was cut into 10  $\mu$ m thick sections using the Leica CM1950 cryostat and placed on super frost glass slides. Cryostat slides were stored at -20°C and dried before staining at room temperature. The immunological labelling procedure was same as described above.

To analyse the immunological staining, the following microscopes were used: Leica SP5 confocal laser scanning microscope equipped with a Mai-Tai multi photon laser (Spectra-Physics) for stimulated emission depletion (STED) microscopy, an inverted confocal microscope (SP5, Leica) equipped with a laser combiner for standard confocal laser scanning microscopy, alternatively Fluoview1000ix81, Olympus equipped with a FV10-MCPSU laser combiner was used for standard confocal laser scanning microscopy as described recently (Subramanian *et al.* 2012).

#### 2.2.4 Axon length measurement

Motoneurons from E14 embryos were cultured for five to seven days *in vitro* and stained by immunocytochemistry (see 2.2.1.2 and 2.2.3.4). Images from anti  $\alpha$ -tubulin labelled cells were captured using a Keyence BZ-8000 fluorescence microscope equipped with the following objective: PlanApo 20x NA0.75. Axon length was measured with ImageJ 1.42i software and statistically analysed with GraphPad Prism 4.02 software. Mean values of at least three independent experiments were presented with the standard error of the mean.

#### 2.2.5 Survival assay

To analyse the survival of motoneurons, 24-well plates were signed at the bottom with a vertical and a horizontal line crossing each well as orientation for counting. Plates were coated with PORN, washed three times with neurobasal medium containing GlutaMax and coated additionally with laminin. Motoneurons were isolated (see 2.2.1.2) and seeded on the coated 24-well plates. After 24 hours of incubation at 37°C in a standard cell culture incubator, living motoneurons were counted using the drawn "pluses" on the bottom of the plates. A defined area of four quadrants along the lines was counted under the phase contrast microscope. Every second day 40% of the medium was exchanged as described in 2.2.1.2 and the counting procedure was repeated at day five and day seven *in vitro*. Percentage survival was calculated on the basis of results obtained at day five and day seven. Survival of motoneurons was compared between several mouse genotypes and between different neurotrophic factor combinations, which were used in the motoneuron complete medium for cell feeding. The neurotrophic factors BDNF (5 ng/ml) and CNTF (5 ng/ml) were used. As control, cells were fed with motoneuron complete medium without any additional factor.



### 2.2.6 Calcium imaging

For  $\text{Ca}^{2+}$  imaging, artificial cerebral spinal fluid (ACSF) ringer solution composed of 127 mM NaCl, 3 mM KCl, 2.5 mM  $\text{NaH}_2\text{PO}_4$ , 2 mM  $\text{CaCl}_2$ , 2 mM  $\text{MgCl}_2$ , 23 mM  $\text{NaHCO}_3$  and 25 mM D-glucose was used. Glucose,  $\text{CaCl}_2$  and  $\text{MgCl}_2$  were added freshly before use and pH was adjusted during the experiment by bubbling the ACSF with carbogen gas. Osmolarity of the solution was verified using the Micro-Osmometer TypOM806 from Vogel. The high-affinity calcium indicator Oregon Green 488 BAPTA-1, AM was prepared as 5 mM stock solution by adding 7.94  $\mu\text{l}$  of 20% Pluronic® F-127 solved in DMSO. After incubation for two minutes in a sonifier water bath (Bandelin), 0.5  $\mu\text{l}$  aliquots were made. For dye loading of cells, 500  $\mu\text{l}$  of ACSF was added to one aliquot of Oregon Green 488 BAPTA-1, AM. Cells, grown on cover glasses were incubated in the solution for 15 minutes at 37°C and 5%  $\text{CO}_2$ . Subsequently the cover glasses were transferred to the imaging setup containing an upright fixed microscope (BXWI, Olympus) equipped with a CoolLED (Visitron Systems) and a X-cite 120Q excitation light source (Lumen dynamics). The microscope system was controlled by Remote Control SM7 (Luigs and Neumann), while imaging was performed in a imaging chamber under continuous perfusion with ACSF warmed to 35°C using a SH-27B In-line Solution Heater (Warner Instrument Cooperation) regulated over Automatic temperature controller (Warner Instrument Cooperation) and a Bridge 500 under the control of Bad Controller V (Luigs & Neumann). For steady flow of the solution, the Minipuls 3 Peristaltic Pump (Gilson) was used and images were captured with the Rolera-XR camera (Qimaging) operated by the StreamPix 4 software (Norpix). During imaging of  $\text{Ca}^{2+}$  dynamics, the following parameters were applied: frame size limited to 600, 200 ms exposure, at a speed of 5 Hz. Oregon Green was excited at a wave length of 470 nm.

To analyse  $\text{Ca}^{2+}$  imaging data, fluorescent intensity in defined regions of interest (ROIs) were obtained using the ImageJ 1.42I software. After ROI definition, change in fluorescence intensity was measured over time using the Time Series Analyzer V2 0 tool. Results were transferred to Microsoft Excel 2003 for further calculations. Here, background noise was subtracted from each ROI at each time point using the average of three background ROIs. To display relative changes of fluorescence intensity over the time ( $\Delta F/F_0$ ), fluorescence intensity at each time point ( $F_{\text{ROI}}$ ) was set in correlation to the basic fluorescence intensity ( $F_0$ ) using the following formula:  $(\Delta F/F_0) = (F_{\text{ROI}} - F_0) / F_0$ . Afterwards peak analysis was done with OriginPro 9.0.0G software (OriginLab Corporation). For this, a baseline was defined and peaks with an amplitude of at least 10% increase over background were defined to represent a calcium transient.

### 3 Results

Earlier experiments by our group showed that pharmacological inhibition of voltage-gated sodium channels (VGSC) causes a reduced spontaneous neural activity as well as decreased axon elongation of cultured embryonic motoneurons (*Jablonka et al. 2007, Subramanian et al. 2012*). During these experiments, VGSC pore blocker saxitoxin appeared to be more efficient than the pore blocker tetrodotoxin (*Subramanian et al. 2012*). Thus, for the discovery of voltage-gated sodium channels, which are responsible for the regulation of  $\text{Ca}^{2+}$  influx and subsequent axon growth in motoneurons, we focused on TTX-insensitive/STX-sensitive VGSCs.

#### 3.1 $\text{Na}_v1.9$ is expressed in spinal cord and motoneurons

Three TTX-resistant voltage-gated sodium channels have been described in the literature: the heart specific  $\text{Na}_v1.5$  channel and the homologues  $\text{Na}_v1.8$  and  $\text{Na}_v1.9$ .  $\text{Na}_v1.8$  and  $\text{Na}_v1.9$  are well known to be highly expressed in dorsal root ganglia neurons (*Dib-Hajj et al. 1998, Catterall et al. 2005, Beyder et al. 2010*). In order to investigate the expression level of all three channels in the spinal cord, where motoneurons are located, and in cultured motoneurons, channel encoding transcripts were amplified by efficiency controlled quantitative RT-PCR (Figure 12A and B). RNA was isolated from spinal cord and dorsal root ganglia at different developmental stages, from cultured embryonic motoneurons at day 7 *in vitro* and as reference for  $\text{Na}_v1.5$  from heart at postnatal day 1 (P1). Representative amplification products and RT-PCR amplification curves are demonstrated in Figure 12A - D. External standard dilution curves with P1 heart RNA (2 ng - 100 ng) and E18 spinal cord RNA (10 ng - 500 pg) provided as references for the amplification of  $\text{Na}_v1.5$  and  $\text{Na}_v1.9$  in cultured motoneurons (Figure 12C and D). In the spinal cord,  $\text{Na}_v1.5$  and  $\text{Na}_v1.9$  transcripts were already detectable at embryonic day 14 (E14), while  $\text{Na}_v1.8$  expression started at E15 (Figure 12A).  $\text{Na}_v1.5$  as well as  $\text{Na}_v1.9$  transcripts were also verified in cultured motoneurons at day *in vitro* (DIV) 7, whereas  $\text{Na}_v1.8$  transcripts were not found (Figure 12B). The amplification efficiency of the  $\text{Na}_v1.8$  qRT-PCR protocol (1.92) was close to the amplification efficiency of the  $\text{Na}_v1.9$  qRT-PCR protocol (1.95). This reveals that  $\text{Na}_v1.9$  mRNA is expressed at relatively high levels in motoneurons (Figure 12B). Interestingly, the relative expression of  $\text{Na}_v1.5$  in cultured motoneurons was at least 27-fold higher than the expression of  $\text{Na}_v1.9$ . Consequently,  $\text{Na}_v1.5$  and  $\text{Na}_v1.9$  are the best candidate proteins that may trigger the VGSC-dependent  $\text{Ca}^{2+}$  transients in motoneurons. However, in comparison to  $\text{Na}_v1.5$ , the  $\text{Na}_v1.9$  channel comprises unique electrophysiological properties, suggesting

him as most likely candidate as an initial trigger of cell-autonomous excitation of motoneurons.  $Na_v1.9$  has a lower activation threshold than  $Na_v1.5$  and is able to mediate spontaneous excitation near the resting potential, at least in dorsal root ganglia and myenteric neurons (Cummins et al. 1999, Herzog et al. 2001, Rugiero et al. 2003, Catterall et al. 2005, Ostman et al. 2008). Hence, we focused in subsequent analysis on  $Na_v1.9$ .

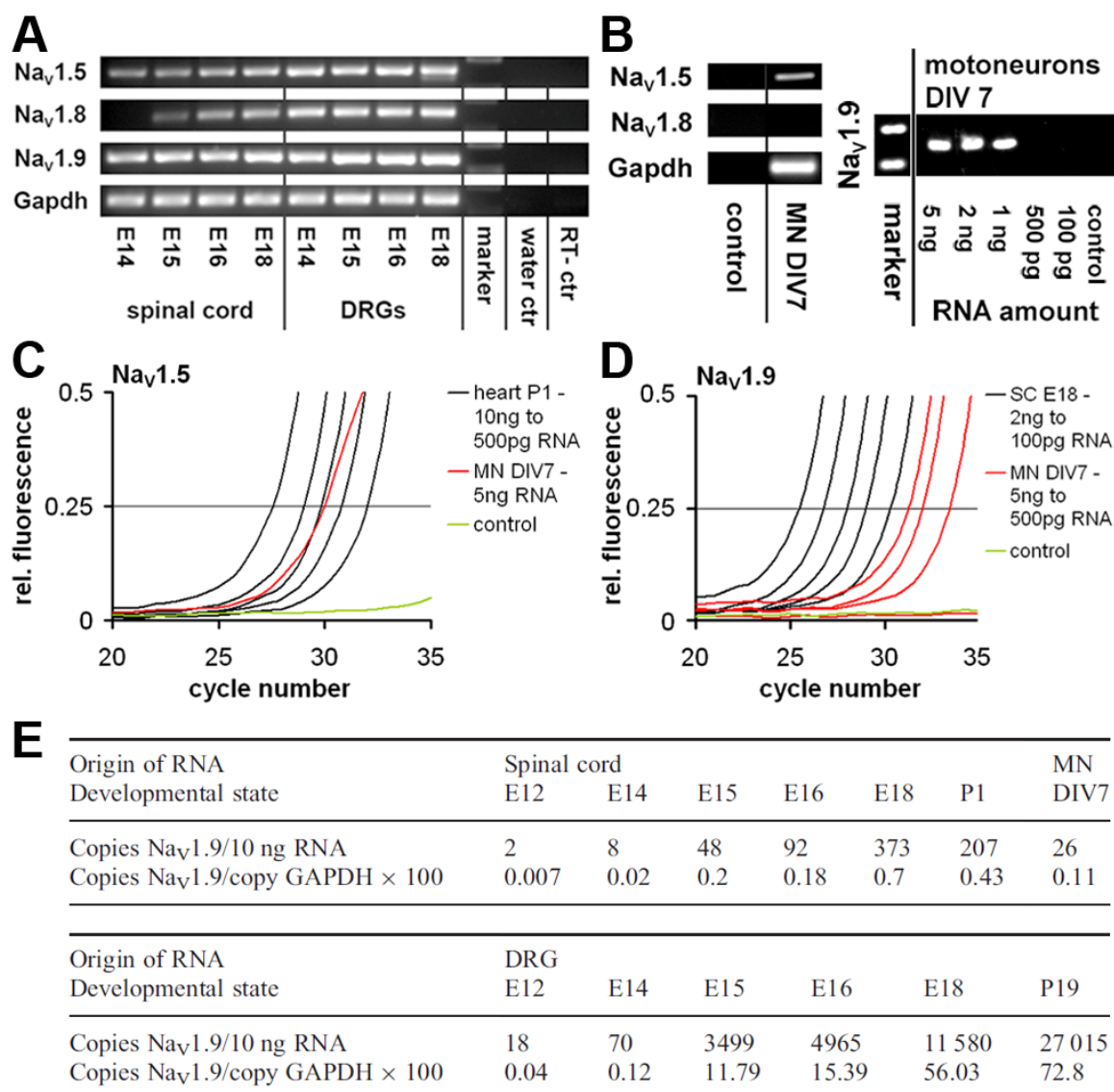


**Figure 12: Expression pattern of TTX-resistant VGSCs in spinal cord, DRGs and motoneurons** (A and B) Representative amplification products after qRT-PCR with indicated cDNA samples. (A) Early expression pattern of transcripts encoding tetrodotoxin-resistant voltage-gated sodium channels in spinal cord and DRG neurons. (B) Expression of transcripts encoding  $Na_v1.9$  (right panel) and  $Na_v1.5$  and  $Na_v1.8$  (left panel) in cultured motoneurons at DIV 7. (C and D) Real-time monitoring of the fluorescence emission of SYBR Green I during PCR amplification of  $Na_v1.5$  (C) and  $Na_v1.9$  (D). In  $Na_v1.5$  amplification, serial dilutions of heart RNA served as external control (black lines in C) and for  $Na_v1.9$ , spinal cord RNA was used as control (black lines in D). (E) Determination of the number of VGSC transcripts per RNA or per number of GAPDH transcripts in spinal cord, cultured motoneurons and DRG neurons. cDNA = copy/complementary deoxyribonucleic acid; DIV = day *in vitro*; E = embryonal; GAPDH = glyceraldehyde 3-phosphate dehydrogenase; MN = motoneuron; P = postnatal; qRT-PCR = quantitative real time polymerase chain reaction; RNA = ribonucleic acid; SC = spinal cord; TTX = tetrodotoxin; VGSC = voltage-gated sodium channel

In some studies, a broad expression pattern of Na<sub>v</sub>1.9 was described (Jeong *et al.* 2000, Ogata *et al.* 2000, Blum *et al.* 2002). However, in contrast to data from dorsal root ganglia and myenteric neurons, these expression data were not supported by a verification of voltage-dependent Na<sub>v</sub>1.9 currents. Earlier studies demonstrated no or only low expression levels for Na<sub>v</sub>1.9 in the spinal cord (Dib-Hajj *et al.* 1998, Jeong *et al.* 2000, Tyrrell *et al.* 2001, Wetzel *et al.* 2013). For that reason, we determined the number of Na<sub>v</sub>1.9 transcripts in the developing spinal cord, in dorsal root ganglia neurons and in cultured motoneurons at DIV 7 (Figure 12E). Quantitative RT-PCR confirmed 26 Na<sub>v</sub>1.9 transcripts per 10 ng RNA in cultured motoneurons and our data indicated that Na<sub>v</sub>1.9 expression increases continuously between E12 (spinal cord: 2 copies/10 ng RNA; DRG: 18 copies/10 ng RNA) and E18 (spinal cord: 373 copies/10 ng RNA; DRG: 11 580 copies/10 ng RNA) in spinal cord and DRG tissue (Figure 12E). In dorsal root ganglia Na<sub>v</sub>1.9 expression became very high in older mice (P19: 27 015 copies/10 ng RNA), while in spinal cord the Na<sub>v</sub>1.9 expression level decreases after birth compared to Na<sub>v</sub>1.9 expression levels at late embryonic stages (E18: 373 copies/10 ng RNA; P1: 207 copies/10 ng RNA). This observation suggests that Na<sub>v</sub>1.9 presence and activity is necessary during early developmental periods, when axon growth of motoneurons occurs. Moreover, Na<sub>v</sub>1.9 transcripts were also found in young motoneurons *in situ* (Subramanian *et al.* 2012). Laser-assisted microdissection of young motoneurons from the anterior horn of the spinal cord exposed a low abundance of Na<sub>v</sub>1.9 transcripts (Subramanian *et al.* 2012). In summary, Na<sub>v</sub>1.9 transcripts are expressed in the spinal cord and in embryonic motoneurons. This raised the question whether Na<sub>v</sub>1.9 protein is also found in motoneurons.

### **3.2 Na<sub>v</sub>1.9 protein is localized in cultured embryonic motoneurons and at the node of Ranvier of motor and sensory nerve fibres**

Voltage-gated sodium channels are transmembrane proteins containing a highly processed  $\alpha$  subunit with a relative molecular weight ( $M_r$ ) of 260 kDa, which is associated with smaller  $\beta$  subunits (Catterall *et al.* 2005). Moreover, multiple phosphorylation sites in the intracellular loops as well as glycosylation sites in the extracellular linkers are common for voltage-gated sodium channels (Dib-Hajj *et al.* 2002, Catterall *et al.* 2005). In the case of Na<sub>v</sub>1.9 protein detection by western blot analysis different results were described (Yiangou *et al.* 2000, Tyrrell *et al.* 2001). Yiangou *et al.*, 2000 identified a 180 kDa band for Na<sub>v</sub>1.9 (Yiangou *et al.* 2000), while Tyrrell *et al.*, 2001 were able to observe a Na<sub>v</sub>1.9-specific antibody reaction at 210 kDa from membrane fractions of adult dorsal root ganglia and trigeminal ganglia, but not from liver or spinal cord (Tyrrell *et al.* 2001).

In order to verify our antibody against the carboxyterminal end of Na<sub>v</sub>1.9, a stable cell line expressing Na<sub>v</sub>1.9 was developed.

### 3.2.1 Generation of a stable Na<sub>v</sub>1.9 expressing cell line

It has shown to be problematic to achieve robust heterologous expression levels of Na<sub>v</sub>1.9 in transfected cell lines, oocytes or other reconstitution models (*Ostman et al. 2008, Smith & Momin 2008, Waxman & Estacion 2008*). Therefore, we established a lentiviral vector with a high DNA packaging capacity and a stabilized DNA amplification backbone. This lentiviral Na<sub>v</sub>1.9 expression vector consists of a rop-element, which enables the stabilization of the Na<sub>v</sub>1.9 DNA amplification in *Escherichia coli* and a shortened "woodchuck hepatitis post-transcriptional regulatory" (WPRE) element. This construction enabled a packaging capacity in the range of 5460 base pairs (bp). The Na<sub>v</sub>1.9 DNA element (5.3 kb) and the retroviral elements kept the vector below 9.8 kb, which is the proposed packaging limit of lentiviral vectors. After packaging using a "second-generation packaging system", HEK 293T cells were infected with these lentiviral particles. A first test via immunocytochemistry and western blot analysis revealed that isolation steps were necessary to increase the amount of Na<sub>v</sub>1.9 expressing HEK 293T cells. Therefore, infected HEK 293T cells were cultivated on uncoated cell culture dishes in suspension to permit the selection of single positive clones (Figure 13A). In the course of a first isolation step, 48 clones were transferred to 24-well plates, where they grew adherent in small colonies for a few days (Figure 13B). Cells were afterwards tested using immunocytochemistry and western blot analysis (Figure 14).

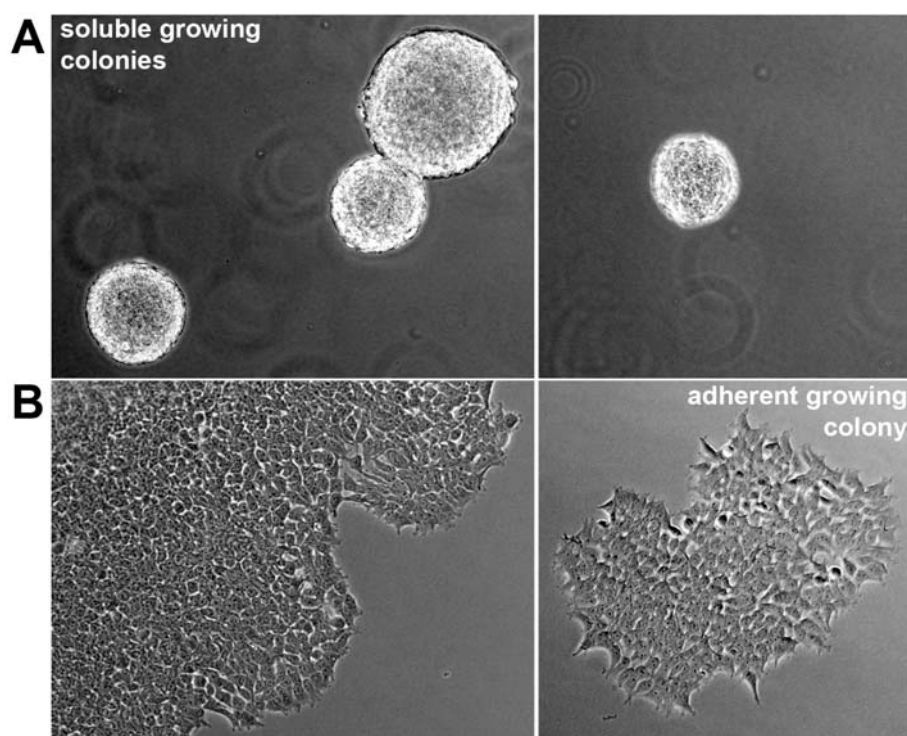


**Figure 13: Isolation process to generate stable Na<sub>v</sub>1.9 expressing cells**

**(A)** After HEK 293T cell infection with lentiviral particles containing recombinant Na<sub>v</sub>1.9 expression vector (719-pLVX1-ROP-mNav1-9), single clones, growing in an uncoated cell culture dish in suspension. **(B)** Single colonies growing on 24-well plates after selection of 48 single clones. HEK = human embryonic kidney

Five out of 48 HEK 293T cell clones were 40 - 50% immuno-positive for Na<sub>v</sub>1.9 (Figure 14A), but only very weak signals were detected via western blot analysis (Figure 14C, clone B16). In a next round of single clone selection, 48 more clones were selected out of cells from a previous Na<sub>v</sub>1.9-positive clone. The second isolation step resulted in five clones that stably express high amounts of mouse Na<sub>v</sub>1.9 protein as indicated in Figure 14B and C (B16A7, B16A8, B16A9, B16A10, B16B18). Lysates of these cells showed two predominant bands for Na<sub>v</sub>1.9, one at approximately 180 kDa and a second at about 280 kDa (Figure 14C). Beside its function as positive control for further protein detection analysis, the newly generated stable Na<sub>v</sub>1.9 expressing cell line display a useful tool for functional analysis of Na<sub>v</sub>1.9.

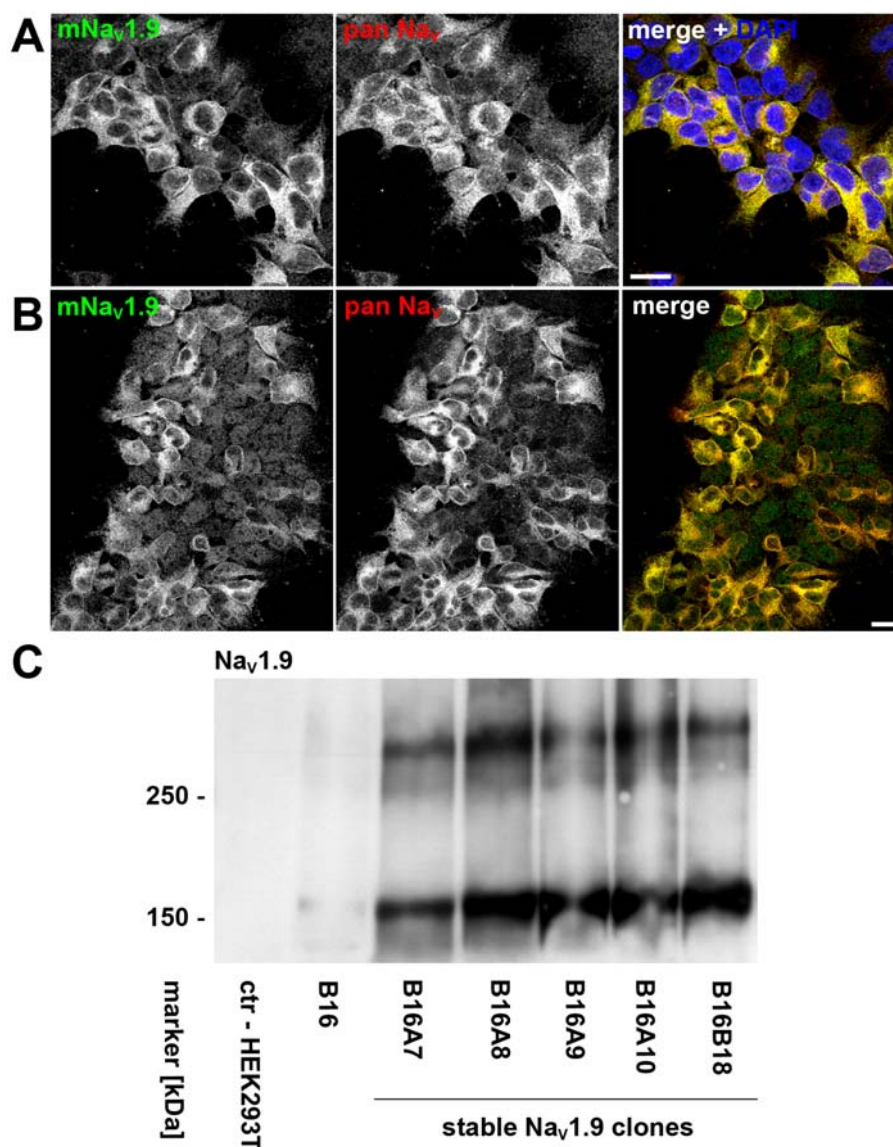


**Figure 14: Verification of the stable Na<sub>v</sub>1.9 expressing cell line**

(A and B) Stable expression of mouse Na<sub>v</sub>1.9 in HEK 293T cells visualized by immunocytochemistry. Anti-Na<sub>v</sub>1.9 staining (left), anti-pan Na<sub>v</sub> staining (middle), and overlap of anti-Na<sub>v</sub>1.9 and anti-pan Na<sub>v</sub> immunoreactivity with or without DAPI stained nuclei (right). Bar: 20 μm. (A) Immuno-stained clone B16 from the first selection step. (B) Immuno-stained clone B16A8 from the second selection step. (C) Stable expression of recombinant mouse Na<sub>v</sub>1.9 in a clone from the first selection step (B16) and in clones from the second selection step displayed by two bands at a M<sub>r</sub> of ~180 kDa and ~280 kDa. DAPI = 4', 6-diamidino-2-phenylindole; kDa = kilo dalton; HEK = human embryonic kidney

### 3.2.2 Verification of the anti-mouse Na<sub>v</sub>1.9 antibody

For the detection of Na<sub>v</sub>1.9 protein, in cultured embryonic motoneurons, anti-mouse Na<sub>v</sub>1.9 antibodies had been provided, which were raised in rabbits. Figure 15A shows the sequence of Peptide 71 in red, which was deduced from the carboxyterminal end of mouse Na<sub>v</sub>1.9 and used for immunization of the rabbits. The Na<sub>v</sub>1.9-specific rabbit antiserum labelled mouse Na<sub>v</sub>1.9 protein in cryostat slides of dorsal root ganglia from wild type mice (Figure 15B; upper panel). In contrast, dorsal root ganglia from Na<sub>v</sub>1.9 knock-out mice were Na<sub>v</sub>1.9 immunonegative (Figure 15B, lower panel). We used DRG tissue for Na<sub>v</sub>1.9 antibody verification, because Na<sub>v</sub>1.9 is known to be highly expressed in neurons of dorsal root ganglia (Figure 12E). Western blot analysis of lysates from wild type lumbar and thoracic dorsal root ganglia demonstrated the typical double band pattern for Na<sub>v</sub>1.9 (Figure 15C). This pattern closely resembles the detection pattern of Na<sub>v</sub>1.9, after stable expression in HEK 293T cells (Figure 14C). No signal for Na<sub>v</sub>1.9 was detectable in dorsal roots alone (Figure 15C). A further western blot experiment revealed the same specific Na<sub>v</sub>1.9 immuno-positive signal in lysates from a stable Na<sub>v</sub>1.9 expressing cell line, which served as positive control and in lysates from wild type dorsal root ganglia (Figure 15D). The signal was absent in dorsal root ganglia lysates harvested from Na<sub>v</sub>1.9 knock-out mice (n = 4). Detection of Trk receptors verified equal loading of protein from wild type and Na<sub>v</sub>1.9 knock-out animals.

Anti-Na<sub>v</sub>1.9 immunohistochemistry experiments with cryostat slides of wild type dorsal root ganglia were difficult to interpret (Figure 16). Here, smaller DRG neurons showed a continuous red staining (Figure 16, triangle arrows). In this assay, the anti-Na<sub>v</sub>1.9 antibody also caused a nuclear label, which was not observed in all cells, but also found in the Na<sub>v</sub>1.9 knock-out, thus labelling e.g. DRG neurons with a bigger diameter size as well (Figure 16, non-triangle arrows). This observation fits perfectly to the description that Na<sub>v</sub>1.9 is preferentially expressed in small (<30 μm diameter) nociceptive neurons of the dorsal root ganglia and trigeminal ganglia (*Dib-Hajj et al. 2002, Fang et al. 2002*).

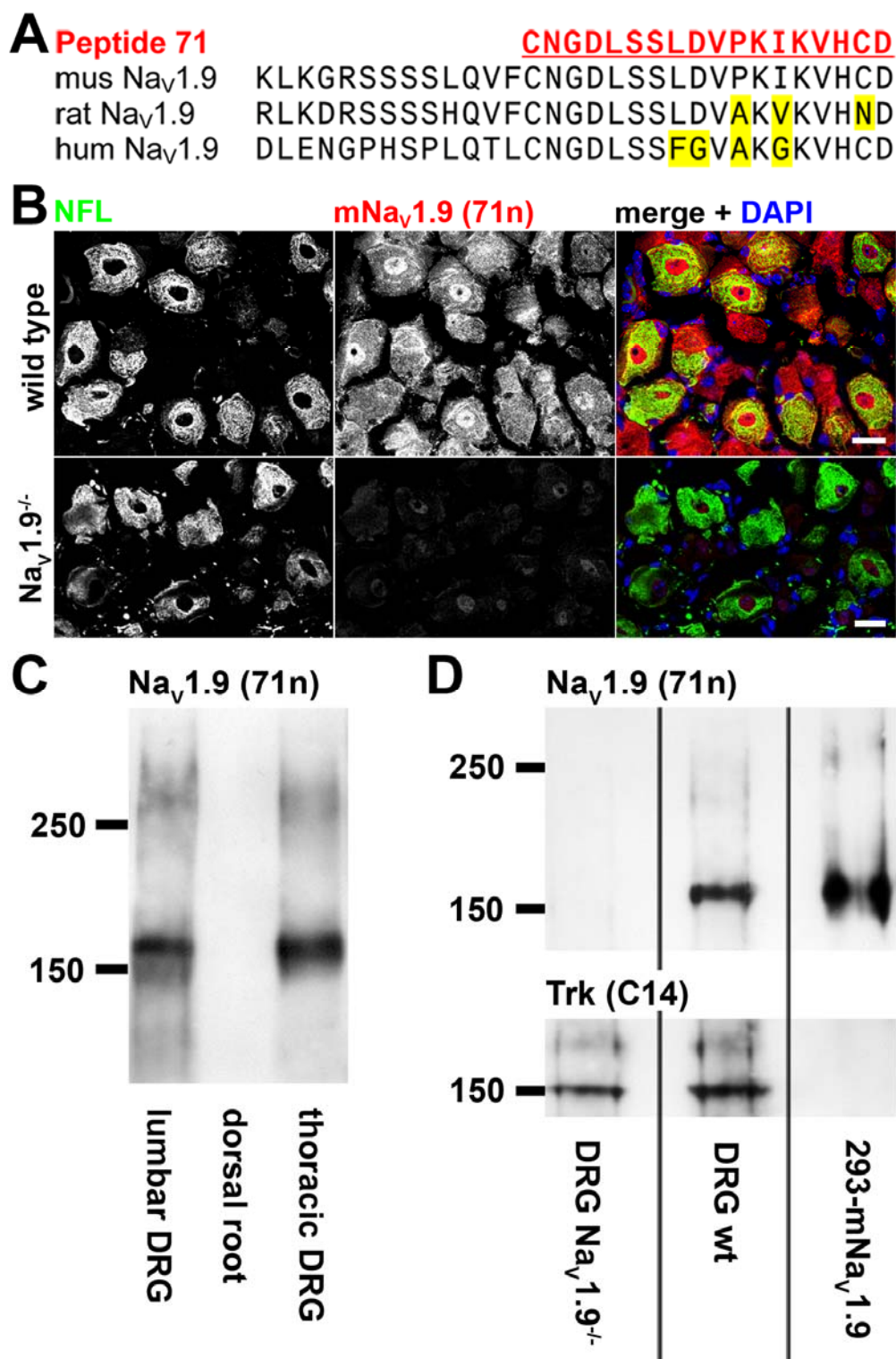


**Figure 15: Verification of the specificity of anti-mouse Na<sub>V</sub>1.9 antibody**

(A) Sequence of Peptide 71, a specific sequence for the carboxyterminal end of mouse Na<sub>V</sub>1.9 (red). Differences to rat or human Na<sub>V</sub>1.9 in yellow. (B) Immunoreactivity of anti-mNa<sub>V</sub>1.9 (71n) (middle) and Neurofilament and DAPI positive nuclei as orientation on cryostat slides of DRG neurons from wild type and Na<sub>V</sub>1.9<sup>-/-</sup> mice. Bar: 20 μm. (C and D) Detection of Na<sub>V</sub>1.9 via western blot analysis displayed by the typical double band pattern with bands at ~180 kDa and ~280 kDa. (C) Endogenous mouse Na<sub>V</sub>1.9 from lumbar and thoracic DRG neurons. (D) Endogenous mouse Na<sub>V</sub>1.9 in DRGs from wild type and Na<sub>V</sub>1.9<sup>-/-</sup> mice and recombinant Na<sub>V</sub>1.9 in the stable cell line 293-mNa<sub>V</sub>1.9. Anti-Trk antibodies served as loading control for DRG tissue. DAPI = 4', 6-diamidino-2-phenylindole; DRG = dorsal root ganglia; kDa = kilo dalton; HEK = human embryonic kidney; NFL = neurofilament; Trk = tropomyosin receptor kinase



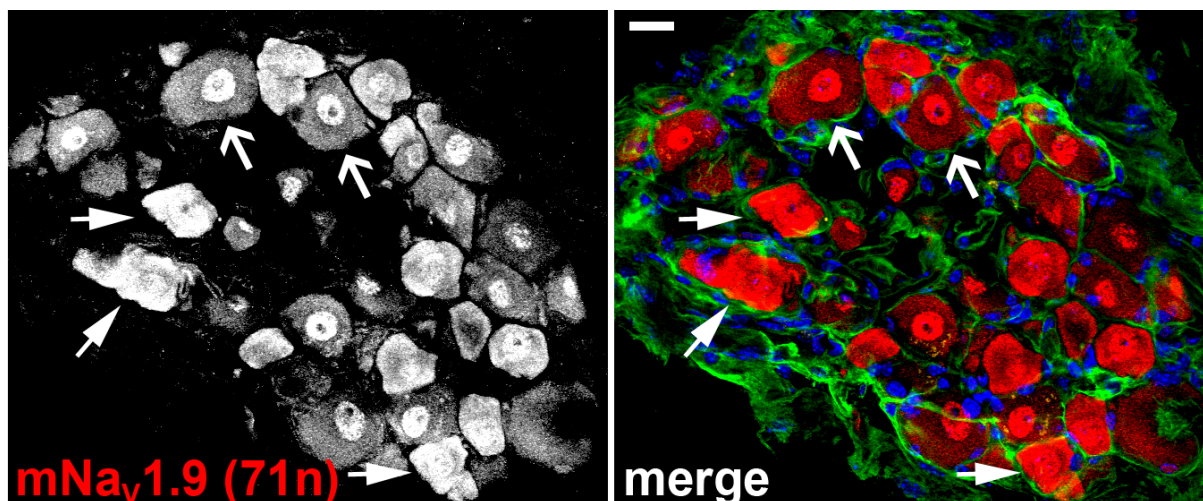


**Figure 16: Immunohistochemistry of Nav1.9 in dorsal root ganglia**

Single confocal sections of anti-mNav<sub>v</sub>1.9 (71n) immunoreactivity on cryostat slides of wild type DRG neurons. Small Nav<sub>v</sub>1.9 positive DRG neurons marked with triangle arrows, Nav<sub>v</sub>1.9 negative DRG neurons marked with non-triangle arrows. Caspr staining (green) and DAPI positive nuclei (blue) served as orientation. Bar: 20  $\mu$ m. Caspr = contactin-associated protein; DAPI = 4', 6-diamidino-2-phenylindole; DRG = dorsal root ganglia

### 3.2.3 Detection of Nav1.9 protein in cultured embryonic motoneurons

In young cultured motoneurons, local Ca<sup>2+</sup> transients appear in the soma, in distal axons and even in growth cones (*Jablonka et al. 2007, Subramanian et al. 2012*). Thus, we expected Nav<sub>v</sub>1.9 protein in these regions, close to voltage-gated calcium channels. To analyse the localization of Nav<sub>v</sub>1.9 protein in cultured embryonic motoneurons, we performed stimulated emission depletion (STED) microscopy combined with standard confocal laser scanning microscopy for the detection of actin and  $\alpha$ -tubulin as structural markers (Figure 17). Nav<sub>v</sub>1.9 protein was found in immuno-positive clusters along the axon and enriched at somatic sites (Figure 17A). In axons and growth cones, anti-mouse Nav<sub>v</sub>1.9 antibody detected high amounts of the protein in distal regions of the axon and in small protrusions (Figure 17B and C). Thereby, Nav<sub>v</sub>1.9 protein was determinable along the cell surface of growth cones in a small punctuated formation (Figure 17C). These results support the concept that Nav<sub>v</sub>1.9 may act as a local trigger for the generation of local calcium transients in the axon of motoneurons.

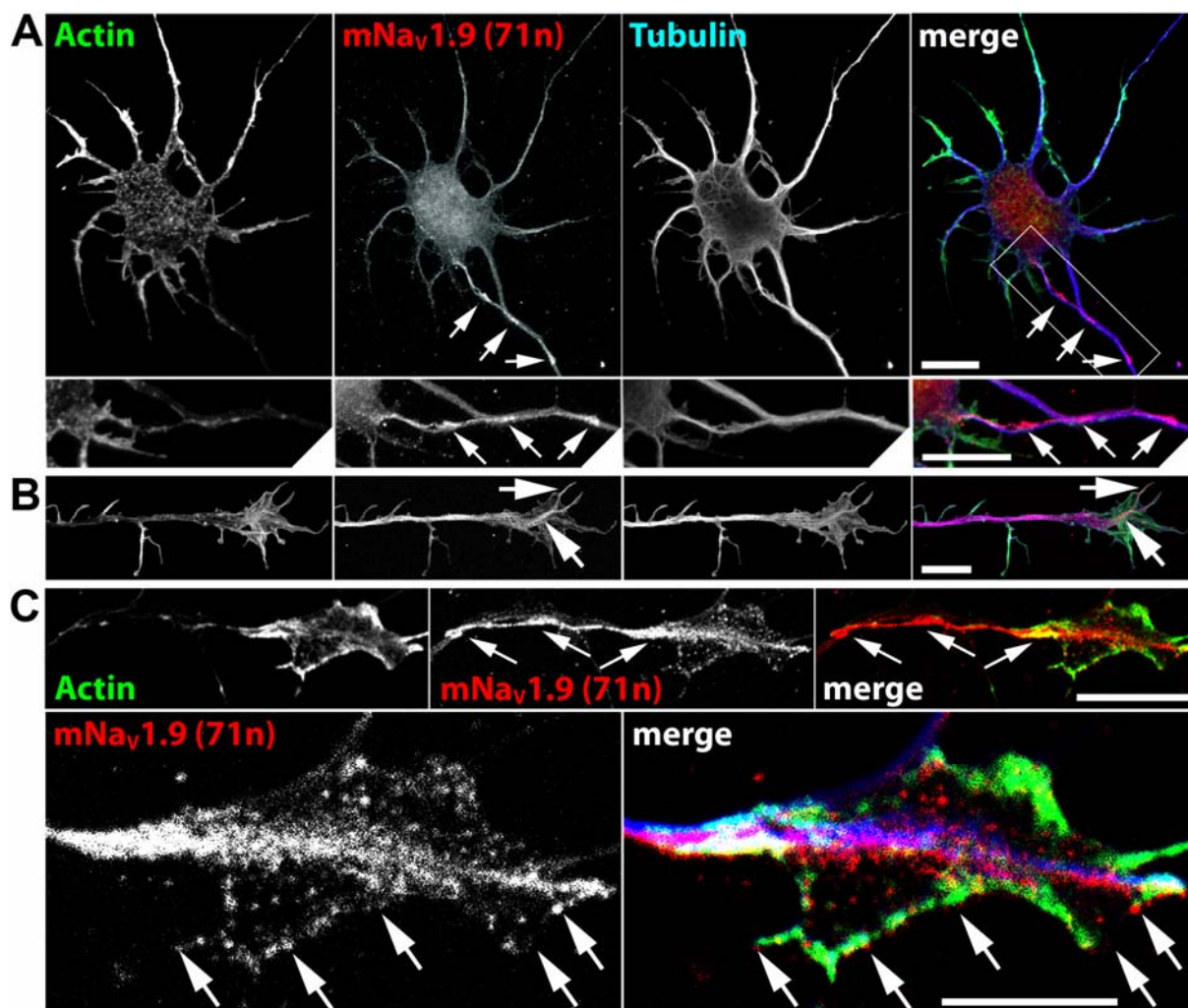


**Figure 17: Detection of Na<sub>v</sub>1.9 protein in cultured embryonic motoneurons**

(A - C) Single confocal sections of anti-mNa<sub>v</sub>1.9 (arrows) stained motoneurons by STED microscopy, combined with standard laser scanning microscopy of actin and  $\alpha$ -tubulin staining. (A) Anti-mouse Na<sub>v</sub>1.9 immunoreactivity, concentrated in axonal regions of DIV 7 motoneurons with enlarged inlet (lower panel). (B) Example of a DIV 3 growth cone with anti-Na<sub>v</sub>1.9 immunoreactivity in a fine protrusion. Bar in A and B: 10  $\mu$ m. (C) Example of a motoneuron growth cone at DIV 7 with Na<sub>v</sub>1.9 immunoreactivity, concentrated in axonal region and then found on the surface of the growth cone in small punctuate-like elements. Bar: 10  $\mu$ m (C, upper panel), 5  $\mu$ m (C, lower panel). DIV = day *in vitro*; STED = stimulated emission depletion

### 3.2.4 Localization of Na<sub>v</sub>1.9 protein in motor and sensory nerve fibres

The Na<sub>v</sub>1.9 channel was previously found at some nodes of Ranvier of thinly myelinated axons of the sciatic nerve – a distribution of Na<sub>v</sub>1.9, which is consistent with its role in nociceptive transmission (Fjell *et al.* 2000). In order to investigate Na<sub>v</sub>1.9 localization in motor nerve fibres *in vivo*, adult wild type and Na<sub>v</sub>1.9 knock-out mice were perfused with 2% PFA and nerves were dissected and separated by teasing on glass slides in 0.5x PBS. Femoral quadriceps nerve fibres as well as teased facial nerve fibres were labelled using anti-mouse Na<sub>v</sub>1.9 antibody and a antibody against the contactin-associated protein (Caspr) as paranode marker (Figure 18 and 19).

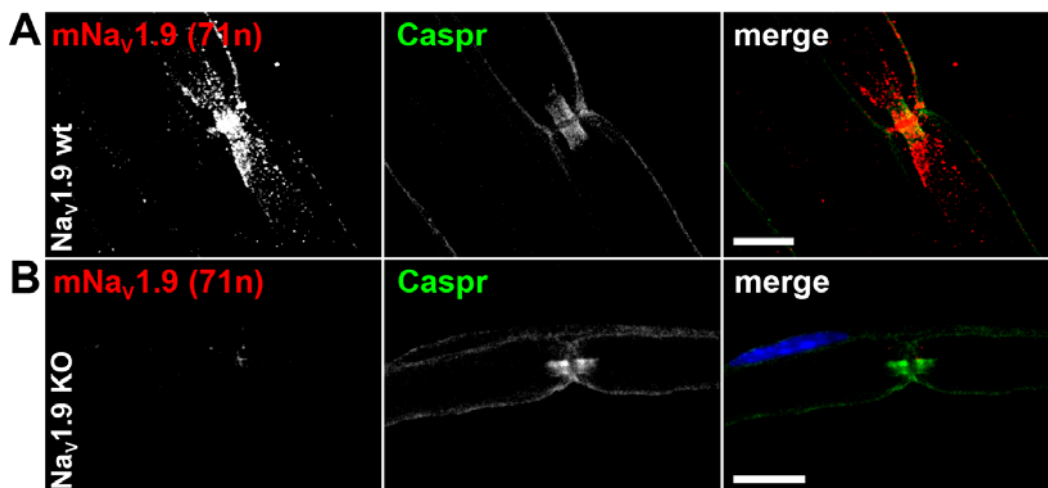


**Figure 18: Detection of Na<sub>v</sub>1.9 protein in femoral quadriceps nerve fibres**

(A and B) Single confocal sections of anti-mouse Na<sub>v</sub>1.9 stained teased fibres of the femoral quadriceps nerve by laser scanning microscopy. Caspr as paranode marker and nuclear DAPI served as counterstain. Bar: 10 μm. (A) Anti-mouse Na<sub>v</sub>1.9 immunoreactivity concentrated at the node of Ranvier of femoral quadriceps nerve fibres from adult wild type mice. (B) Mouse Na<sub>v</sub>1.9 protein is not detectable at the node of Ranvier of quadriceps nerve fibres from adult Na<sub>v</sub>1.9<sup>-/-</sup> mice. Caspr = contactin-associated protein; DAPI = 4', 6-diamidino-2-phenylindole

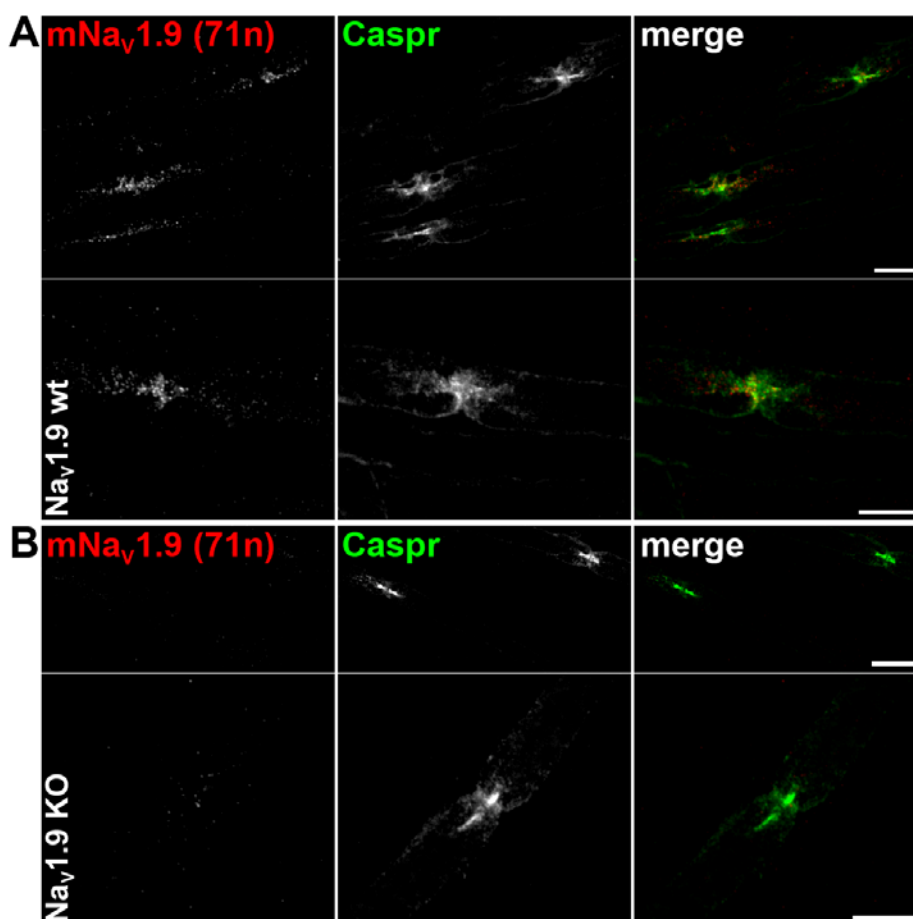


**Figure 19: Detection of Na<sub>v</sub>1.9 protein in facial nerve fibres**

(A and B) Representative confocal sections of anti-mouse Na<sub>v</sub>1.9 stained teased fibres of the facial nerve by laser scanning microscopy. Caspr staining served as control. Bar: 10 μm (A) Anti-mouse Na<sub>v</sub>1.9 immunoreactivity concentrated at the node of Ranvier of facial nerve fibres from adult wild type mice (B) Mouse Na<sub>v</sub>1.9 protein is not detectable at the node of Ranvier of facial nerve fibres from adult Na<sub>v</sub>1.9<sup>-/-</sup> mice. Caspr = contactin-associated protein

Mouse and rat facial motoneurons are important for the innervation of whisker muscles and motoneurons of the femoral quadriceps nerve innervate the quadriceps muscle. Our immunohistochemistry experiments revealed a signal for Na<sub>v</sub>1.9 protein at nodes of Ranvier of femoral quadriceps nerve fibres as well as of facial nerve fibres from wild type mice (Figure 18A and 19A). Na<sub>v</sub>1.9 appeared partially in a very strong punctuated formation at nodes of Ranvier in both wild type nerves. The signal was not found at nodes of Ranvier of femoral quadriceps nerve fibres and of facial nerve fibres isolated from Na<sub>v</sub>1.9 knock-out mice (Figure 18B and 19B). This observation verified the specificity of this finding.

### 3.3 The axons of motoneurons from Na<sub>v</sub>1.9<sup>-/-</sup> mice are shorter

As indicated previously, treatment of cultured motoneurons with voltage-gated sodium channel pore blockers resulted in a reduction of spontaneous neural activity and axon expansion (*Jablonka et al. 2007, Subramanian et al. 2012*). To investigate the role of Na<sub>v</sub>1.9 in activity-dependent axon growth, motoneurons were isolated from Na<sub>v</sub>1.9 knock-out and strain-matched wild type mice and cultured for 7 days *in vitro* at low density. Immunocytochemistry experiments performed by Dr. Narayan Subramanian and PD Dr. Robert Blum verified no anti-mouse Na<sub>v</sub>1.9 signal in motoneurons from Na<sub>v</sub>1.9 knock-out mice compared to motoneurons from wild type mice (*Subramanian et al. 2012*). Furthermore, Na<sub>v</sub>1.9 knock-out motoneurons show reduced rates of global Ca<sup>2+</sup> transients, distributed all over the cell, and local spontaneous Ca<sup>2+</sup> transients, in the soma and growth cones (*Subramanian et al. 2012*).

Analysis regarding the axon length of motoneurons revealed a 38% reduction of axon length from Na<sub>v</sub>1.9 knock-out motoneurons compared to axon length from wild type motoneurons (Figure 20), which is in accordance with a reduced level of local calcium transients in the distal axon and growth cone (*Jablonka et al. 2007, Subramanian et al. 2012, Wetzel et al. 2013*). Consequently, the Na<sub>v</sub>1.9 channel seems to play an important role in the process of activity-dependent axon augmentation of young motoneurons.

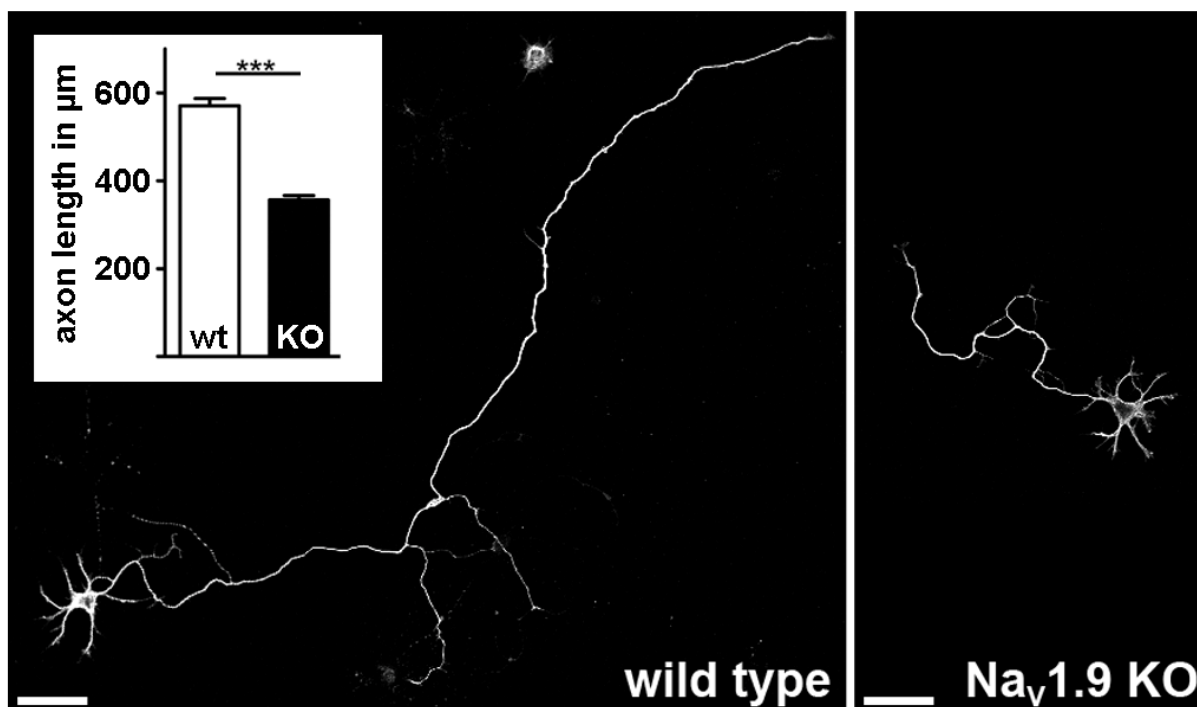


**Figure 20: Axon length of motoneurons from Na<sub>v</sub>1.9 wild type and knock-out mice**

Reduced axon elongation of motoneurons from Na<sub>v</sub>1.9 knock-out mice. Representative confocal sections of DIV 7, α-tubulin stained motoneurons from wild type and Na<sub>v</sub>1.9<sup>-/-</sup> mice. Bar: 40 μm. Statistical analysis performed by Dr. Narayan Subramanian (wild type: n = 286, Na<sub>v</sub>1.9<sup>-/-</sup>: n = 447, 3 independent cultures) Results represent the mean ±SEM of pooled data. \*\*\* P < 0.001 tested by two-tailed nonparametric Mann-Whitney test. DIV = day *in vitro*; KO = knock-out; wt = wild type

### 3.4 Reduced axon growth of Na<sub>v</sub>1.9<sup>-/-</sup> motoneurons can be rescued by a Na<sub>v</sub>1.9 encoding virus

The axon growth of motoneurons from Na<sub>v</sub>1.9 knock-out mice is reduced compared to wild type littermates (Figure 20). To analyse whether this knock-out effect can be rescued, low density motoneurons were infected with a Na<sub>v</sub>1.9 encoding virus. The same virus was used to generate a stable Na<sub>v</sub>1.9 expressing cell line as described under "3.2.1 Generation of a stable Na<sub>v</sub>1.9 expressing cell line". Motoneurons were infected directly after plating. They grew for 5 days *in vitro* and axon length was measured directly after immunocytochemistry and confocal microscopy. Axons of infected wild type motoneurons were longer compared to axons from wild type motoneurons without Na<sub>v</sub>1.9 virus infection (Figure 21C). The same experiment was performed with motoneurons from Na<sub>v</sub>1.9 knock-out mice. Axons of Na<sub>v</sub>1.9 knock-out motoneurons with Na<sub>v</sub>1.9 virus infection grew longer than axons of untransduced Na<sub>v</sub>1.9 knock-out motoneurons (Figure 21A, B and D). Thus, re-expression of Na<sub>v</sub>1.9 in Na<sub>v</sub>1.9-deficient motoneurons can partially rescue activity-dependent axon elongation (Figure 21D).

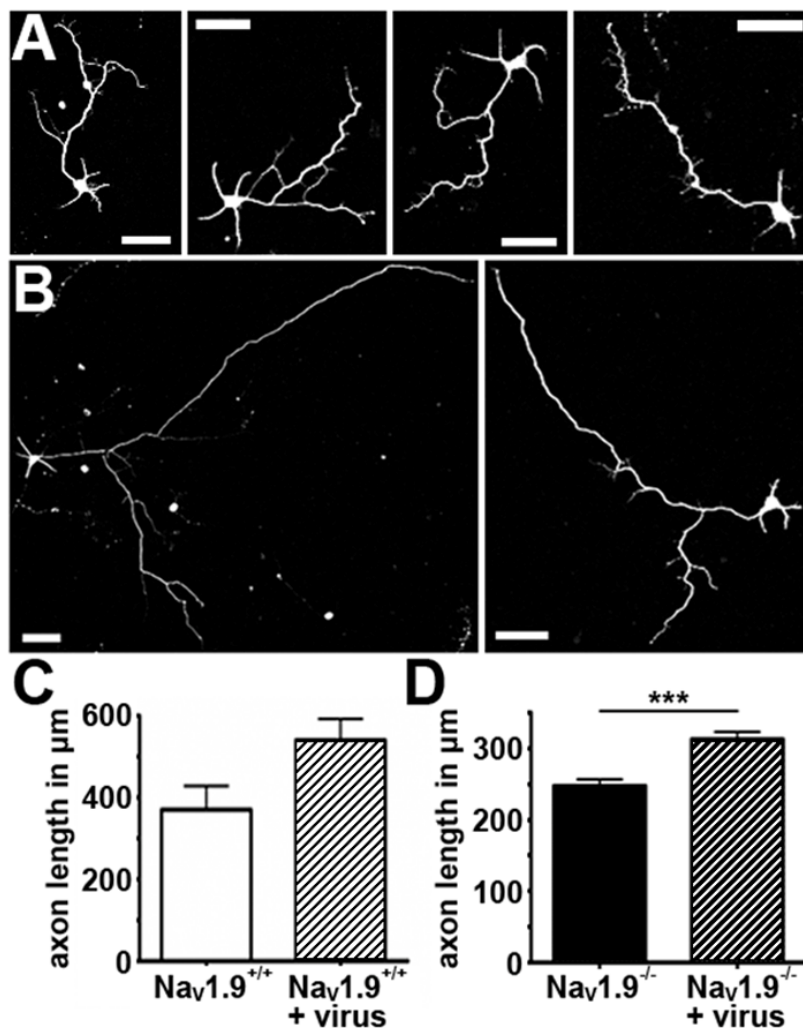


**Figure 21: Axon length of motoneurons from  $Nav_1.9$  wild type and knock-out mice with and without  $Nav_1.9$  virus infection**

Increased axon elongation of DIV 5 motoneurons from wild type and  $Nav_1.9^{-/-}$  mice after  $Nav_1.9$  encoding virus infection. **(A and B)** Representative single confocal sections of  $\alpha$ -tubulin stained motoneurons from  $Nav_1.9^{-/-}$  mice without (A) and with  $Nav_1.9$  virus infection (B). Bar: 50  $\mu m$ . **(C)** Axon length of wild type motoneurons with and without  $Nav_1.9$  virus infection (wild type: n = 30, wild type + virus: n = 35, 1 independent culture). **(D)** Statistical analysis of axonal elongation of  $Nav_1.9$  knock-out motoneurons with and without  $Nav_1.9$  virus infection ( $Nav_1.9^{-/-}$ : n = 136,  $Nav_1.9^{-/-}$  + virus: n = 216, 2 independent cultures). Results represent the mean  $\pm$ SEM of pooled data. \*\*\*  $P < 0.0001$  tested by two-tailed nonparametric Mann-Whitney test. DIV = day *in vitro*; SEM = standard error of the mean

### 3.5 $Nav_1.9$ protein is present in growth cones of motoneurons from $Smn^{-/-}$ - $SMN2tg$ mice

Our results demonstrated that the  $Nav_1.9$  channel is important for the process of axon growth in motoneurons. In a mouse model for the motoneuron disease, spinal muscular atrophy (SMA), spontaneous  $Ca^{2+}$  transients are reduced because of defects in  $Ca_v2.2$  clustering at axonal terminals, which correlates with decreased axon growth (Jablonka *et al.* 2007). In order to investigate whether these observations in motoneurons from  $Smn$ -deficient mice are also influenced by a disturbed distribution of the  $Nav_1.9$  channel,  $Smn^{-/-}$ - $SMN2tg$  motoneurons were cultured for 7 days *in vitro*, fixed and labelled with anti-mouse  $Nav_1.9$  antibody. As indicated in Figure 22,  $Nav_1.9$  protein was still found in axons and axonal growth cones of  $Smn^{-/-}$ - $SMN2tg$  motoneurons (Figure 22). Additional experiments via qPCR revealed normal expression levels of  $Nav_1.9$  in motoneurons from  $Smn$ -deficient and wild type mice (Subramanian *et al.* 2012). Moreover, treatment of  $Smn^{-/-}$ - $SMN2tg$  motoneurons with 10 nM STX led to an unchanged axon elongation, thus functional block of VGSCs had

no further growth inhibiting effect (Subramanian *et al.* 2012), indicating that Na<sub>v</sub>1.9 may serve as a target molecule to restore neuronal activity in SMA-diseased motoneurons.

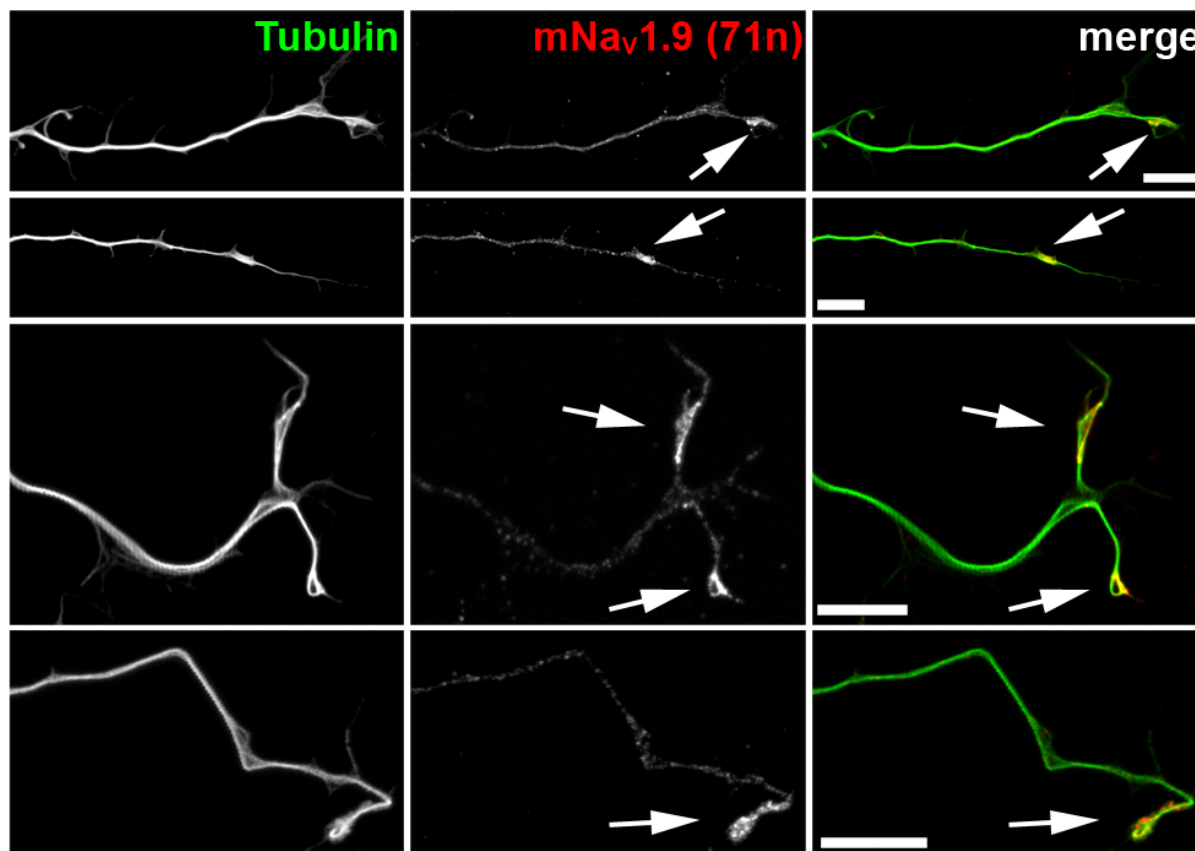


**Figure 22: Na<sub>v</sub>1.9 labelling in motoneurons from *Smn*<sup>-/-</sup>-*SMN2tg* mice**

Single confocal sections of anti-mouse Na<sub>v</sub>1.9 staining in motoneurons from *Smn*<sup>-/-</sup>-*SMN2tg* mice by standard laser scanning microscopy of  $\alpha$ -tubulin staining. Anti-mouse Na<sub>v</sub>1.9 immunoreactivity concentrated in distal axonal regions and growth cones (arrows). Bar: 10  $\mu$ m. SMN = survival motoneuron; tg = transgene

### 3.6 Mutant Na<sub>v</sub>1.9 is expressed in DRGs from *Scn11a*<sup>+L788P</sup> mice

In parallel to this work our cooperation partners in Jena identified a specific *de novo* missense mutation in the *SCN11A* gene, encoding the Na<sub>v</sub>1.9 channel in human (Leipold *et al.* 2013). The mutation results in the replacement of leucine 811 by proline at the distal end of the sixth transmembrane segment in domain II of Na<sub>v</sub>1.9, a highly conserved position. Affected individuals showed self-mutilations, slow-healing wounds and multiple painless fractures as result of the inability to feel pain since birth. Interestingly, these patients also developed a mild muscular weakness and delayed motor development, probably due to the role of Na<sub>v</sub>1.9 in the development of motoneurons.

To understand the pathogenicity of the human Leu811Pro alteration, heterozygous knock-in mice were generated that carry the orthologous mutation (Leipold *et al.* 2013). These *Scn11a*<sup>+L799P</sup> (Na<sub>v</sub>1.9<sup>+P</sup>) mice displayed reduced sensitivity to pain, self-inflicted tissue

lesions and a prominent gain-of-function phenotype, increasing the basal activity of  $\text{Na}_v1.9$  channels. We supported the study by the providing of our verified  $\text{Na}_v1.9$  encoding vectors. In order to characterize  $\text{Na}_v1.9^{+/P}$  mice molecularly, the mRNA level as well as the protein level of wild type and mutant  $\text{Na}_v1.9$  in DRG neurons from certain mouse lines were analysed (Figure 23).

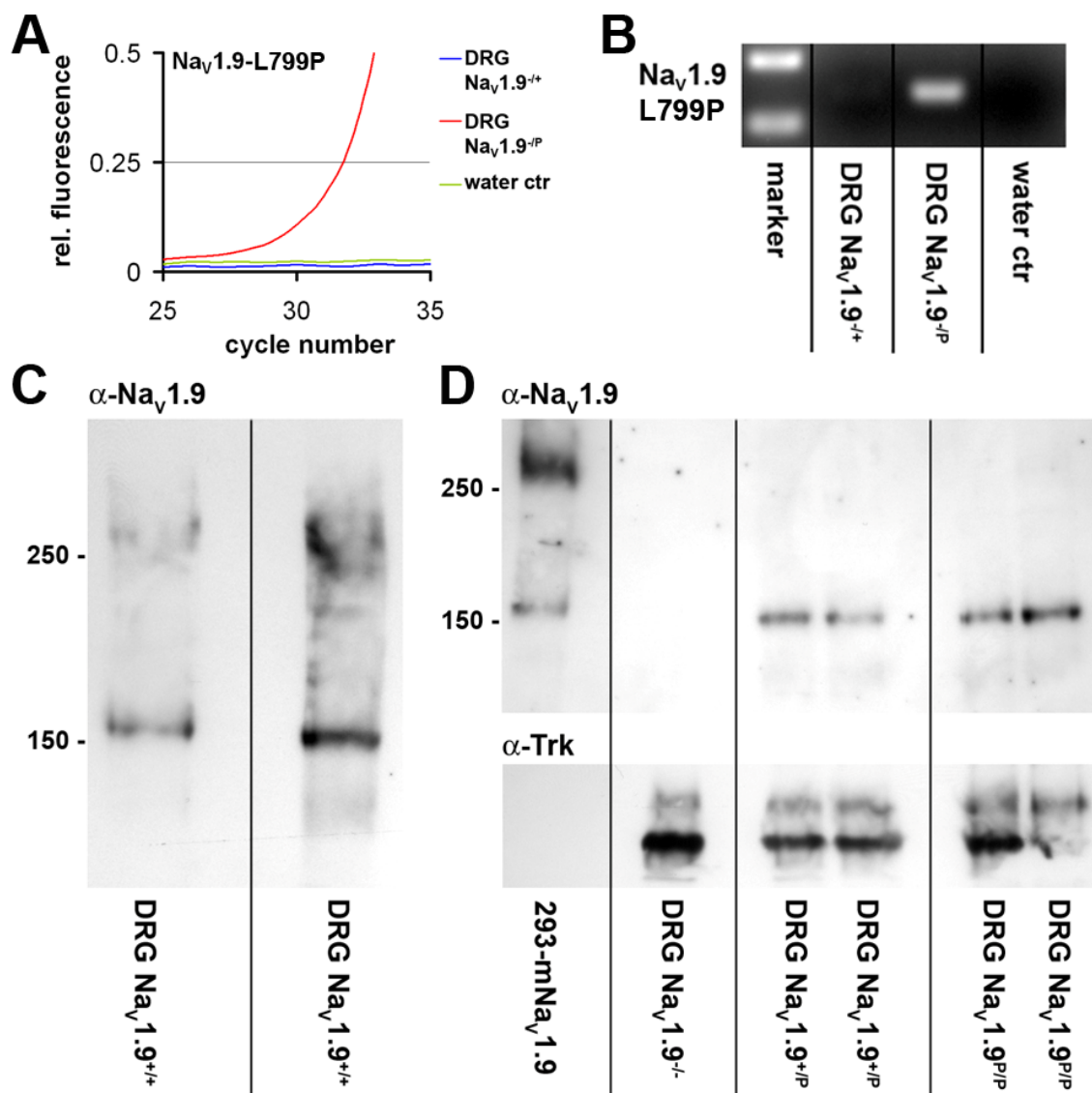


**Figure 23: Detection of mutant  $\text{Na}_v1.9$  transcripts and  $\text{Na}_v1.9$  protein in dorsal root ganglia from wild type and mutant mice**

**(A and B)** Representative amplification products after  $\text{Na}_v1.9\text{-L799P}$  qRT-PCR with indicated cDNA samples. **(A)** Real-time monitoring of the fluorescence emission of SYBR Green I during PCR amplification of mutant  $\text{Na}_v1.9\text{-L799P}$  in DRG neurons from different mouse lines. **(B)** Expression of mutant  $\text{Na}_v1.9\text{-L799P}$  transcripts only in DRGs of  $\text{Na}_v1.9^{P/P}$  mice. **(C and D)** Detection of  $\text{Na}_v1.9$  protein via western blot analysis displayed by the typical double band pattern with bands at approximately 180 kDa and ~280 kDa. Endogenous mouse  $\text{Na}_v1.9$  from lumbar and thoracic DRG neurons from wild type (C),  $\text{Na}_v1.9^{-/-}$ ,  $\text{Na}_v1.9^{+/P}$  and  $\text{Na}_v1.9^{P/P}$  mice and as control recombinant  $\text{Na}_v1.9$  in the stable cell line 293-m $\text{Na}_v1.9$  (D). Anti-Trk antibodies served as loading control for DRG tissue. cDNA = copy/complementary deoxyribonucleic acid; ctr = control; DRG = dorsal root ganglia; HEK = human embryonic kidney; kDa = kilo dalton; Trk = tropomyosin receptor kinase; qRT-PCR = quantitative real time polymerase chain reaction



For the amplification of mutant Na<sub>v</sub>1.9 transcripts, RNA was isolated from DRG tissue of heterozygous mice encoding either one copy of wild type Na<sub>v</sub>1.9 (Na<sub>v</sub>1.9<sup>-/+</sup>) or one copy of mutant Na<sub>v</sub>1.9 (Na<sub>v</sub>1.9<sup>-P</sup>). Representative amplification products and RT-PCR amplification curves are shown in Figure 23A and B. Mutant Na<sub>v</sub>1.9 transcripts were identified in DRG neurons from heterozygous mice encoding one copy of mutant Na<sub>v</sub>1.9 (Na<sub>v</sub>1.9<sup>-P</sup>). This observation raised the question whether mutant Na<sub>v</sub>1.9 protein is found in DRGs of mutant knock-in mice, too.

Western blot analysis demonstrated the typical double band pattern with a band at ~180 kDa and a band at ~280 kDa for Na<sub>v</sub>1.9 in DRG neurons from wild type mice and in the stable Na<sub>v</sub>1.9 expressing cell line (Figure 23C and D). This signal was absent in DRG neurons from Na<sub>v</sub>1.9 knock-out mice, while Na<sub>v</sub>1.9 detection in heterozygous and homozygous mutant DRG neurons (Na<sub>v</sub>1.9<sup>+P</sup> and Na<sub>v</sub>1.9<sup>P/P</sup>) appeared at least in one band at ~180 kDa (Figure 23D). Western blots with a longer exposure time confirmed the typical band at ~280 kDa for Na<sub>v</sub>1.9 control littermates and in DRG tissue from Na<sub>v</sub>1.9<sup>+P</sup> and Na<sub>v</sub>1.9<sup>P/P</sup> mice. In summary, mutated Na<sub>v</sub>1.9 protein was stably expressed in DRG tissue from heterozygous and homozygous Na<sub>v</sub>1.9 knock-in mice, carrying one or two copies of the orthologous missense mutation.

### **3.7 TrkB protein is localized in cultured embryonic motoneurons and at the node of Ranvier of facial nerve fibres**

Na<sub>v</sub>1.9 channels play an important role in activity-dependent axon growth in motoneurons (*Subramanian et al. 2012*). However the analysis of mechanisms that regulate the opening of Na<sub>v</sub>1.9 channels became a critical issue. Studies on fast excitatory transients after BDNF application proposed a link between Na<sub>v</sub>1.9 channel opening and BDNF induced activation of TrkB receptors in central neurons (*Blum et al. 2002, Lang et al. 2007*). In order to identify a possible trigger that increases the open probability of Na<sub>v</sub>1.9 channels in motoneurons, thus regulating activity-dependent Ca<sup>2+</sup> influx and axon elongation, TrkB full knock-out mice were analysed.

#### **3.7.1 Detection of TrkB protein in cultured embryonic motoneurons**

In cultured embryonic motoneurons, the Na<sub>v</sub>1.9 channel was detectable along the axon and enriched at soma and growth cone sites (see 3.2.3), where local Ca<sup>2+</sup> transients are observed. When TrkB receptors are triggers for local Na<sub>v</sub>1.9 channel opening, these receptor tyrosine kinases should be present in close proximity to Na<sub>v</sub>1.9. To test this hypothesis, cultured motoneurons from wild type and TrkB knock-out mice were analysed by

immunocytochemistry. Anti-TrkB antibodies detected TrkB in wild type motoneurons, but not in motoneurons from TrkB knock-out mice (Figure 24). TrkB receptors were localized at positions where  $\text{Na}_V1.9$  channels are also found in young cultured motoneurons. Anti-TrkB immunoreactivity was enriched at somatic sites, in axon terminals and represented a punctuated formation along the axon (Figure 24A). Thus, TrkB receptors are possible candidates for  $\text{Na}_V1.9$  channel triggering in motoneurons during the process of axon growth.

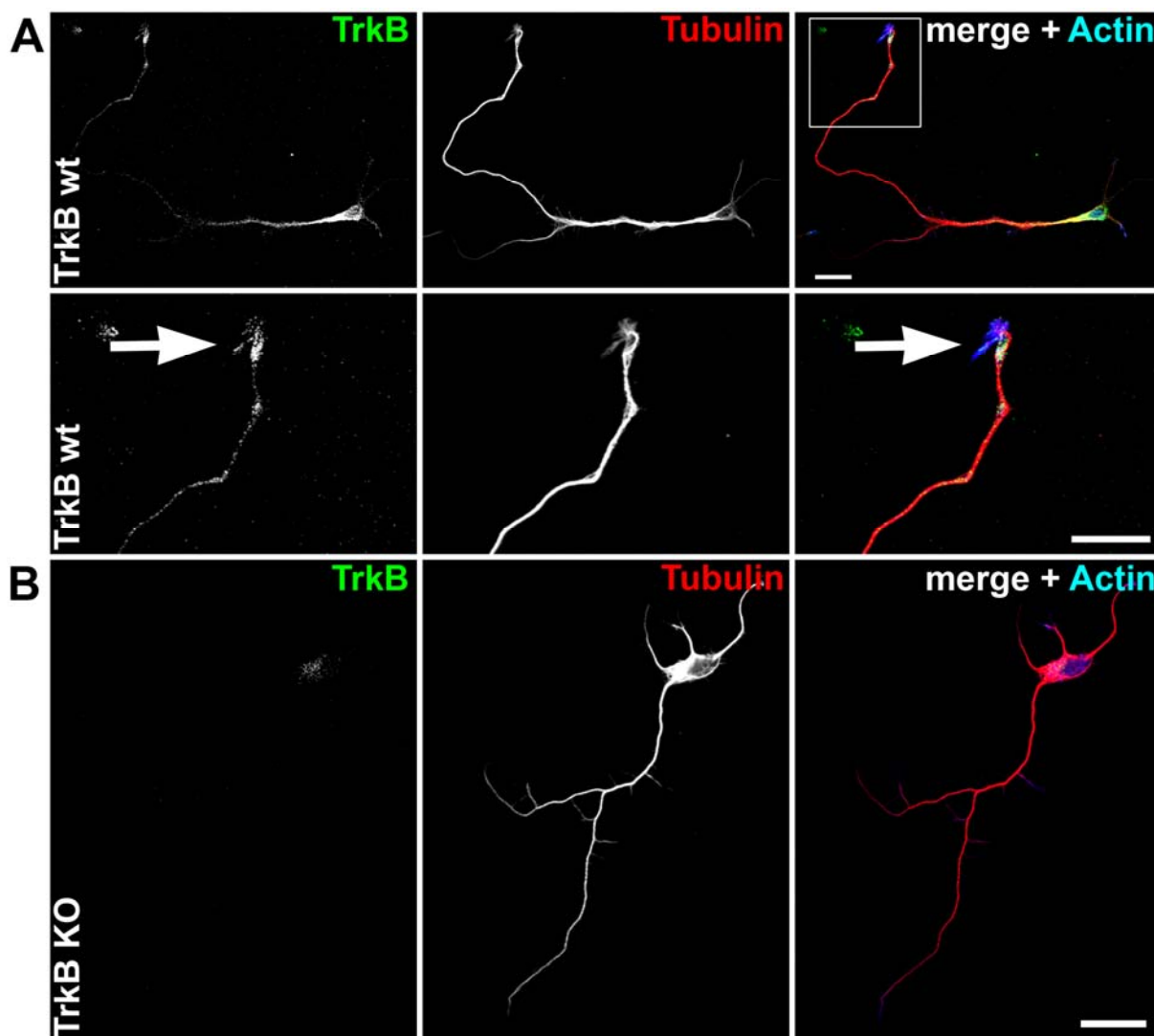


**Figure 24: Recognition of TrkB protein in cultured embryonic motoneurons**

**(A and B)** Representative single confocal sections of anti-TrkB stained, DIV 5 motoneurons by standard laser scanning microscopy. Actin and  $\alpha$ -tubulin staining served as reference. Bar: 20  $\mu\text{m}$ . **(A)** Anti-TrkB immunoreactivity, concentrated in the soma and in axon terminal regions of wild type motoneurons with enlarged inlet of the axonal growth cone (lower panel). **(B)** TrkB signal is not detectable in motoneurons from TrkB knock-out mice. DIV = day *in vitro*; KO = knock-out; Trk = tropomyosin receptor kinase; wt = wild type

### 3.7.2 Localization of TrkB protein in facial nerve fibres

Na<sub>v</sub>1.9 channel was found at the node of Ranvier of teased fibres of motor and sensory nerves of adult wild type mice *in vivo* (see 3.2.4). To test whether TrkB is also present at the node of Ranvier, facial nerves were dissected and stained with anti-TrkB antibody and anti-Caspr antibody. The latter antibody was used to identify the nodes of Ranvier along the myelinated axon.

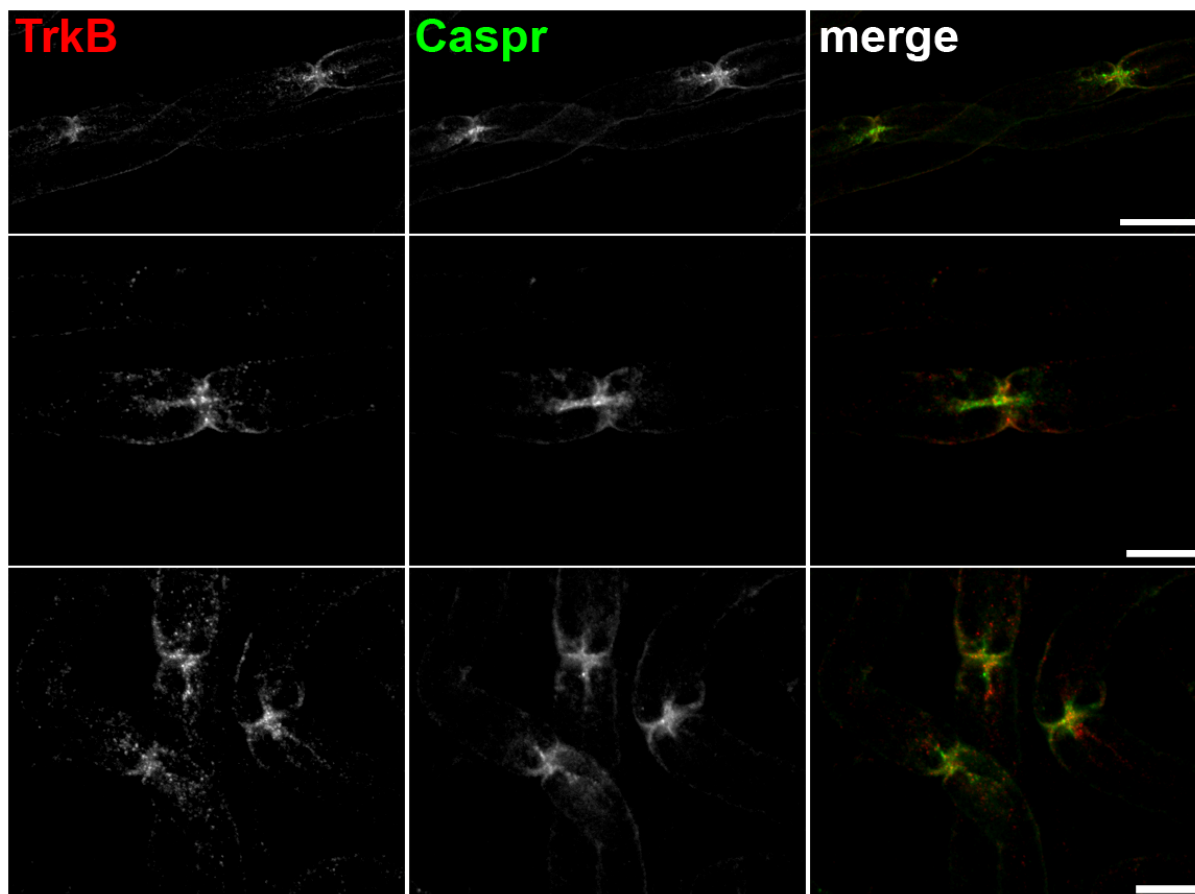


**Figure 25: Labelling of TrkB protein at the node of Ranvier of facial nerve fibres**

Representative confocal sections of TrkB labelled teased fibres of the facial nerve by laser scanning microscopy. Caspr staining provided as control. Bar: 20  $\mu$ m (upper panel) and 10  $\mu$ m (middle and lower panel). Anti-TrkB immunoreactivity concentrated at the node of Ranvier of facial nerve fibres from adult wild type mice. Caspr = contactin-associated protein; Trk = tropomyosin receptor kinase

Anti-TrkB antibodies identified TrkB protein at nodes of Ranvier of facial nerve fibres of adult wild type mice (Figure 25). The anti-TrkB signal appeared in a strong punctuated formation at the nodes of Ranvier. This reveals that TrkB as well as Na<sub>v</sub>1.9 are both present at nodes of Ranvier.

### 3.8 Spontaneous activity is reduced in motoneurons from TrkB<sup>-/-</sup> mice

In order to test whether the loss of TrkB receptors affects spontaneous excitability, motoneurons of TrkB knock-out mice were isolated and cultured for four and seven days *in vitro*. Motoneurons were loaded with the high affinity intracellular calcium indicator Oregon Green 488 BAPTA-1, AM and spontaneous Ca<sup>2+</sup> transients were measured under continuous perfusion with ACSF-Ringer. Wild type motoneurons exhibited peak like Ca<sup>2+</sup> transients at DIV 4 and DIV 7, while in growth cones more Ca<sup>2+</sup> transients were observed than in somatodendritic regions (Figure 26). Motoneurons of TrkB knock-out mice revealed significantly reduced rates of spontaneous Ca<sup>2+</sup> transients compared to strain-matched wild type controls at DIV 4 and DIV 7, in the soma and the growth cone (Figure 26), indicating that the loss of TrkB receptors affects global and local Ca<sup>2+</sup> transients in motoneurons.

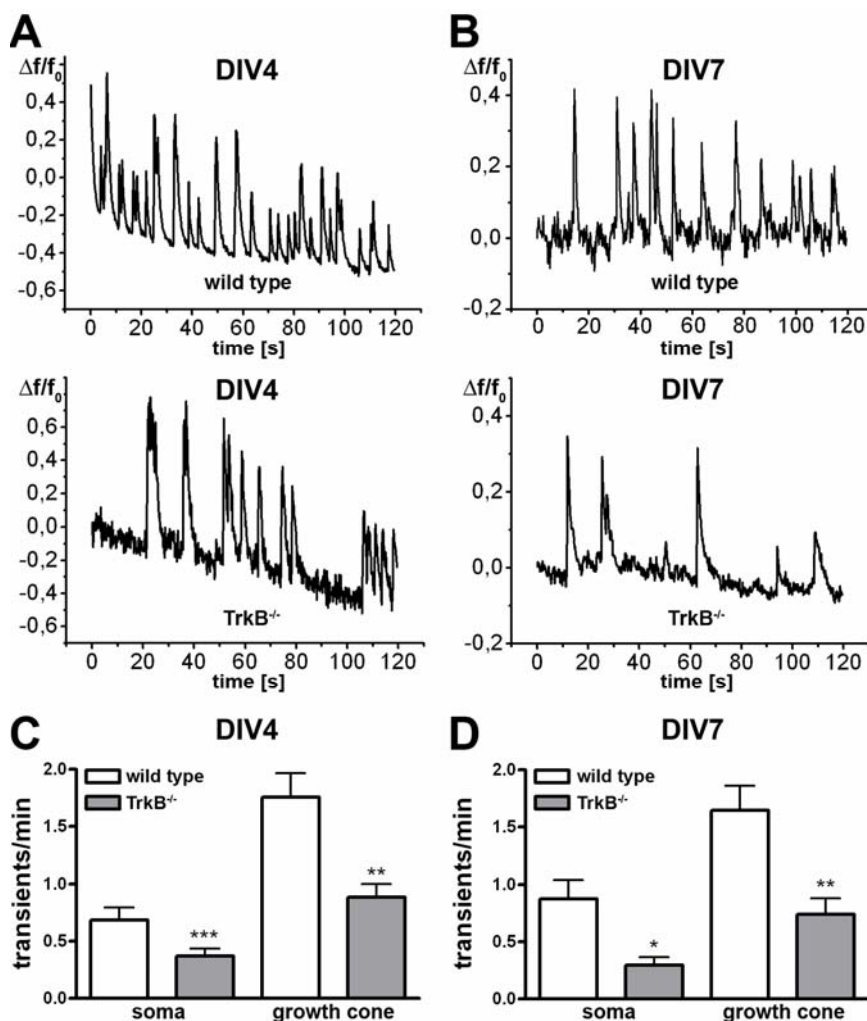


**Figure 26: Spontaneous activity of motoneurons from wild type and TrkB<sup>-/-</sup> mice**

Spontaneous calcium transients in wild type and TrkB<sup>-/-</sup> motoneurons loaded with Oregon Green 488 BAPTA-1, AM at DIV 4 (A and C) and DIV 7 (B and D). (A and B) Representative curves showing calcium-dependent changes in fluorescence intensity ( $\Delta f/f_0$ ) measured in growth cone regions of motoneurons from wild type (upper panel) and TrkB<sup>-/-</sup> (lower panel) mice at DIV 4 (A) and DIV 7 (B). (C and D) Statistical analysis of the frequency of spontaneous Ca<sup>2+</sup> transients (transients/min) determined at DIV 4 (C) and DIV 7 (D) at the soma and growth cone of wild type and TrkB<sup>-/-</sup> motoneurons (DIV 4: soma: wt = 85, KO = 98, growth cone: wt = 94, KO = 114, 4 independent cultures; DIV 7: soma:

wt = 73, KO = 71, growth cone: wt = 95, KO = 81; 4 independent cultures). Results represent the mean  $\pm$ SEM of pooled data. \*\*\*  $P < 0.001$ , \*\*  $P < 0.01$ , \*  $P < 0.05$  tested by two-tailed nonparametric Mann-Whitney test. DIV = day *in vitro*; KO = knock-out; SEM = standard error of the mean; Trk = tropomyosin receptor kinase; wt = wild type

### 3.9 The axons of motoneurons from $TrkB^{-/-}$ mice are shorter

With the intention to clarify whether TrkB receptors are also involved in the regulation of activity-dependent axon elongation of motoneurons, the axon length of TrkB knock-out motoneurons and control littermates was analysed. Motoneurons were isolated from wild type and TrkB knock-out mice and cultured for five and seven days *in vitro*. Then, motoneurons were fixed and labelled with anti- $\alpha$ -tubulin antibodies and the axon length was determined. Axons of TrkB knock-out motoneurons were shorter than axons of wild type motoneurons at DIV 5 and DIV 7 (Figure 27). Hence, the loss of TrkB receptors affects the process of axon growth in motoneurons, too.

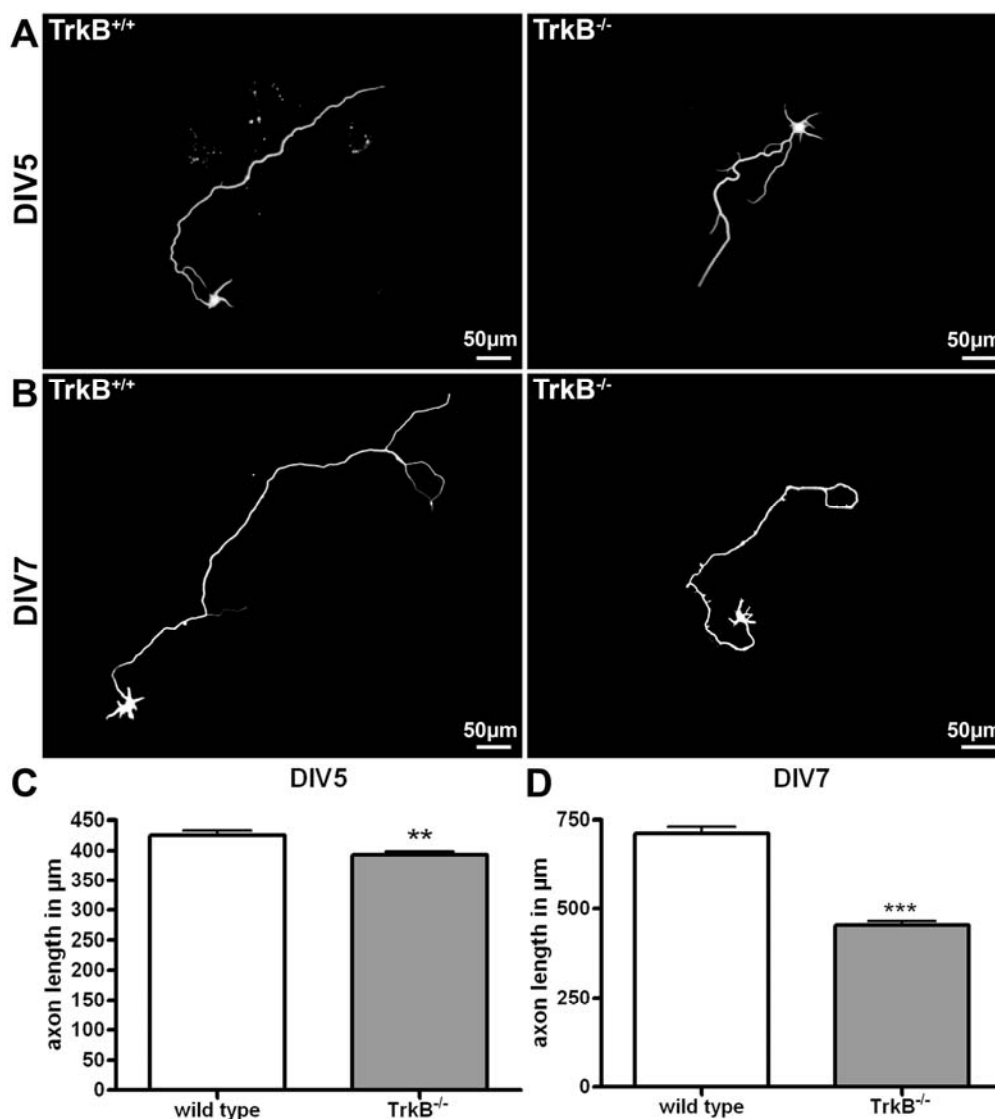


**Figure 27: Axon length of cultured motoneurons from wild type and  $TrkB^{-/-}$  mice**

Reduced axon growth of motoneurons from TrkB knock-out mice. **(A and B)** Representative confocal sections of DIV 5 (A) and DIV 7 (B),  $\alpha$ -tubulin stained motoneurons from wild type and  $TrkB^{-/-}$  mice. Bar: 50  $\mu$ m. **(C and D)** Statistical analysis of the axon length of motoneurons from wild type and  $TrkB^{-/-}$  mice at DIV 5 (wild type: n = 465,  $TrkB^{-/-}$ : n = 563, 2 independent cultures) (C) and DIV 7 (wild type: n = 284,  $TrkB^{-/-}$ : n = 310, 3 independent cultures) (D). Results represent the mean  $\pm$ SEM of pooled data. \*\*\*  $P < 0.001$ , \*\*  $P < 0.01$  tested by two-tailed nonparametric Mann-Whitney test. DIV = day *in vitro*; SEM = standard error of the mean; Trk = tropomyosin receptor kinase

### 3.10 BDNF and TrkB mediate motoneuron survival by two independent mechanisms

Neurotrophic factors like BDNF, CNTF, NT-3 and NT-4 support the survival of motoneurons (Arakawa *et al.* 1990, Sendtner *et al.* 2000). These molecules act through members of the Trk family of receptor tyrosine kinases (TrkB and TrkC) or in the case of CNTF through complex membrane receptors like gp130, LIFR $\beta$  and CNTFR $\alpha$  (Sendtner *et al.* 2000, Chao *et al.* 2006). The pharmacological inhibition of voltage-gated sodium channels and the loss of Na<sub>v</sub>1.9 channels in motoneurons did not affect motoneuron survival (Subramanian *et al.* 2012). Nevertheless, to test whether the loss of TrkB had an effect on neurotrophin-mediated motoneuron survival, wild type and TrkB<sup>-/-</sup> motoneurons were cultivated with either BDNF (5 ng/ml) or CNTF (5 ng/ml) or with and without both factors together. After five or seven days *in vitro* the percentage survival of motoneurons relative to originally plated cells was determined. A cultivation of wild type and TrkB<sup>-/-</sup> motoneurons with CNTF only or BDNF and CNTF together promoted motoneuron survival. In contrast, in presence of BDNF alone the survival of TrkB<sup>-/-</sup> motoneurons was reduced after five and seven days *in vitro* (Figure 28).

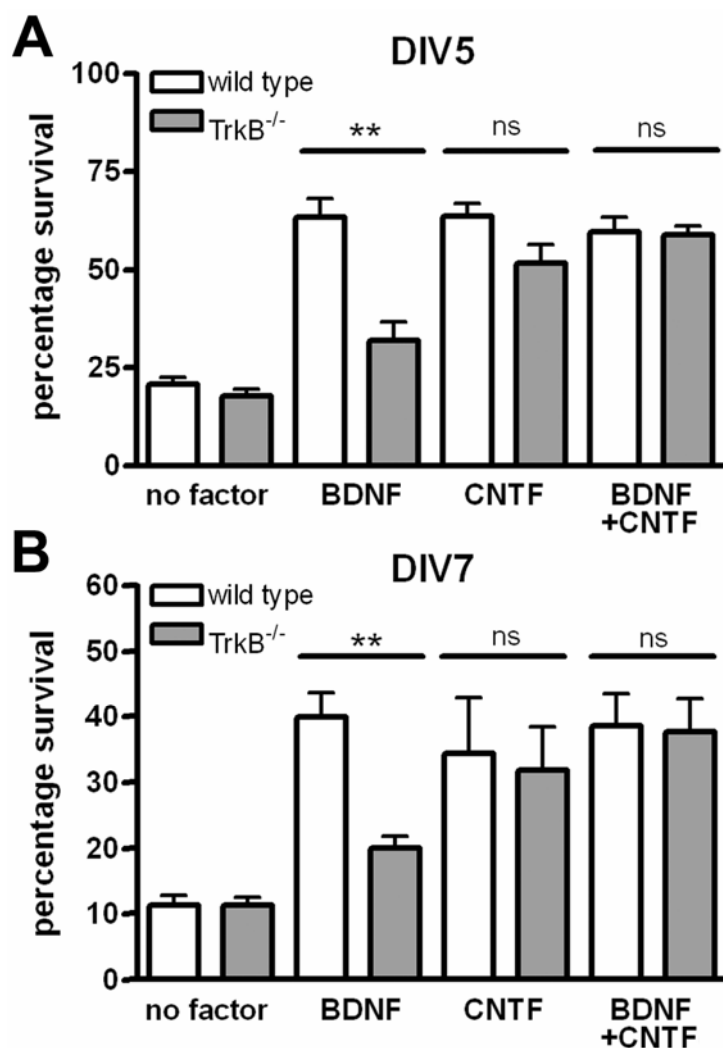


**Figure 28: Survival of cultured motoneurons from TrkB<sup>+/+</sup> and TrkB<sup>-/-</sup> mice**

(A and B) Statistical analysis of motoneuron survival of DIV 5 (A) and DIV 7 (B) motoneurons from wild type and TrkB<sup>-/-</sup> mice in the presence or absence of neurotrophic factors (DIV 5: BDNF: n = 5 independent cultures; CNTF: n = 4 independent cultures; BDNF + CNTF: n = 6 independent cultures; DIV 7: BDNF: n = 5 independent cultures; CNTF: n = 4 independent cultures; BDNF + CNTF: n = 7 independent cultures). Results represent the mean  $\pm$ SEM of pooled data. \*\*  $P < 0.01$  tested by two-tailed nonparametric Mann-Whitney test. BDNF = brain-derived neurotrophic factor; CNTF = ciliary neurotrophic factor; DIV = day *in vitro*; SEM = standard error of the mean; Trk = tropomyosin receptor kinase

Interestingly, despite a complete lack of all TrkB receptors, BDNF still had a substantial effect on motoneuron survival. Whether this BDNF-dependent survival affects only a subfraction of all motoneurons, or whether this effect is caused by BDNF activation of the TrkC receptor is not clear yet. TrkC is expressed in motoneurons and is able to bind BDNF with a low but functionally relevant affinity (*Philo et al. 1994, Sendtner et al. 2000*).

## 4 Discussion

Spontaneous neuronal activity plays an important role during development of the nervous system (O'Donovan & Landmesser 1987, Gu & Spitzer 1995, Spitzer 2006, Wang et al. 2009). Motoneurons become spontaneously active before they make synaptic interactions with their target tissue (Nishimaru et al. 1996, Milner & Landmesser 1999, Hanson & Landmesser 2004, Subramanian et al. 2012). This spontaneous calcium ion influx is important for growth cone differentiation and axon extension in cultured motoneurons (Jablonka et al. 2007, Subramanian et al. 2012). The aim of this thesis was the molecular discovery and characterization of regulators for spontaneous neuronal activity and activity-dependent axon growth in motoneurons. Voltage-gated sodium channels are key proteins for neuronal activity and action potential initiation, but spontaneous electrical activity in motoneurons is also a local event, and is therefore unlikely to be mediated by ligand-dependent initiation of action potentials (Wetzel et al. 2013). Basing on initial pharmacological hints in combination with its specific electrophysiological properties, the VGSC Na<sub>v</sub>1.9 became the most likely candidate for a sodium channel that can act as a local trigger of voltage-dependent calcium influx. This sodium channel is able to mediate subthreshold excitability and this specific feature may explain the initiation of local excitation events. Indeed, in cultured embryonic motoneurons, Na<sub>v</sub>1.9 was found at the soma, along the axon and enriched at the growth cone, a region where spontaneous neuronal activity is observed (Hanson & Landmesser 2004, Blankenship & Feller 2010, Subramanian et al. 2012). Moreover, Na<sub>v</sub>1.9 was found at the node of Ranvier of isolated nerve fibres, which represents the principle site of action potential generation in axons of adult motoneurons (Rumsey et al. 2009). Live cell imaging experiments performed by my colleagues demonstrated that spontaneous neuronal activity in motoneurons from Na<sub>v</sub>1.9 knock-out mice is reduced (Subramanian et al. 2012). As a consequence, activity-dependent axon elongation is reduced in motoneurons from these mice, too. This phenotype could not be compensated by other members of the family of voltage-gated sodium channels. Spontaneous excitation and the subsequent process of axon growth are disturbed in motoneurons from TrkB knock-out mice. Thus, TrkB acts as regulator for activity-dependent axon expansion in motoneurons, too, but it is not clear yet whether Na<sub>v</sub>1.9 and TrkB-dependent events are linked or independent events. A better understanding of the interplay of TrkB and Na<sub>v</sub>1.9 during the process of axon elongation and synapse maintenance would be helpful for the development of therapies for motoneuron diseases like spinal muscular atrophy.



## 4.1 The Na<sub>v</sub>1.9 channel is found in motoneurons

It was surprising that we found Na<sub>v</sub>1.9 channel expression in motoneurons. The channel is normally prominent for its expression in pain sensory neurons (*Dib-Hajj et al. 2002*) and earlier studies excluded Na<sub>v</sub>1.9 expression in central neurons, the spinal cord or embryonic tissue (*Dib-Hajj et al. 1998, Fukuoka et al. 2010*). Our data confirmed an exceptionally high expression level for Na<sub>v</sub>1.9 in dorsal root ganglia neurons and revealed Na<sub>v</sub>1.9 expression during early neuronal development in spinal cord tissue, where young motoneurons reside. Moreover, substantial amounts of Na<sub>v</sub>1.9 transcripts were found in cultured embryonic motoneurons at day 7, as well. In dorsal root ganglia, Na<sub>v</sub>1.9 expression increased continuously and became very high in older mice. In spinal cord, on the other hand, Na<sub>v</sub>1.9 expression decreased after birth. This observation suggests that Na<sub>v</sub>1.9 presence and activity seem to be necessary during early developmental periods, when axon growth of motoneurons takes place. In addition, expression of Na<sub>v</sub>1.9 in motoneurons was much lower than in DRG neurons, indicating that even low expression levels of Na<sub>v</sub>1.9 are sufficient to enhance neuronal excitability, to regulate spontaneous voltage-dependent calcium ion influx, and to support activity-dependent axon growth in motoneurons.

To localize Na<sub>v</sub>1.9 protein in cultured embryonic motoneurons, a Na<sub>v</sub>1.9 specific antibody was used which recognizes the C-terminal end of mouse Na<sub>v</sub>1.9. In western blot analysis the anti-mouse Na<sub>v</sub>1.9 antibody showed a double band pattern with one band at ~180 kDa and another band at ~280 kDa in DRG tissue as well as in lysates of a stable Na<sub>v</sub>1.9 expressing cell line. The signal was absent in DRG tissue from Na<sub>v</sub>1.9 knock-out mice. Immunocytochemistry experiments combined with super resolution imaging using stimulated emission depletion microscopy (STED) showed Na<sub>v</sub>1.9 localization preferentially in axons and axonal growth cones, regions where local calcium ion influx is pronounced (*Cohan et al. 1987, Hanson & Landmesser 2004, Jablonka et al. 2007, Blankenship & Feller 2010, Subramanian et al. 2012*). The Na<sub>v</sub>1.9 localization pattern in motoneurons is in accordance with a local excitatory action of the channel.

Beside the finding that Na<sub>v</sub>1.9 protein was detectable in embryonic motoneurons *in vitro*, immunohistochemistry experiments, using isolated nerve fibres, revealed Na<sub>v</sub>1.9 localization at the node of Ranvier, the general site of action potential generation in axons of adult motoneurons (*Rumsey et al. 2009*). Na<sub>v</sub>1.9 channel was previously found at some nodes of Ranvier of thinly myelinated axons of the sciatic nerve (*Fjell et al. 2000*). The peripheral facial nerve is a primary motor nerve (*Sendtner et al. 1996*) leading to the conclusion that Na<sub>v</sub>1.9 may regulate the excitability at nodes of Ranvier as well.

## 4.2 Is Na<sub>v</sub>1.9 a therapeutic target for motor defects?

The findings of this dissertation reveal that the Na<sub>v</sub>1.9 channel is an important trigger for activity-dependent axon outgrowth in young cultured motoneurons. To understand this mechanism in detail is of central interest for the development of therapies for motoneuron diseases like spinal muscular atrophy. Isolated motoneurons from a mouse model for spinal muscular atrophy show defects in synapse maintenance. A reduced number of  $\beta$ -actin mRNA and locally synthesised  $\beta$ -actin protein was observed in growth cones of *Smn*-deficient motoneurons (Rossoll *et al.* 2003, Rathod *et al.* 2012). This cytoskeletal defects result in an affected cell-surface clustering of the N-type calcium channel Ca<sub>v</sub>2.2, leading to reduced local calcium influx (Jablonka *et al.* 2007, Ruiz *et al.* 2010, Wetzel *et al.* 2013). Isolated motoneurons from *Smn*-deficient mice have shorter axons than wild type littermates (Rossoll *et al.* 2003, Jablonka *et al.* 2007). Immunocytochemical experiments indicated that the Na<sub>v</sub>1.9 channel distribution is not affected in growth cones of *Smn*<sup>-/-</sup>-*SMN2*<sup>tg</sup> motoneurons. Substantial amounts of the channel are present in motoneurons of *Smn*-deficient mice. Earlier publications have confirmed that intracellular signalling pathways can modulate persistent sodium currents by Na<sub>v</sub>1.9 (Rush & Waxman 2004, Ostman *et al.* 2008) and we observed that lentiviral overexpression of Na<sub>v</sub>1.9 rescues the phenotype of impaired axon growth in motoneurons from Na<sub>v</sub>1.9 knock-out mice. These findings raise the hope that pharmacological increase of the open probability of Na<sub>v</sub>1.9 might support synapse maintenance of motoneurons suffering from SMA deficiency and therefore making Na<sub>v</sub>1.9 to a possible therapeutic target for spinal muscular atrophy and even axon regeneration.

Beside other more prominent symptoms like the inability to feel pain since birth, the motor system is also affected in patients with a missense mutation in the *SCN11A* gene, encoding Na<sub>v</sub>1.9 (Leipold *et al.* 2013). Affected individuals suffer from a mild muscular weakness and delayed motor development. Muscle biopsy and electromyography are normal in these patients, but electroneurography showed slightly reduced motor and sensory nerve conduction velocities with normal amplitudes (Leipold *et al.* 2013). Investigations of nerves by sural biopsy did not show sensory axonal loss (Leipold *et al.* 2013). The muscular weakness might be attributed to the developmental role of the Na<sub>v</sub>1.9 channel in motoneurons (Subramanian *et al.* 2012, Wetzel *et al.* 2013).

### 4.3 Na<sub>v</sub>1.5 might act downstream of Na<sub>v</sub>1.9-mediated excitation

Spontaneous calcium influx to motoneurons largely depends on the activity of the N-type voltage-gated calcium channel Ca<sub>v</sub>2.2 (Jablonka *et al.* 2007). This channel is known to open at high voltages, in the range of approximately +5 to +10 mV (Catterall *et al.* 2005). This raises the question how subthreshold activity of Na<sub>v</sub>1.9 is enhanced. In DRG neurons, the concomitant partners of Na<sub>v</sub>1.9 are Na<sub>v</sub>1.8 and Na<sub>v</sub>1.7 (Wood *et al.* 2004, Dib-Hajj *et al.* 2010). However, Na<sub>v</sub>1.8 is not expressed in embryonic (see 3.1, Figure 12) (Subramanian *et al.* 2012) and adult motoneurons (Moldovan *et al.* 2011) and Na<sub>v</sub>1.7 is sensitive to tetrodotoxin (Catterall *et al.* 2005). Interestingly, quantitative analysis revealed high expression levels of the TTX-insensitive VGSC Na<sub>v</sub>1.5 in cultured motoneurons. This channel is normally found in electromechanical systems like heart and gut (Beyder *et al.* 2010) and is important for action potential initiation and conduction with a voltage activation around -47 mV (Catterall *et al.* 2005). The activation threshold of Na<sub>v</sub>1.9 is much lower than the activation threshold of Na<sub>v</sub>1.5, which gives him the possibility to open spontaneously near the resting potential (Cummins *et al.* 1999, Herzog *et al.* 2001, Rugiero *et al.* 2003, Ostman *et al.* 2008). In conclusion, the Na<sub>v</sub>1.5 channel would be an ideal physiological partner to potentiate Na<sub>v</sub>1.9-mediated excitation. It may be that Na<sub>v</sub>1.9 could first activate Na<sub>v</sub>1.5, which afterwards initiates a rapid depolarization and a fast voltage-dependent gating of clustered Ca<sub>v</sub>2.2 channels at axonal terminals of growing motoneurons (Figure 29).

### 4.4 Is TrkB upstream of Na<sub>v</sub>1.9-mediated excitation?

Spontaneous excitation of motoneurons is not a continuous process. Motoneurons switch between phases of no or low activity and phases of high activity (Wetzel *et al.* 2013). This leads to the question how phases of high activity are initiated. It is known that G protein-dependent signalling cascades and their interaction with intracellular signalling cascades can increase Na<sub>v</sub>1.9 activity (Baker *et al.* 2003, Ostman *et al.* 2008). Despite this initial hint it is still a puzzling issue how Na<sub>v</sub>1.9 activity is regulated.

In brain neurons the neurotrophin BDNF acts through the receptor tyrosine kinase TrkB and can activate Na<sub>v</sub>1.9-mediated excitation (Blum *et al.* 2002). Therefore, it was tested whether TrkB is also involved in the generation of spontaneous calcium transients. Indeed, motoneurons cultured from a mouse model lacking the complete TrkB receptor gene show a reduced number of spontaneous calcium transients in the soma and growth cone and have shorter axons. TrkB protein was localized in axons and growth cones, indicating that there is a close proximity between the Na<sub>v</sub>1.9 channel and the TrkB kinase. At least in motoneurons, it may be that TrkB is upstream of Na<sub>v</sub>1.9 activity, but it is possible that this interaction is



through the activation of the TrkB-PLC $\gamma$  pathway seems to be the most immediate action of BDNF in central neurons. However, Lang et al. described a fast BDNF-evoked calcium influx in hippocampal neurons that extend the findings from Kafitz et al., 1999 and Blum et al., 2002, who published a BDNF caused depolarization within a few milliseconds that require the activity of voltage-dependent sodium channels as well as fast calcium transients through the opening of voltage-gated calcium channels (*Berninger et al. 1993, Kafitz et al. 1999, Blum et al. 2002, Kovalchuk et al. 2002, Lang et al. 2007*). Nevertheless, activation of Trp channels in motoneuron growth cones seems to be another possibility to initiate spontaneous excitation and subsequent axon elongation. TrpC3 contributes to BDNF-mediated survival and growth cone guidance of cerebellar granule neurons (*Li et al. 2005, Trebak 2010*). However, TrpC3 is barely detectable in embryonic motoneurons, whereas TrpC5 has shown to be highly expressed in motoneuron growth cones (*Jablonka et al. 2007*). Moreover, TrpC5 is known to regulate neurite growth and growth cone morphology, at least in hippocampal neurons (*Greka et al. 2003*). In motoneurons, it is not clear yet how the components interact with each other, but it is possible that kinase-active TrkB first acts via PLC $\gamma$  recruitment to increase neuronal excitability by a non-selective ion influx through TrpC channels. This weak and local TrpC-dependent increase in excitability may cause Na $_v$ 1.9 activation and that gates voltage-dependent calcium influx (Figure 29). On the other hand, there could be an interaction between TrkB, Na $_v$ 1.9 and VGCC independent of TrpC channels or Na $_v$ 1.9 may act spontaneously without TrkB activation.

Future physiological and molecular analysis has to clarify in detail the exact signalling pathways, leading to motoneuron differentiation and activity-dependent axon elongation in developing motoneurons.

In summary, this study contributed to better understanding of the role of subthreshold, cell-autonomous excitation in neurons. It will be a challenging endeavour to unravel the role of Na $_v$ 1.9 as an amplifier of subthreshold excitability for synapse formation and synapse maintenance, not only at the motor endplate, but also at chemical synapses in the brain.

## References

1. Agnew, W. S., Moore, A. C., Levinson, S. R., and Raftery, M. A. (1980) Identification of a large molecular weight peptide associated with a tetrodotoxin binding protein from the electroplax of *Electrophorus electricus*, *Biochem Biophys Res Commun* 92, 860-866.
2. Amaral, M. D., and Pozzo-Miller, L. (2007) TRPC3 channels are necessary for brain-derived neurotrophic factor to activate a nonselective cationic current and to induce dendritic spine formation, *J Neurosci* 27, 5179-5189.
3. Amaya, F., Wang, H., Costigan, M., Allchorne, A. J., Hatcher, J. P., Egerton, J., Stean, T., Morisset, V., Grose, D., Gunthorpe, M. J., Chessell, I. P., Tate, S., Green, P. J., and Woolf, C. J. (2006) The voltage-gated sodium channel Na(v)1.9 is an effector of peripheral inflammatory pain hypersensitivity, *J Neurosci* 26, 12852-12860.
4. Arakawa, Y., Sendtner, M., and Thoenen, H. (1990) Survival effect of ciliary neurotrophic factor (CNTF) on chick embryonic motoneurons in culture: comparison with other neurotrophic factors and cytokines, *J Neurosci* 10, 3507-3515.
5. Araque, A., and Perea, G. (2004) Glial modulation of synaptic transmission in culture, *Glia* 47, 241-248.
6. Baker, M. D., Chandra, S. Y., Ding, Y., Waxman, S. G., and Wood, J. N. (2003) GTP-induced tetrodotoxin-resistant Na<sup>+</sup> current regulates excitability in mouse and rat small diameter sensory neurones, *J Physiol* 548, 373-382.
7. Balkowiec, A., Kunze, D. L., and Katz, D. M. (2000) Brain-derived neurotrophic factor acutely inhibits AMPA-mediated currents in developing sensory relay neurons, *J Neurosci* 20, 1904-1911.
8. Barde, Y. A. (1994) Neurotrophins: a family of proteins supporting the survival of neurons, *Prog Clin Biol Res* 390, 45-56.
9. Berninger, B., Garcia, D. E., Inagaki, N., Hahnel, C., and Lindholm, D. (1993) BDNF and NT-3 induce intracellular Ca<sup>2+</sup> elevation in hippocampal neurones, *Neuroreport* 4, 1303-1306.
10. Beyder, A., Rae, J. L., Bernard, C., Strege, P. R., Sachs, F., and Farrugia, G. (2010) Mechanosensitivity of Nav1.5, a voltage-sensitive sodium channel, *J Physiol* 588, 4969-4985.
11. Bezzi, P., and Volterra, A. (2001) A neuron-glia signalling network in the active brain, *Curr Opin Neurobiol* 11, 387-394.
12. Bibel, M., Hoppe, E., and Barde, Y. A. (1999) Biochemical and functional interactions between the neurotrophin receptors trk and p75NTR, *The EMBO journal* 18, 616-622.
13. Blankenship, A. G., and Feller, M. B. (2010) Mechanisms underlying spontaneous patterned activity in developing neural circuits, *Nature reviews. Neuroscience* 11, 18-29.
14. Blum, R., Kafitz, K. W., and Konnerth, A. (2002) Neurotrophin-evoked depolarization requires the sodium channel Na(V)1.9, *Nature* 419, 687-693.
15. Blum, R., and Konnerth, A. (2005) Neurotrophin-Mediated Rapid Signaling in the Central Nervous System: Mechanisms and Functions, In *Physiology*, pp 70-78.
16. Briese, M., Esmaili, B., and Sattelle, D. B. (2005) Is spinal muscular atrophy the result of defects in motor neuron processes?, *Bioessays* 27, 946-957.

17. Brigadski, T., Hartmann, M., and Lessmann, V. (2005) Differential vesicular targeting and time course of synaptic secretion of the mammalian neurotrophins, *J Neurosci* 25, 7601-7614.
18. Brunet, A., Datta, S. R., and Greenberg, M. E. (2001) Transcription-dependent and -independent control of neuronal survival by the PI3K-Akt signaling pathway, *Curr Opin Neurobiol* 11, 297-305.
19. Burghes, A. H., and Beattie, C. E. (2009) Spinal muscular atrophy: why do low levels of survival motor neuron protein make motor neurons sick?, *Nat Rev Neurosci* 10, 597-609.
20. Bulet, P., Huber, C., Bertrand, S., Ludosky, M. A., Zwaenepoel, I., Clermont, O., Roume, J., Delezoide, A. L., Cartaud, J., Munnich, A., and Lefebvre, S. (1998) The distribution of SMN protein complex in human fetal tissues and its alteration in spinal muscular atrophy, *Hum Mol Genet* 7, 1927-1933.
21. Carroll, R. C., Beattie, E. C., von Zastrow, M., and Malenka, R. C. (2001) Role of AMPA receptor endocytosis in synaptic plasticity, *Nat Rev Neurosci* 2, 315-324.
22. Catterall, W. A. (2000) From ionic currents to molecular mechanisms: the structure and function of voltage-gated sodium channels, *Neuron* 26, 13-25.
23. Catterall, W. A. (2010) Ion channel voltage sensors: structure, function, and pathophysiology, *Neuron* 67, 915-928.
24. Catterall, W. A. (2012) Voltage-gated sodium channels at 60: structure, function and pathophysiology, *J Physiol* 590, 2577-2589.
25. Catterall, W. A., Goldin, A. L., and Waxman, S. G. (2005) International Union of Pharmacology. XLVII. Nomenclature and structure-function relationships of voltage-gated sodium channels, *Pharmacol Rev* 57, 397-409.
26. Catterall, W. A., Perez-Reyes, E., Snutch, T. P., and Striessnig, J. (2005) International Union of Pharmacology. XLVIII. Nomenclature and structure-function relationships of voltage-gated calcium channels, *Pharmacol Rev* 57, 411-425.
27. Cestele, S., and Catterall, W. A. (2000) Molecular mechanisms of neurotoxin action on voltage-gated sodium channels, *Biochimie* 82, 883-892.
28. Chan, Y. B., Miguel-Aliaga, I., Franks, C., Thomas, N., Trulzsch, B., Sattelle, D. B., Davies, K. E., and van den Heuvel, M. (2003) Neuromuscular defects in a Drosophila survival motor neuron gene mutant, *Hum Mol Genet* 12, 1367-1376.
29. Chao, M. V. (2003) Neurotrophins and their receptors: a convergence point for many signalling pathways, *Nature reviews Neuroscience* 4, 299-309.
30. Chao, M. V., Rajagopal, R., and Lee, F. S. (2006) Neurotrophin signalling in health and disease, *Clin Sci (Lond)* 110, 167-173.
31. Cheng, Q., and Yeh, H. H. (2003) Brain-derived neurotrophic factor attenuates mouse cerebellar granule cell GABA(A) receptor-mediated responses via postsynaptic mechanisms, *J Physiol* 548, 711-721.
32. Christensen, R. K., Petersen, A. V., and Perrier, J. F. (2013) How do glial cells contribute to motor control?, *Curr Pharm Des* 19, 4385-4399.
33. Ciccolini, F., Collins, T. J., Sudhoelter, J., Lipp, P., Berridge, M. J., and Bootman, M. D. (2003) Local and global spontaneous calcium events regulate neurite outgrowth and onset of GABAergic phenotype during neural precursor differentiation, *J Neurosci* 23, 103-111.
34. Clapham, D. E. (2003) TRP channels as cellular sensors, *Nature* 426, 517-524.

35. Cohan, C. S., Connor, J. A., and Kater, S. B. (1987) Electrically and chemically mediated increases in intracellular calcium in neuronal growth cones, *J Neurosci* 7, 3588-3599.
36. Coover, D. D., Le, T. T., McAndrew, P. E., Strasswimmer, J., Crawford, T. O., Mendell, J. R., Coulson, S. E., Androphy, E. J., Prior, T. W., and Burghes, A. H. (1997) The survival motor neuron protein in spinal muscular atrophy, *Hum Mol Genet* 6, 1205-1214.
37. Crawford, T. O., and Pardo, C. A. (1996) The neurobiology of childhood spinal muscular atrophy, *Neurobiol Dis* 3, 97-110.
38. Crowder, R. J., and Freeman, R. S. (1998) Phosphatidylinositol 3-kinase and Akt protein kinase are necessary and sufficient for the survival of nerve growth factor-dependent sympathetic neurons, *J Neurosci* 18, 2933-2943.
39. Cummins, T. R., Dib-Hajj, S. D., Black, J. A., Akopian, A. N., Wood, J. N., and Waxman, S. G. (1999) A novel persistent tetrodotoxin-resistant sodium current in SNS-null and wild-type small primary sensory neurons, *J Neurosci* 19, RC43.
40. Daub, H., Weiss, F. U., Wallasch, C., and Ullrich, A. (1996) Role of transactivation of the EGF receptor in signalling by G-protein-coupled receptors, *Nature* 379, 557-560.
41. Dechant, G., and Barde, Y.-A. (2002) The neurotrophin receptor p75(NTR): novel functions and implications for diseases of the nervous system, *Nature Neuroscience* 5, 1131-1136.
42. Dechant, G., and Barde, Y. A. (1997) Signalling through the neurotrophin receptor p75NTR, *Curr Opin Neurobiol* 7, 413-418.
43. Dekkers, M. P., Nikolettou, V., and Barde, Y. A. (2013) Cell biology in neuroscience: Death of developing neurons: New insights and implications for connectivity, *J Cell Biol* 203, 385-393.
44. Dib-Hajj, S., Black, J. A., Cummins, T. R., and Waxman, S. G. (2002) Na<sub>v</sub>1.9: a sodium channel with unique properties, *Trends Neurosci* 25, 253-259.
45. Dib-Hajj, S. D., Cummins, T. R., Black, J. A., and Waxman, S. G. (2010) Sodium channels in normal and pathological pain, *Annu Rev Neurosci* 33, 325-347.
46. Dib-Hajj, S. D., Tyrrell, L., Black, J. A., and Waxman, S. G. (1998) Na<sub>v</sub>, a novel voltage-gated Na channel, is expressed preferentially in peripheral sensory neurons and down-regulated after axotomy, *Proc Natl Acad Sci U S A* 95, 8963-8968.
47. Dib-Hajj, S. D., Tyrrell, L., Escayg, A., Wood, P. M., Meisler, M. H., and Waxman, S. G. (1999) Coding sequence, genomic organization, and conserved chromosomal localization of the mouse gene Scn11a encoding the sodium channel Na<sub>v</sub>, *Genomics* 59, 309-318.
48. Dubowitz, V. (1999) Very severe spinal muscular atrophy (SMA type 0): an expanding clinical phenotype, *Eur J Paediatr Neurol* 3, 49-51.
49. Dull, T., Zufferey, R., Kelly, M., Mandel, R. J., Nguyen, M., Trono, D., and Naldini, L. (1998) A third-generation lentivirus vector with a conditional packaging system, *J Virol* 72, 8463-8471.
50. Durand, G. M., Marandi, N., Herberger, S. D., Blum, R., and Konnerth, A. (2006) Quantitative single-cell RT-PCR and Ca<sup>2+</sup> imaging in brain slices, *Pflugers Arch* 451, 716-726.
51. Fang, X., Djouhri, L., Black, J. A., Dib-Hajj, S. D., Waxman, S. G., and Lawson, S. N. (2002) The presence and role of the tetrodotoxin-resistant sodium channel Na<sub>v</sub>1.9 (Na<sub>v</sub>) in nociceptive primary afferent neurons, *J Neurosci* 22, 7425-7433.



52. Finkbeiner, S., Tavazoie, S. F., Maloratsky, A., Jacobs, K. M., Harris, K. M., and Greenberg, M. E. (1997) CREB: a major mediator of neuronal neurotrophin responses, *Neuron* 19, 1031-1047.
53. Fjell, J., Hjelmstrom, P., Hormuzdiar, W., Milenkovic, M., Aglieco, F., Tyrrell, L., Dib-Hajj, S., Waxman, S. G., and Black, J. A. (2000) Localization of the tetrodotoxin-resistant sodium channel NaN in nociceptors, *Neuroreport* 11, 199-202.
54. Fozzard, H. A., and Hanck, D. A. (1996) Structure and function of voltage-dependent sodium channels: comparison of brain II and cardiac isoforms, *Physiol Rev* 76, 887-926.
55. Frade, J. M., Rodriguez-Tebar, A., and Barde, Y. A. (1996) Induction of cell death by endogenous nerve growth factor through its p75 receptor, *Nature* 383, 166-168.
56. Franke, T. F., Kaplan, D. R., and Cantley, L. C. (1997) PI3K: downstream AKTion blocks apoptosis, *Cell* 88, 435-437.
57. Fujisawa, S., Yamada, M. K., Nishiyama, N., Matsuki, N., and Ikegaya, Y. (2004) BDNF boosts spike fidelity in chaotic neural oscillations, *Biophysical journal* 86, 1820-1828.
58. Fukuoka, T., Kobayashi, K., and Noguchi, K. (2010) Laminae-specific distribution of alpha-subunits of voltage-gated sodium channels in the adult rat spinal cord, *Neuroscience* 169, 994-1006.
59. Gartner, A., Polnau, D. G., Staiger, V., Sciarretta, C., Minichiello, L., Thoenen, H., Bonhoeffer, T., and Korte, M. (2006) Hippocampal long-term potentiation is supported by presynaptic and postsynaptic tyrosine receptor kinase B-mediated phospholipase Cgamma signaling, *J Neurosci* 26, 3496-3504.
60. Goldin, A. L., Barchi, R. L., Caldwell, J. H., Hofmann, F., Howe, J. R., Hunter, J. C., Kallen, R. G., Mandel, G., Meisler, M. H., Netter, Y. B., Noda, M., Tamkun, M. M., Waxman, S. G., Wood, J. N., and Catterall, W. A. (2000) Nomenclature of voltage-gated sodium channels, *Neuron* 28, 365-368.
61. Gomez, T. M., and Spitzer, N. C. (1999) In vivo regulation of axon extension and pathfinding by growth-cone calcium transients, *Nature* 397, 350-355.
62. Graham, F. L., Smiley, J., Russell, W. C., and Nairn, R. (1977) Characteristics of a human cell line transformed by DNA from human adenovirus type 5, *J Gen Virol* 36, 59-74.
63. Greka, A., Navarro, B., Oancea, E., Duggan, A., and Clapham, D. E. (2003) TRPC5 is a regulator of hippocampal neurite length and growth cone morphology, *Nat Neurosci* 6, 837-845.
64. Gu, X. N., Olson, E. C., and Spitzer, N. C. (1994) Spontaneous Neuronal Calcium Spikes and Waves during Early Differentiation, *Journal of Neuroscience* 14, 6325-6335.
65. Gu, X. N., and Spitzer, N. C. (1995) Distinct Aspects of Neuronal Differentiation Encoded by Frequency of Spontaneous Ca<sup>2+</sup> Transients, *Nature* 375, 784-787.
66. Hallbook, F. (1999) Evolution of the vertebrate neurotrophin and Trk receptor gene families, *Curr Opin Neurobiol* 9, 616-621.
67. Hamburger, V. (1934) The effects of wing bud extirpation on the development of the central nervous system in chick embryos, *J Exp Zool* 68, 449-494.
68. Hamburger, V. (1975) Cell-Death in Development of Lateral Motor Column of Chick-Embryo, *Journal of Comparative Neurology* 160, 535-546.

69. Hanson, M. G., and Landmesser, L. T. (2003) Characterization of the circuits that generate spontaneous episodes of activity in the early embryonic mouse spinal cord, *J Neurosci* 23, 587-600.
70. Hanson, M. G., and Landmesser, L. T. (2004) Normal patterns of spontaneous activity are required for correct motor axon guidance and the expression of specific guidance molecules, *Neuron* 43, 687-701.
71. Heinemann, S. H., Terlau, H., Stuhmer, W., Imoto, K., and Numa, S. (1992) Calcium channel characteristics conferred on the sodium channel by single mutations, *Nature* 356, 441-443.
72. Hempstead, B. L., Martin-Zanca, D., Kaplan, D. R., Parada, L. F., and Chao, M. V. (1991) High-affinity NGF binding requires coexpression of the trk proto-oncogene and the low-affinity NGF receptor, *Nature* 350, 678-683.
73. Herzog, R. I., Cummins, T. R., and Waxman, S. G. (2001) Persistent TTX-resistant Na<sup>+</sup> current affects resting potential and response to depolarization in simulated spinal sensory neurons, *Journal of neurophysiology* 86, 1351-1364.
74. Huang, E. J., and Reichardt, L. F. (2001) Neurotrophins: roles in neuronal development and function, *Annu Rev Neurosci* 24, 677-736.
75. Huang, E. J., and Reichardt, L. F. (2003) Trk receptors: roles in neuronal signal transduction, *Annu Rev Biochem* 72, 609-642.
76. Isom, L. L. (2001) Sodium channel beta subunits: anything but auxiliary, *Neuroscientist* 7, 42-54.
77. Jablonka, S., Beck, M., Lechner, B. D., Mayer, C., and Sendtner, M. (2007) Defective Ca<sup>2+</sup> channel clustering in axon terminals disturbs excitability in motoneurons in spinal muscular atrophy, *J Cell Biol* 179, 139-149.
78. Jablonka, S., Holtmann, B., Meister, G., Bandilla, M., Rossoll, W., Fischer, U., and Sendtner, M. (2002) Gene targeting of Gemin2 in mice reveals a correlation between defects in the biogenesis of U snRNPs and motoneuron cell death, *Proc Natl Acad Sci U S A* 99, 10126-10131.
79. Jablonka, S., Karle, K., Sandner, B., Andreassi, C., von Au, K., and Sendtner, M. (2006) Distinct and overlapping alterations in motor and sensory neurons in a mouse model of spinal muscular atrophy, *Hum Mol Genet* 15, 511-518.
80. Jeong, S. Y., Goto, J., Hashida, H., Suzuki, T., Ogata, K., Masuda, N., Hirai, M., Isahara, K., Uchiyama, Y., and Kanazawa, I. (2000) Identification of a novel human voltage-gated sodium channel alpha subunit gene, SCN12A, *Biochemical and biophysical research communications* 267, 262-270.
81. Kafitz, K. W., Rose, C. R., Thoenen, H., and Konnerth, A. (1999) Neurotrophin-evoked rapid excitation through TrkB receptors, *Nature* 401, 918-921.
82. Kang, H., and Schuman, E. M. (1995) Long-lasting neurotrophin-induced enhancement of synaptic transmission in the adult hippocampus, *Science* 267, 1658-1662.
83. Kaplan, D. R., and Miller, F. D. (2000) Neurotrophin signal transduction in the nervous system, *Curr Opin Neurobiol* 10, 381-391.
84. Kariya, S., Re, D. B., Jacquier, A., Nelson, K., Przedborski, S., and Monani, U. R. (2012) Mutant superoxide dismutase 1 (SOD1), a cause of amyotrophic lateral sclerosis, disrupts the recruitment of SMN, the spinal muscular atrophy protein to nuclear Cajal bodies, *Hum Mol Genet* 21, 3421-3434.

85. Kohl, B., Fischer, S., Groh, J., Wessig, C., and Martini, R. (2010) MCP-1/CCL2 modifies axon properties in a PMP22-overexpressing mouse model for Charcot-Marie-tooth 1A neuropathy, *Am J Pathol* 176, 1390-1399.
86. Kong, L., Wang, X., Choe, D. W., Polley, M., Burnett, B. G., Bosch-Marce, M., Griffin, J. W., Rich, M. M., and Sumner, C. J. (2009) Impaired synaptic vesicle release and immaturity of neuromuscular junctions in spinal muscular atrophy mice, *J Neurosci* 29, 842-851.
87. Korte, M., Carroll, P., Wolf, E., Brem, G., Thoenen, H., and Bonhoeffer, T. (1995) Hippocampal long-term potentiation is impaired in mice lacking brain-derived neurotrophic factor, *Proc Natl Acad Sci U S A* 92, 8856-8860.
88. Kovalchuk, Y., Hanse, E., Kafitz, K. W., and Konnerth, A. (2002) Postsynaptic Induction of BDNF-Mediated Long-Term Potentiation, *Science (New York, N Y)* 295, 1729-1734.
89. Kovalchuk, Y., Holthoff, K., and Konnerth, A. (2004) Neurotrophin action on a rapid timescale, *Curr Opin Neurobiol* 14, 558-563.
90. Kwiatkowski, T. J., Jr., Bosco, D. A., Leclerc, A. L., Tamrazian, E., Vanderburg, C. R., Russ, C., Davis, A., Gilchrist, J., Kasarskis, E. J., Munsat, T., Valdmanis, P., Rouleau, G. A., Hosler, B. A., Cortelli, P., de Jong, P. J., Yoshinaga, Y., Haines, J. L., Pericak-Vance, M. A., Yan, J., Ticozzi, N., Siddique, T., McKenna-Yasek, D., Sapp, P. C., Horvitz, H. R., Landers, J. E., and Brown, R. H., Jr. (2009) Mutations in the FUS/TLS gene on chromosome 16 cause familial amyotrophic lateral sclerosis, *Science* 323, 1205-1208.
91. Lang, S. B., Stein, V., Bonhoeffer, T., and Lohmann, C. (2007) Endogenous brain-derived neurotrophic factor triggers fast calcium transients at synapses in developing dendrites, *J Neurosci* 27, 1097-1105.
92. Lebkowski, J. S., Clancy, S., and Calos, M. P. (1985) Simian virus 40 replication in adenovirus-transformed human cells antagonizes gene expression, *Nature* 317, 169-171.
93. Lee, F. S., and Chao, M. V. (2001) Activation of Trk neurotrophin receptors in the absence of neurotrophins, *Proc Natl Acad Sci U S A* 98, 3555-3560.
94. Lee, F. S., Rajagopal, R., Kim, A. H., Chang, P. C., and Chao, M. V. (2002) Activation of Trk neurotrophin receptor signaling by pituitary adenylate cyclase-activating polypeptides, *The Journal of biological chemistry* 277, 9096-9102.
95. Lefebvre, S., Burglen, L., Reboullet, S., Clermont, O., Burlet, P., Viollet, L., Benichou, B., Cruaud, C., Millasseau, P., Zeviani, M., and et al. (1995) Identification and characterization of a spinal muscular atrophy-determining gene, *Cell* 80, 155-165.
96. Leipold, E., Liebmann, L., Korenke, G. C., Heinrich, T., Giesselmann, S., Baets, J., Ebbinghaus, M., Goral, R. O., Stodberg, T., Hennings, J. C., Bergmann, M., Altmuller, J., Thiele, H., Wetzel, A., Nurnberg, P., Timmerman, V., De Jonghe, P., Blum, R., Schaible, H. G., Weis, J., Heinemann, S. H., Hubner, C. A., and Kurth, I. (2013) A de novo gain-of-function mutation in SCN11A causes loss of pain perception, *Nat Genet.*
97. Leipold, E., Liebmann, L., Korenke, G. C., Heinrich, T., Giesselmann, S., Baets, J., Ebbinghaus, M., Goral, R. O., Stodberg, T., Hennings, J. C., Bergmann, M., Altmuller, J., Thiele, H., Wetzel, A., Nurnberg, P., Timmerman, V., De Jonghe, P., Blum, R., Schaible, H. G., Weis, J., Heinemann, S. H., Hubner, C. A., and Kurth, I. (2013) A de novo gain-of-function mutation in SCN11A causes loss of pain perception, *Nature genetics* 45, 1399-1404.

98. Leo, S., D'Hooge, R., and Meert, T. (2010) Exploring the role of nociceptor-specific sodium channels in pain transmission using Nav1.8 and Nav1.9 knockout mice, *Behav Brain Res* 208, 149-157.
99. Lessmann, V., Gottmann, K., and Malcangio, M. (2003) Neurotrophin secretion: current facts and future prospects, *Prog Neurobiol* 69, 341-374.
100. Levi-Montalcini, R. (1987) The nerve growth factor 35 years later, *Science (New York, N Y)* 237, 1154-1162.
101. Levine, E. S., Crozier, R. A., Black, I. B., and Plummer, M. R. (1998) Brain-derived neurotrophic factor modulates hippocampal synaptic transmission by increasing N-methyl-D-aspartic acid receptor activity, *Proc Natl Acad Sci U S A* 95, 10235-10239.
102. Levine, E. S., Dreyfus, C. F., Black, I. B., and Plummer, M. R. (1995) Brain-derived neurotrophic factor rapidly enhances synaptic transmission in hippocampal neurons via postsynaptic tyrosine kinase receptors, *Proc Natl Acad Sci U S A* 92, 8074-8077.
103. Li, H. S., Xu, X. Z., and Montell, C. (1999) Activation of a TRPC3-dependent cation current through the neurotrophin BDNF, *Neuron* 24, 261-273.
104. Li, Y., Calfa, G., Inoue, T., Amaral, M. D., and Pozzo-Miller, L. (2010) Activity-dependent release of endogenous BDNF from mossy fibers evokes a TRPC3 current and Ca<sup>2+</sup> elevations in CA3 pyramidal neurons, *J Neurophysiol* 103, 2846-2856.
105. Li, Y., Jia, Y. C., Cui, K., Li, N., Zheng, Z. Y., Wang, Y. Z., and Yuan, X. B. (2005) Essential role of TRPC channels in the guidance of nerve growth cones by brain-derived neurotrophic factor, *Nature* 434, 894-898.
106. Lin, S. Y., Wu, K., Levine, E. S., Mount, H. T., Suen, P. C., and Black, I. B. (1998) BDNF acutely increases tyrosine phosphorylation of the NMDA receptor subunit 2B in cortical and hippocampal postsynaptic densities, *Brain Res Mol Brain Res* 55, 20-27.
107. Linseman, D. A., Benjamin, C. W., and Jones, D. A. (1995) Convergence of angiotensin II and platelet-derived growth factor receptor signaling cascades in vascular smooth muscle cells, *J Biol Chem* 270, 12563-12568.
108. Liu, M., and Wood, J. N. (2011) The roles of sodium channels in nociception: implications for mechanisms of neuropathic pain, *Pain Med* 12 Suppl 3, S93-99.
109. Liu, X., Ernfor, P., Wu, H., and Jaenisch, R. (1995) Sensory but not motor neuron deficits in mice lacking NT4 and BDNF, *Nature* 375, 238-241.
110. Lohof, A. M., Ip, N. Y., and Poo, M. M. (1993) Potentiation of developing neuromuscular synapses by the neurotrophins NT-3 and BDNF, *Nature* 363, 350-353.
111. Lorson, C. L., Hahnen, E., Androphy, E. J., and Wirth, B. (1999) A single nucleotide in the SMN gene regulates splicing and is responsible for spinal muscular atrophy, *Proc Natl Acad Sci U S A* 96, 6307-6311.
112. Lu, B., Pang, P. T., and Woo, N. H. (2005) The yin and yang of neurotrophin action, *Nature reviews. Neuroscience* 6, 603-614.
113. Luttrell, L. M., Daaka, Y., and Lefkowitz, R. J. (1999) Regulation of tyrosine kinase cascades by G-protein-coupled receptors, *Curr Opin Cell Biol* 11, 177-183.
114. McGovern, V. L., Gavrilina, T. O., Beattie, C. E., and Burghes, A. H. M. (2008) Embryonic motor axon development in the severe SMA mouse, *Hum Mol Genet* 17, 2900-2909.
115. Michaud, M., Arnoux, T., Bielli, S., Durand, E., Rotrou, Y., Jablonka, S., Robert, F., Giraudon-Paoli, M., Riessland, M., Mattei, M. G., Andriambeloso, E., Wirth, B., Sendtner, M., Gallego, J., Pruss, R. M., and Bordet, T. (2010) Neuromuscular defects

- and breathing disorders in a new mouse model of spinal muscular atrophy, *Neurobiol Dis* 38, 125-135.
116. Milner, L. D., and Landmesser, L. T. (1999) Cholinergic and GABAergic inputs drive patterned spontaneous motoneuron activity before target contact, *J Neurosci* 19, 3007-3022.
  117. Minichiello, L. (2009) TrkB signalling pathways in LTP and learning, *Nature reviews. Neuroscience* 10, 850-860.
  118. Minichiello, L., Calella, A. M., Medina, D. L., Bonhoeffer, T., Klein, R., and Korte, M. (2002) Mechanism of TrkB-mediated hippocampal long-term potentiation, *Neuron* 36, 121-137.
  119. Mizuno, M., Yamada, K., He, J., Nakajima, A., and Nabeshima, T. (2003) Involvement of BDNF receptor TrkB in spatial memory formation, *Learn Mem* 10, 108-115.
  120. Moldovan, M., Alvarez, S., Pinchenko, V., Klein, D., Nielsen, F. C., Wood, J. N., Martini, R., and Krarup, C. (2011) Na(v)1.8 channelopathy in mutant mice deficient for myelin protein zero is detrimental to motor axons, *Brain* 134, 585-601.
  121. Monani, U. R. (2005) Spinal muscular atrophy: a deficiency in a ubiquitous protein; a motor neuron-specific disease, *Neuron* 48, 885-896.
  122. Monani, U. R., Sendtner, M., Coover, D. D., Parsons, D. W., Andreassi, C., Le, T. T., Jablonka, S., Schrank, B., Rossoll, W., Prior, T. W., Morris, G. E., and Burghes, A. H. (2000) The human centromeric survival motor neuron gene (SMN2) rescues embryonic lethality in *Smn(-/-)* mice and results in a mouse with spinal muscular atrophy, *Hum Mol Genet* 9, 333-339.
  123. Montell, C., Birnbaumer, L., and Flockerzi, V. (2002) The TRP channels, a remarkably functional family, *Cell* 108, 595-598.
  124. Murray, L. M., Lee, S., Baumer, D., Parson, S. H., Talbot, K., and Gillingwater, T. H. (2010) Pre-symptomatic development of lower motor neuron connectivity in a mouse model of severe spinal muscular atrophy, *Hum Mol Genet* 19, 420-433.
  125. Nikolettou, V., Lickert, H., Frade, J. M., Rencurel, C., Giallonardo, P., Zhang, L., Bibel, M., and Barde, Y. A. (2010) Neurotrophin receptors TrkA and TrkC cause neuronal death whereas TrkB does not, *Nature* 467, 59-63.
  126. Nishimaru, H., Iizuka, M., Ozaki, S., and Kudo, N. (1996) Spontaneous motoneuronal activity mediated by glycine and GABA in the spinal cord of rat fetuses in vitro, *J Physiol* 497 ( Pt 1), 131-143.
  127. Noda, M., Ikeda, T., Suzuki, H., Takeshima, H., Takahashi, T., Kuno, M., and Numa, S. (1986) Expression of functional sodium channels from cloned cDNA, *Nature* 322, 826-828.
  128. O'Donovan, M. J., and Landmesser, L. (1987) The development of hindlimb motor activity studied in the isolated spinal cord of the chick embryo, *J Neurosci* 7, 3256-3264.
  129. Ogata, K., Jeong, S. Y., Murakami, H., Hashida, H., Suzuki, T., Masuda, N., Hirai, M., Isahara, K., Uchiyama, Y., Goto, J., and Kanazawa, I. (2000) Cloning and expression study of the mouse tetrodotoxin-resistant voltage-gated sodium channel alpha subunit NaT/Scn11a, *Biochemical and biophysical research communications* 267, 271-277.
  130. Ostman, J. A., Nassar, M. A., Wood, J. N., and Baker, M. D. (2008) GTP up-regulated persistent Na<sup>+</sup> current and enhanced nociceptor excitability require NaV1.9, *J Physiol* 586, 1077-1087.
  131. Park, H., and Poo, M. M. (2013) Neurotrophin regulation of neural circuit development and function, *Nat Rev Neurosci* 14, 7-23.

132. Patino, G. A., and Isom, L. L. (2010) Electrophysiology and beyond: multiple roles of Na<sup>+</sup> channel beta subunits in development and disease, *Neurosci Lett* 486, 53-59.
133. Pearn, J. H., Hudgson, P., and Walton, J. N. (1978) A clinical and genetic study of spinal muscular atrophy of adult onset: the autosomal recessive form as a discrete disease entity, *Brain* 101, 591-606.
134. Penzotti, J. L., Fozzard, H. A., Lipkind, G. M., and Dudley, S. C., Jr. (1998) Differences in saxitoxin and tetrodotoxin binding revealed by mutagenesis of the Na<sup>+</sup> channel outer vestibule, *Biophys J* 75, 2647-2657.
135. Philo, J., Talvenheimo, J., Wen, J., Rosenfeld, R., Welcher, A., and Arakawa, T. (1994) Interactions of neurotrophin-3 (NT-3), brain-derived neurotrophic factor (BDNF), and the NT-3.BDNF heterodimer with the extracellular domains of the TrkB and TrkC receptors, *J Biol Chem* 269, 27840-27846.
136. Poo, M. M. (2001) Neurotrophins as synaptic modulators, *Nature reviews Neuroscience* 2, 24-32.
137. Priest, B. T., Murphy, B. A., Lindia, J. A., Diaz, C., Abbadie, C., Ritter, A. M., Liberator, P., Iyer, L. M., Kash, S. F., Kohler, M. G., Kaczorowski, G. J., MacIntyre, D. E., and Martin, W. J. (2005) Contribution of the tetrodotoxin-resistant voltage-gated sodium channel NaV1.9 to sensory transmission and nociceptive behavior, *Proc Natl Acad Sci U S A* 102, 9382-9387.
138. Puehringer, D., Orel, N., Luningschror, P., Subramanian, N., Herrmann, T., Chao, M. V., and Sendtner, M. (2013) EGF transactivation of Trk receptors regulates the migration of newborn cortical neurons, *Nature Neuroscience* 16, 407-415.
139. Rajagopal, R., and Chao, M. V. (2006) A role for Fyn in Trk receptor transactivation by G-protein-coupled receptor signaling, *Molecular and cellular neurosciences* 33, 36-46.
140. Rajagopal, R., Chen, Z. Y., Lee, F. S., and Chao, M. V. (2004) Transactivation of Trk neurotrophin receptors by G-protein-coupled receptor ligands occurs on intracellular membranes, *J Neurosci* 24, 6650-6658.
141. Rathod, R., Havlicek, S., Frank, N., Blum, R., and Sendtner, M. (2012) Laminin induced local axonal translation of beta-actin mRNA is impaired in SMN-deficient motoneurons, *Histochem Cell Biol* 138, 737-748.
142. Reichardt, L. F. (2003) Neurobiology: signals that make waves, *Nature* 426, 25-26.
143. Reichardt, L. F. (2006) Neurotrophin-regulated signalling pathways, *Philosophical transactions of the Royal Society of London Series B, Biological sciences* 361, 1545-1564.
144. Rodriguez-Tebar, A., Dechant, G., and Barde, Y. A. (1990) Binding of brain-derived neurotrophic factor to the nerve growth factor receptor, *Neuron* 4, 487-492.
145. Rohrer, B., Korenbrot, J. I., LaVail, M. M., Reichardt, L. F., and Xu, B. (1999) Role of neurotrophin receptor TrkB in the maturation of rod photoreceptors and establishment of synaptic transmission to the inner retina, *J Neurosci* 19, 8919-8930.
146. Rose, C. R., Blum, R., Pichler, B., Lepier, A., Kafitz, K. W., and Konnerth, A. (2003) Truncated TrkB-T1 mediates neurotrophin-evoked calcium signalling in glia cells, *Nature* 426, 74-78.
147. Rosenberg, S. S., and Spitzer, N. C. (2011) Calcium signaling in neuronal development, *Cold Spring Harb Perspect Biol* 3, a004259.
148. Rossoll, W., Jablonka, S., Andreassi, C., Kroning, A. K., Karle, K., Monani, U. R., and Sendtner, M. (2003) Smn, the spinal muscular atrophy-determining gene product,

- modulates axon growth and localization of beta-actin mRNA in growth cones of motoneurons, *J Cell Biol* 163, 801-812.
149. Rossoll, W., Kroning, A.-K., Ohndorf, U.-M., Steegborn, C., Jablonka, S., and Sendtner, M. (2002) Specific interaction of Smn, the spinal muscular atrophy determining gene product, with hnRNP-R and gry-rbp/hnRNP-Q: a role for Smn in RNA processing in motor axons?, *Hum Mol Genet* 11, 93-105.
  150. Rugiero, F., Mistry, M., Sage, D., Black, J. A., Waxman, S. G., Crest, M., Clerc, N., Delmas, P., and Gola, M. (2003) Selective expression of a persistent tetrodotoxin-resistant Na<sup>+</sup> current and Nav1.9 subunit in myenteric sensory neurons, *J Neurosci* 23, 2715-2725.
  151. Ruiz, R., Casanas, J. J., Torres-Benito, L., Cano, R., and Tabares, L. (2010) Altered intracellular Ca<sup>2+</sup> homeostasis in nerve terminals of severe spinal muscular atrophy mice, *J Neurosci* 30, 849-857.
  152. Rumsey, J. W., Das, M., Stancescu, M., Bott, M., Fernandez-Valle, C., and Hickman, J. J. (2009) Node of Ranvier formation on motoneurons in vitro, *Biomaterials* 30, 3567-3572.
  153. Rush, A. M., and Waxman, S. G. (2004) PGE2 increases the tetrodotoxin-resistant Nav1.9 sodium current in mouse DRG neurons via G-proteins, *Brain Res* 1023, 264-271.
  154. Sanes, J. R., and Lichtman, J. W. (1999) Development of the vertebrate neuromuscular junction, *Annu Rev Neurosci* 22, 389-442.
  155. Satin, J., Kyle, J. W., Chen, M., Bell, P., Cribbs, L. L., Fozzard, H. A., and Rogart, R. B. (1992) A mutant of TTX-resistant cardiac sodium channels with TTX-sensitive properties, *Science* 256, 1202-1205.
  156. Sendtner, M. (2010) Therapy development in spinal muscular atrophy, *Nature Neuroscience* 13, 795-799.
  157. Sendtner, M., Holtmann, B., and Hughes, R. A. (1996) The response of motoneurons to neurotrophins, *Neurochem Res* 21, 831-841.
  158. Sendtner, M., Holtmann, B., Kolbeck, R., Thoenen, H., and Barde, Y. A. (1992) Brain-derived neurotrophic factor prevents the death of motoneurons in newborn rats after nerve section, *Nature* 360, 757-759.
  159. Sendtner, M., Kreutzberg, G. W., and Thoenen, H. (1990) Ciliary neurotrophic factor prevents the degeneration of motor neurons after axotomy, *Nature* 345, 440-441.
  160. Sendtner, M., Pei, G., Beck, M., Schweizer, U., and Wiese, S. (2000) Developmental motoneuron cell death and neurotrophic factors, *Cell and tissue research* 301, 71-84.
  161. Shaywitz, A. J., and Greenberg, M. E. (1999) CREB: a stimulus-induced transcription factor activated by a diverse array of extracellular signals, *Annu Rev Biochem* 68, 821-861.
  162. Sivilotti, L., Okuse, K., Akopian, A. N., Moss, S., and Wood, J. N. (1997) A single serine residue confers tetrodotoxin insensitivity on the rat sensory-neuron-specific sodium channel SNS, *FEBS Lett* 409, 49-52.
  163. Skaper, S. D. (2008) The biology of neurotrophins, signalling pathways, and functional peptide mimetics of neurotrophins and their receptors, *CNS & neurological disorders drug targets* 7, 46-62.
  164. Smith, E. S., and Momin, A. (2008) Persistent pain: the contribution of Na(V)1.9, *J Physiol* 586, 2249-2250.
  165. Spitzer, N. C. (2006) Electrical activity in early neuronal development, *Nature* 444, 707-712.

166. Spitzer, N. C. (2008) Calcium: first messenger, *Nature neuroscience* 11, 243-244.
167. Spitzer, N. C., Lautermilch, N. J., Smith, R. D., and Gomez, T. M. (2000) Coding of neuronal differentiation by calcium transients, *BioEssays : news and reviews in molecular, cellular and developmental biology* 22, 811-817.
168. Stevens, M., Peigneur, S., and Tytgat, J. (2011) Neurotoxins and their binding areas on voltage-gated sodium channels, *Front Pharmacol* 2, 71.
169. Subramanian, N., Wetzel, A., Dombert, B., Yadav, P., Havlicek, S., Jablonka, S., Nassar, M. A., Blum, R., and Sendtner, M. (2012) Role of Nav1.9 in activity-dependent axon growth in motoneurons, *Hum Mol Genet*.
170. Suen, P. C., Wu, K., Levine, E. S., Mount, H. T., Xu, J. L., Lin, S. Y., and Black, I. B. (1997) Brain-derived neurotrophic factor rapidly enhances phosphorylation of the postsynaptic N-methyl-D-aspartate receptor subunit 1, *Proc Natl Acad Sci U S A* 94, 8191-8195.
171. Thoenen, H. (1993) Role played by neurotrophic factors in the maintenance and repair of the peripheral nervous system, *Diabet Med* 10 Suppl 2, 7S-9S.
172. Trebak, M. (2010) The puzzling role of TRPC3 channels in motor coordination, *Pflugers Arch* 459, 369-375.
173. Tucker, K., and Fadool, D. A. (2002) Neurotrophin modulation of voltage-gated potassium channels in rat through TrkB receptors is time and sensory experience dependent, *J Physiol* 542, 413-429.
174. Tyrrell, L., Renganathan, M., Dib-Hajj, S. D., and Waxman, S. G. (2001) Glycosylation alters steady-state inactivation of sodium channel Nav1.9/NaN in dorsal root ganglion neurons and is developmentally regulated, *J Neurosci* 21, 9629-9637.
175. Vizard, T. N., O'Keefe, G. W., Gutierrez, H., Kos, C. H., Riccardi, D., and Davies, A. M. (2008) Regulation of axonal and dendritic growth by the extracellular calcium-sensing receptor, *Nature neuroscience* 11, 285-291.
176. Wang, S., Polo-Parada, L., and Landmesser, L. T. (2009) Characterization of rhythmic Ca<sup>2+</sup> transients in early embryonic chick motoneurons: Ca<sup>2+</sup> sources and effects of altered activation of transmitter receptors, *J Neurosci* 29, 15232-15244.
177. Waxman, S. G., Dib-Hajj, S., Cummins, T. R., and Black, J. A. (1999) Sodium channels and pain, *Proc Natl Acad Sci U S A* 96, 7635-7639.
178. Waxman, S. G., and Estacion, M. (2008) Nav1.9, G-proteins, and nociceptors, *J Physiol* 586, 917-918.
179. West, J. W., Patton, D. E., Scheuer, T., Wang, Y., Goldin, A. L., and Catterall, W. A. (1992) A cluster of hydrophobic amino acid residues required for fast Na<sup>(+)</sup>-channel inactivation, *Proc Natl Acad Sci U S A* 89, 10910-10914.
180. Wetzel, A., Jablonka, S., and Blum, R. (2013) Cell-autonomous axon growth of young motoneurons is triggered by a voltage-gated sodium channel, *Channels (Austin)* 7, 51-56.
181. Wiese, S., Herrmann, T., Drepper, C., Jablonka, S., Funk, N., Klausmeyer, A., Rogers, M.-L., Rush, R., and Sendtner, M. (2010) Isolation and enrichment of embryonic mouse motoneurons from the lumbar spinal cord of individual mouse embryos, *Nat Protoc* 5, 31-38.
182. Wiese, S., Jablonka, S., Holtmann, B., Orel, N., Rajagopal, R., Chao, M. V., and Sendtner, M. (2007) Adenosine receptor A2A-R contributes to motoneuron survival by transactivating the tyrosine kinase receptor TrkB, *Proc Natl Acad Sci U S A* 104, 17210-17215.



- 
183. Wirth, B. (2000) An update of the mutation spectrum of the survival motor neuron gene (SMN1) in autosomal recessive spinal muscular atrophy (SMA), *Hum Mutat* 15, 228-237.
  184. Wood, J. N., Boorman, J. P., Okuse, K., and Baker, M. D. (2004) Voltage-gated sodium channels and pain pathways, *J Neurobiol* 61, 55-71.
  185. Yiangou, Y., Birch, R., Sangameswaran, L., Eglon, R., and Anand, P. (2000) SNS/PN3 and SNS2/NaN sodium channel-like immunoreactivity in human adult and neonate injured sensory nerves, *FEBS Lett* 467, 249-252.
  186. Yoshii, A., and Constantine-Paton, M. (2010) Postsynaptic BDNF-TrkB signaling in synapse maturation, plasticity, and disease, *Dev Neurobiol* 70, 304-322.
  187. Zhou, F. Q., and Snider, W. D. (2006) Intracellular control of developmental and regenerative axon growth, *Philos Trans R Soc Lond B Biol Sci* 361, 1575-1592.
  188. Zufferey, R., Dull, T., Mandel, R. J., Bukovsky, A., Quiroz, D., Naldini, L., and Trono, D. (1998) Self-inactivating lentivirus vector for safe and efficient in vivo gene delivery, *J Virol* 72, 9873-9880.

## Affidavit

I hereby confirm that my thesis entitled "The role of TrkB and Na<sub>v</sub>1.9 in activity-dependent axon growth in motoneurons" is the result of my own work. I did not receive any help or support from commercial consultants. All sources and / or materials applied are listed and specified in the thesis.

Furthermore, I confirm that this thesis has not yet been submitted as part of another examination process neither in identical nor in similar form.

---

Place, Date

---

Signature

## Eidesstattliche Erklärung

Hiermit erkläre ich an Eides statt, die Dissertation mit dem Titel "Die Rolle von TrkB und Na<sub>v</sub>1.9 in aktivitätsabhängigem Axonwachstum von Motoneuronen" eigenständig, d.h. insbesondere selbständig und ohne Hilfe eines kommerziellen Promotionsberaters, angefertigt und keine anderen als die von mir angegebenen Quellen und Hilfsmittel verwendet zu haben.

Ich erkläre außerdem, dass die Dissertation weder in gleicher noch in ähnlicher Form bereits in einem anderen Prüfungsverfahren vorgelegen hat.

---

Ort, Datum

---

Unterschrift

# Curriculum Vitae

## PERSONAL INFORMATION

Name: Andrea Wetzel  
 Date of Birth: 06/23/1985  
 Place of Birth: Erfurt  
 Nationality: German

## SCIENTIFIC EXPERIENCE

- 09/2010 - present      Institute for Clinical Neurobiology at the University Hospital of Wuerzburg, Germany
- PhD student at the Institute of Prof. Dr. Michael Sendtner, at the research group of PD Dr. Robert Blum
  - Title of the dissertation: "The role of TrkB and Na<sub>v</sub>1.9 in activity-dependent axon growth in motoneurons"
- 02/2009 - 04/2010      Center for Molecular Biomedicine, Institute for Molecular Cell Biology at Friedrich Schiller University in Jena, Germany
- Diploma student at the Laboratory of Prof. Dr. Frank-D. Böhmer
  - Title of the diploma thesis: "DEP-1/CD148 effects on PDGF receptor signalling in meningioma cells"

## EDUCATION

- 10/2004 - 06/2010      Friedrich Schiller University of Jena, Germany
- Graduate studies of Biology: Average grade 1.1
- 07/1996 - 06/2004      Cooperative comprehensive school, Erfurt, Germany
- Abitur: Average grade 2.1

## PUBLICATIONS

- Leipold E, Liebmann L, Korenke GC, Heinrich T, Gießelmann S, Baets J, Ebbinghaus M, Goral RO, Stöberg T, Hennings JC, Bergmann M, Altmüller J, Thiele H, **Wetzel A**, Nürnberg P, Timmerman V, De Jonghe P, Blum R, Schaible HG, Weis J, Heinemann HH, Hübner CA, Kurth I; "A *de novo* gain-of-function mutation in *SCN11A* causes loss of pain perception"; Nature Genetics 2013
- **Wetzel A**, Jablonka S, Blum R; "Cell-autonomous axon growth of young motoneurons is triggered by a voltage-gated sodium channel"; Channels (Austin) 2013
- Subramanian N\*, **Wetzel A\***, Dombert B, Yadav P, Havlicek H, Jablonka S, Nassar MA, Blum R, Sendtner M; "Role of Na<sub>v</sub>1.9 in activity-dependent axon growth in motoneurons"; Human Molecular Genetics 2012 (\* equally contributing authors)

- Petermann A, Haase D, **Wetzel A**, Balavenkatraman KK, Tenev T, Gührs KH, Friedrich S, Nakamura M, Mawrin C, Böhmer FD; "Loss of the Protein-Tyrosine Phosphatase DEP-1/PTPRJ Drives Meningioma Cell Motility"; Brain Pathology 2011

## GRANTS

- Travel grant                      From the German Neuroscience Society for participation at the international conference of the Federation of European Neurosciences (FENS) in Barcelona, 2012

## INTERNATIONAL CONFERENCES

- |         |   |
|---------|---|
| 10/2012 | Poster presentation, 7 <sup>th</sup> International Symposium of the Graduate School of Life Sciences - EPOS, Wuerzburg, Germany |
| 07/2012 | Poster presentation, International Conference of the Federation of European Neurosciences (FENS), Barcelona, Spain              |
| 06/2012 | Oral presentation, International NGF Meeting, Wuerzburg, Germany  |
| 04/2012 | Poster presentation, International Symposium of SFB 581, Wuerzburg, Germany   |
| 03/2011 | Participation, 9 <sup>th</sup> Goettingen Meeting of the German Neuroscience Society, Goettingen, Germany                       |

## Acknowledgements

I would like to thank all people who gave me the possibility to complete this thesis:

At first, I thank Prof. Dr. Michael Sendtner for giving me the opportunity to do my thesis in such a well equipped institute with great people. Further, I thank him for his support as one of my supervisors and for all the inspiring comments, not only during the seminars.

A very special thanks goes to PD Dr. Robert Blum as my first supervisor. I thank you for your continuing support, for a very warm welcome and start, for your introduction in many new methods and for your ideas and help over the whole time. Thank you for being my thesis advisor. I learned a lot!

I thank Prof. Dr. Erhard Wischmeyer for his support as my supervisor and for the evaluation of my thesis and Prof. Dr. Utz Fischer as chairperson for completing my committee.

I express my gratitude to Dr. Narayan Subramanian, Benjamin Dombert, Preeti Yadav, Steven Havlicek, PD Dr. Sibylle Jablonka, Dr. Mohammed A. Nassar for a wonderful collaboration on the manuscript "Role of  $\text{Na}_v1.9$  in activity-dependent axon growth in motoneurons".

I would like to thank our cooperation partners from Jena, OA PD Dr. Ingo Kurth and Prof. Dr. Christian Hübner from the Institute of Human Genetics and Dr. Enrico Leipold and Prof. Dr. Stefan H. Heinemann from the Institute of Biochemistry and Biophysics for the nice collaboration on the manuscript "A *de novo* gain-of-function mutation in *SCN11A* causes loss of pain perception".

Furthermore, I place my gratitude to our cooperation partners Dennis Klein and Prof. Dr. Rudolf Martini from the Department of Neurology, University Hospital Würzburg for the help and introduction in the work with teased fibres. In this context, I would like to thank our rotating student Simone Fellmoser who supported this experiments, too.

A big thanks goes to Michaela Keßler, Zuzana Fouskova, Simone Rink, Elena Ferber, Nicole Elflein, Elke Spirk, Hildegard Troll, Christian Mehling, Manuela Kohles and Nadine Vornberger for their excellent support, for the introduction in new techniques and for answering many questions. Special thanks to Michi (GBM No. II), Zuzi and Simi. Work with you was always fun!

I would like to thank all the people from the animal facility. Without the work of Regine Sendtner, Victor Buterus, Joachim Horschig, Galina Gribanova, Richard Taylor and Helga Brunner this thesis would not have been possible. In this context, I thank Prof. Dr. John Wood from London who kindly provided the  $\text{Na}_v1.9^{-/-}$  mice.

I thank Judita Kiehl, Urveen Oberoi-Lehrieder and Birgit Christ for their support in all administrative processes.

I am very grateful for a pleasant working atmosphere and help by all members and former members of the Institute for Clinical Neurobiology. Warm thanks to Samira Samtleben, Lena Saal and Dr. Michael Briese for a funny and beneficial lunch time. I thank Preeti Yadav, Dr. Reena Rathod, Dr. Bhuvaneish Thangaraj Selvaraj and Rajeeve Sivadasan for inspiring discussions mostly on evenings and weekends in lab. Hence, I am sure that Preeti will never forget: यह सब तुम्हारी गलती है and Rajeeve is the most holy devil, I ever met ☺! For Isabella Lengfelder I will always have a pocketful of sunshine and I was impressed by Juliane Jäpel-Schael, Elisa Meneghetti and Caroline Fecher. It was great to meet and work with all of you!

I gratefully appreciate the financial support of the Deutsche Forschungsgemeinschaft, the Hermann und Lilly Schilling Stiftung im Stifterverband der Deutschen Wissenschaft and the German Neuroscience Society as well as I thank the University Hospital of Würzburg and the Graduate School of Life Sciences, University of Würzburg that made it possible to complete my thesis.

Last, but not least I would like to give a heartfelt thanks to my family and friends, especially to my parents who always supported me in my life and who always believe in me. Thank you for your constant encouragements!

PS: Thank you Hans Riegel for the invention of gummy bears...☺